UNDERSTANDING THE MIXING DYNAMICS AND STRUCTURAL FUNCTIONALITY OF GLUTEN SUBUNITS TAGGED WITH QUANTUM DOTS IN WHEAT DOUGH AND ANALYZED BY QUANTITATIVE IMAGING TECHNIQUES

by

Jose Carlos Bonilla Oliva

A Dissertation

Submitted to the Faculty of Purdue University

In Partial Fulfillment of the Requirements for the degree of

Doctor of Philosophy
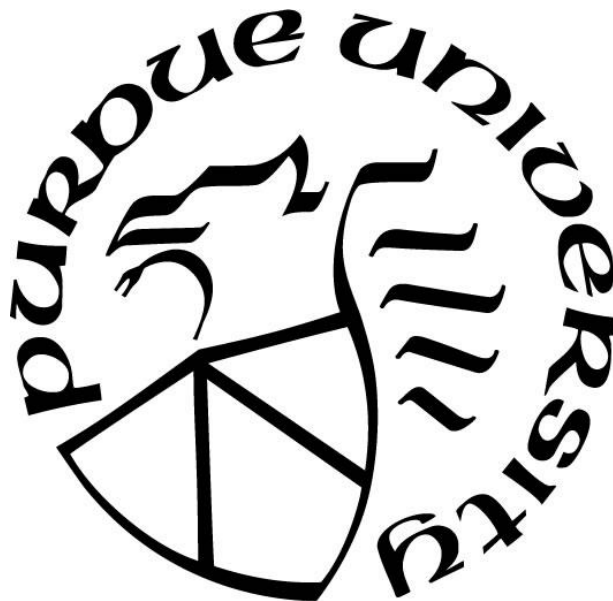
Department of Food Science

West Lafayette, Indiana

May 2020

THE PURDUE UNIVERSITY GRADUATE SCHOOL
STATEMENT OF COMMITTEE APPROVAL

Dr. Jozef Kokini, Chair

Department of Food Science

Dr. Arun Bhunia

Department of Food Science

Dr. Bruce Hamaker

Department of Food Science

Dr. Yuan Yao

Department of Food Science

Dr. James Schaber

Bindley Bioscience Center

Dr. Osvaldo Campanella

Department of Agricultural and Biological Engineering

Approved by:

Dr. Arun Bhunia

To my parents Delcy Oliva and Cesar Bonilla, and to my brother and sisters, Cesar, Jeannie, and Carolina for your immense support and love

To my nieces and nephews, Isabella, Allan, Cesar, Andrea, and Mila for being my inspiration and motivation

ACKNOWLEDGMENTS

TABLE OF CONTENTS

LIST OF TABLES

LIST OF FIGURES

ABSTRACT

Gluten is a group of wheat proteins with viscoelastic properties not seen in any other material on earth, these properties are given by its subunits, gliadins (more viscous) and glutenins (more elastic). The differences in these viscoelastic properties in gluten from different types of wheat flours make a wide variety of wheat products available worldwide, placing wheat products among the most consumed staple foods in the human diet. The objective of this research is to gain new insights about the structural functionality of the gluten subunits, low molecular weight (LMW) glutenins, high molecular weight (HMW) glutenins, and gliadins in wheat dough. To this end, a new staining procedure using antibodies conjugated with fluorescent quantum dots has been developed in order to visualize each gluten subunits individually; a new microscopy procedure with Confocal Laser Scanning Microscopy has also been developed. The fluorescent images have been processed with a protein network analysis software and with a co-localization technique. The use of these two quantitative imaging techniques has helped us move from a qualitative description of the images to quantitative and comparable data collected from the confocal microscopy images. These two techniques provide information about the structural integrity of the network from each gluten subunit, and information about the interactions of the different gluten subunits. It was shown how the three gluten protein subunits interact closely together at the time of dough maximum strength during mixing. As mixing continues, LMW glutenins separate from three-gluten subunits network first, being responsible for the initial decay in dough strength; HMW glutenins agglomerates later in the mixing, being more responsible for the long-term decay in dough strength. It was also shown that the HMW glutenins do not re-distribute themselves when the dough shows high resistance to mixing, and that the three gluten subunits disrupt similarly when the dough has low resistance to mixing. Lastly, the important role of LMW glutenins in keeping the structural integrity of semolina doughs was proven by a direct correlation of the elastic rheological component of the dough and protein network parameters of LMW glutenins. This was proven further when it was shown that gliadins and HMW glutenins stick together during different rheological deformations of the dough. The applications of the fundamental knowledge from this work can be applied by wheat breeders and food product developers to increase the variety of products made for wheat and/or improve the quality of current wheat products.

CHAPTER 1.   INTRODUCTION

1.1 Importance of gluten in wheat products

Wheat is responsible for many of the most consumed staple foods around the world over the centuries. Wheat constitutes the biggest portion of calorie intake in the human diet and occupies more land area than any other crop for human consumption (FAO, 2017). Wheat is consumed in a wide variety of products with different textural attributes, from cakes to pasta. These differences in textural attributes are given by the differences in gluten content and gluten composition in flours from different types of wheat (Finnie and Atwell, 2016). Gluten proteins have been classified by their solubility into gliadins, which are soluble diluted alcohol solutions, and glutenins, which are soluble in under acidic conditions (Osborne, 1907). Describing the properties of gluten as one large matrix of proteins presents the challenge of not being able to discriminate between the contributions of individual gluten subunits. Many studies have also been done using the extracts of the two largest group of gluten proteins, gliadins and glutenin. Gliadins have been found responsible for the viscosity of viscoelastic gluten, while glutenins are more responsible for the elastic component of gluten (Delcour and Hoseney, 2010). High molecular weight (HMW) glutenins have been particularly related to the elastic component of gluten, since it forms intra- and inter- molecular disulfide bonds, compared to low molecular weight (LMW) glutenins which only form inter- molecular disulfide bonds. HMW glutenins have been found to be strongly related with bread quality aspects like loaf volume and dough strengths. (Gupta et al., 1991; Nieto-Taladriz et al., 1994). Gluten and its subunits, glutenins and gliadins have characterized by rheological experiments in the linear (SAOS) and non-linear (LAOS) regions in order to gain information about the molecular organization of their structure in wheat dough (Khatkar et al., 2002, 1995; Yazar et al., 2017). The information obtained from the isolated gluten factions has helped researchers understand better how gluten behaves in a dough matrix. However, the material studied is not the gluten in the dough, but the isolated gluten proteins, which have gone through irreversible conformational changes in their structure due the use of solvents during extraction.

1.2   Recent advances in gluten microscopy and imaging techniques

In the last two decades, colorful images of gluten networks obtained by elegant microscopy techniques, especially confocal laser scanning microscopy (CLSM), have been decorating cereal science papers. These images have been used for qualitative descriptions of the gluten network studied under different conditions. Nowadays, new a more sophisticated staining, microscopy, and image processing methods have become available. One specific gluten subunit, gliadin, has been individually imaged and studied under confocal laser scanning microscopy with the use specific gliadins antibodies and inorganic quantum dots (QDs) in wheat dough (Ansari et al., 2015; Bozkurt, 2013). These previous studies proved that QDs are suitable dyes for specific protein subunits staining in wheat doughs. Among the characteristics of QDs, we find that they have a broad excitation spectrum and a very narrow emission spectrum. They also present low photobleaching, which gives them long-term stability. Due the optical characteristics of QDs, coupling them with CLSM brings the opportunity of simultaneous multispectral imaging, since the CLSM can detect and split different emission wavelengths coming from the sample. The advances in molecular biology techniques and proteomics present also the opportunity of developing specific antibodies that can also be conjugated to QDs for imaging and tracking of other proteins. Moreover, the use image processing techniques, like 'co-localization studies', extensively used in other fields like biology can be used to move from qualitative descriptions of gluten networks to qualitatively measures of the internal structure of gluten subunits in dough images.

1.3   Objective

The overall objective of this research project is to develop and adapt new and existing staining, microscopy, and image processing techniques in order to gain new insights about the role of each gluten subunit, LMW glutenins, HMW glutenins, and gliadins in wheat dough mixing and rheology. In order to approach this objective, five different studies were conducted and are presented in this dissertation. These studies show from the development of individual antibodies for glutenins and their conjugation with QDs to explanations of the role of LMW glutenins, HMW glutenins, and gliadins in different wheat doughs under different mixing rheological tests.

1.4   Hypothesis

Our hypothesis is that we can gain new information about the structural functionality of HMW glutenins, LMW glutenins, and gliadins, in semolina, soft wheat, and hard wheat doughs using antibodies-quantum dots complexes and quantitative data from the protein network analysis and co-localization coefficients.

1.5   References

Ansari, S., Bozkurt, F., Yazar, G., Ryan, V., Bhunia, A., Kokini, J., 2015. Probing the distribution of gliadin proteins in dough and baked bread using conjugated quantum dots as a labeling tool. J. Cereal Sci. 63, 41–48. https://doi.org/10.1016/j.jcs.2014.12.001

Bozkurt, F., 2013. In situ observation of the distribution and location of gliadin as a function of mixing time in wheat flour dough using quantum dots. University of Illinois at Urbana-Champaign, Urbana, Illinois.

Delcour, J.A., Hoseney, R.C., 2010. Principles of cereal science and technology authors provide insight into the current state of cereal processing. Cereal Foods World 55(1), 21-22. Cereal Foods World 55, 21–22.

FAO, 2017. FAO Cereal Supply and Demand Brief | FAO | Food and Agriculture Organization of the United Nations [WWW Document]. URL http://www.fao.org/worldfoodsituation/csdb/en/ (accessed 4.8.17).

Finnie, S.M., Atwell, W.A., 2016. Wheat Flour. Elsevier. https://doi.org/10.1016/C2015-0-06189-5

Gupta, R.B., MacRitchie, F., Shepherd, K.W., Ellison, F., 1991. Relative Contributions of LMW and HMW Glutenin Subunits to Dough Strengh and Dough Stickness of Bread Wheat, in: Gluten Proteins 1990. American Association of Cereal Chemists, St. Paul, Minnesota USA.

Khatkar, B.S., Bell, A.E., Schofield, J.D., 1995. The dynamic rheological properties of glutens and gluten sub-fractions from wheats of good and poor bread making quality. J. Cereal Sci. 22, 29–44. https://doi.org/10.1016/S0733-5210(05)80005-0

Khatkar, B.S., Fido, R.J., Tatham, A.S., Schofield, J.D., 2002. Functional Properties of Wheat Gliadins. II. Effects on Dynamic Rheological Properties of Wheat Gluten. J. Cereal Sci. 35, 307–313. https://doi.org/10.1006/jcrs.2001.0430

Nieto-Taladriz, M.T., Perretant, M.R., Rousset, M., 1994. Effect of gliadins and HMW and LMW subunits of glutenin on dough properties in the F6 recombinant inbred lines from a bread wheat cross. Theor. Appl. Genet. 88, 81–88. https://doi.org/10.1007/BF00222398

Osborne, T., 1907. The proteins of the wheat kernel. Carnegie Institution of Washington - Press of Judd and Detweiler, Washington D.C.

Yazar, G., Duvarci, O., Tavman, S., Kokini, J.L., 2017. Non-linear rheological behavior of gluten-free flour doughs and correlations of LAOS parameters with gluten-free bread properties. J. Cereal Sci. 74, 28–36. https://doi.org/10.1016/j.jcs.2017.01.008

CHAPTER 2. CONJUGATION OF SPECIFICALLY DEVELOPED ANTIBODIES FOR HIGH- AND LOW-MOLECULAR-WEIGHT GLUTENINS WITH FLUORESCENT QUANTUM DOTS AS A TOOL FOR THEIR DETECTION IN WHEAT FLOUR DOUGH

2.1   Abstract

The importance of gluten proteins, gliadins and glutenins, is well-known in the quality of wheat products. To gain more specific information about the role of glutenins in wheat dough, the two major subunits of glutenin, high- and low-molecular-weight (HMW and LMW) glutenins, were extracted, isolated, and identified by mass spectrometry. Antibodies for HMW and LMW glutenins were developed using the proteomic information on the characterized glutenin subunits. The antibodies were found to be specific to each subunit by western immunoblots and were then conjugated to quantum dots (QDs) using site-click conjugation, a new method to keep antibody integrity. A fluorescence-link immunosorbent assay tested the successful QD conjugation. The QD-conjugated antibodies were applied to dough samples, where they recognized glutenin subunits and were visualized using a confocal laser scanning microscope.

2.2   Introduction

Wheat flour doughs have unique viscoelastic properties not seen in any other material. The machinability, moldability, and surface properties of the dough strongly depend upon the unique gluten structure and its rheology (Janssen et al., 1991). It is now well-accepted that gluten proteins (gliadins and glutenins) and their subunits are closely related to dough quality and baking performance (He and Hoseney, 1991; Huang and Kokini, 1993; Kokini et al., 1994; Micard and Guilbert, 2000; Shewry and Tatham, 1990). The wheat proteins in dough form a three-dimensional gluten network, where starch is suspended and held together. The strength of this gluten complex

is dependent upon the rheological properties and extensibility, in particular, of its subfractions, glutenin and gliadin (Hoseney, 1994). Studies performed on extracted gliadins and glutenins have shown how gliadins are more liquid-like viscoelastic, while glutenins are more solid-like viscoelastic and provide much of the elasticity to gluten (Delcour and Hoseney, 2010). A great deal has been learned over the last several decades about the behavior of gluten, gliadins, and glutenins in terms of affecting the quality and rheology of the dough, but not enough is known about the contribution of high- and low-molecular-weight (HMW and LMW) glutenins individually. The LMW glutenin subunits have molecular weights ranging from 30 to 60 kDa, and HMW glutenin subunits have molecular weights ranging from 65 to over 90 kDa (Delcour and Hoseney, 2010).

Gliadins and LMW glutenins aggregate together when extracted with aqueous alcohol solutions (Tatham et al., 1987). The LMW glutenin and gliadin amino acid sequences are closely related because of the allelic variation at the Glu-3 and Gli-1 loci, which encode LMW glutenins and gliadins, respectively. The Glu-3 and Gli-1 loci are genetically linked, and they are believed to come from the same ancestral group of genes (Singh and Shepherd, 1988). Because LMW glutenins and gliadins are genetically linked, they have been studied together and have shown a positive contribution on loaf volume in the bread-making process (Clarke et al., 2003). They have also been studied together when trying to select wheat varieties with optimum bread-making properties (Bonafede et al., 2015). However, in more detailed studies of how the Glu-3 and Gli-1 loci affect the dough strength, it was demonstrated that the gliadins (encoded by the Gli-1 locus) did not account for the positive effect on dough strength associated with the Glu-3/Gli-1 loci, leading to attribution of these positive effects to the Glu-3 locus, related to LMW glutenins (Gupta and MacRitchie, 1994).

On the other hand, the HMW glutenins, encoded by the genetically distant Glu-1 locus, have been demonstrated to have a major impact on dough strength when compared to LMW glutenins (Gupta et al., 1991; Nieto-Taladriz et al., 1994). HMW glutenins have been found to be the principal subunit responsible for dough elasticity related to dough strength (Tatham et al., 1985). In a now classical and elegant study, a Glu-1 quality score was developed, which increased with an increasing HMW content and was used to classify 84 British-grown wheat varieties (Payne et al.,

1987). They found a positive relationship between the Glu-1 quality score and bread-making quality, confirming the importance of HMW glutenins in the bread-making process.

The effect of gluten subunits on dough rheology and bread-making process has been studied using wheat varieties with different genetic compositions related to those specific gluten subunits, accurately attributing the role of genetic differences on dough properties and baking quality. In recent research, commercial anti-gliadin antibodies have been used for targeting and studying the distribution of gliadin in dough and bread samples by conjugating fluorescent quantum dots (QDs) to these antibodies (Ansari et al., 2015; Bozkurt et al., 2014). These studies show how gliadin behaves in situ in wheat flour dough during mixing and baking, giving detailed explanations of the role of gliadin during the mixing and baking. To obtain a more complete understanding of how gluten fractions behave and distribute in the dough, it is very important to study LMW and HMW glutenin subunits as well. To accomplish this goal, specific antibodies need to be manufactured because they are not commercially available; after the antibodies are manufactured, they can be conjugated to fluorescent QDs to visualize these two very important subunits of glutenin in wheat flour dough. The use of peptides from the amino acid sequences of glutenins has been used to develop antibodies to study the HMW and LMW glutenins and their differences on the N-terminal conformations before (Denery-Papini et al., 1996; Sissons et al., 1999), and also to test whether specific peptides of the HMW subunit are involved in intra- and intermolecular disulfide bonds (Mills et al., 2000).

In this research, our objective is to develop antibodies for LMW and HMW glutenins using proteomics tools with accurate characterization of the HMW and LMW glutenin subunits and then conjugate these antibodies with QDs for imaging of the glutenin subunits in dough samples. Detailed characterization of proteins is obtained using the extensive protein databases, including the National Center for Biotechnology Information (NCBI), UniProt, and ExPASy. Matrix-assisted laser desorption/ionization time-of-flight mass spectrometry (MALDI/TOF–MS) is used for protein identification, where the identified peptides are compared to sequences in the databases for successful protein identification (Clauser et al., 1999; Gasteiger et al., 2005; Perkins et al., 1999). We then conjugated the developed LMW and HMW antibodies to fluorescent QDs to develop a method that will allow us successful detection of LMW and HMW glutenins during

wheat dough mixing. This has never been done before and offers the ability to simultaneously detect HMW and LMW glutenin fractions during dough development using imaging tools, such as confocal laser scanning microscopy.

2.3 Materials and Methods

2.3.1 Protein extraction

Glutenin and gliadin extraction from gluten

Gluten was extracted from soft wheat flour obtained from Siemer Milling Company (Teutopolis, IL, U.S.A.) following the official American Association of Cereal Chemists (AACC) method 38-10. The moisture of the soft wheat flour was determined with a rapid moisture analyzer (Mettler Toledo, Columbus, OH, U.S.A.). The dough was then prepared following the official AACC method 38-20 using a Brabender Faringraph. Starch and water-soluble proteins (albumins) were washed and removed with distilled and deionized water (dd water), and salt-soluble proteins (globulins) were dissolved and removed by washing the dough with a 3% NaCl solution. The dough was washed until the dd water came out clear. The remaining sticky sample is wet gluten. The gluten was then washed 3 times in a beaker with 150 mL of 70% ethanol to dissolve alcohol-soluble gliadins. The sample was then centrifuged in a Sorvall legend X1R centrifuge (Thermo Fisher Scientific, Waltham, MA, U.S.A.) at 10 000 rpm for 10 min at 4 °C. The precipitate was lyophilized in a Freezone 4.5 freeze drier (Labconco Corporation, Kansas City, MO, U.S.A.) and was labeled as "crude glutenin". Ethanol (70%) also solubilizes a glutenin fraction. To reduce the presence of glutenins during our gliadin extraction, gliadin was extracted from a different wet gluten sample using 50% 1-propanol to solubilize gliadin and then increasing the 1-propanol concentration to 70%, which precipitated some alcohol-soluble glutenin proteins (Sapirstein and Fu, 2000).

Pure glutenin extraction

The pure glutenin extraction uses wheat flour instead of dough and gluten. Following the method of Tatham et al. (2000), a sample of 100 g of wheat flour was washed with 800 mL of chloroform twice to remove the lipid fraction and then washed with 800 mL of 70% ethanol followed by a second wash with 600 mL of 70% ethanol and 1% 2-mercaptoethanol to dissolve and remove gliadins. The supernatant was separated from the precipitate by centrifugation (5000g for 10 min at 20 °C).(27) Glutenins were then dissolved in a solution containing 500 mL of 50% 1-propanol, 2% 2-mercaptoethanol, and 1% acetic acid and collected by centrifugation (5000g for 10 min at 20 °C). A 1.5 M NaCl solution was then added to precipitate the glutenins, which were separated from the supernatant by centrifugation (10000g for 10 min at 4 °C). The precipitate was then washed with dd water and lyophilized.

Glutenins were separated into HMW and LMW subunits by solubilizing the lyophilized pellets of glutenin in 400 mL of 50% 2-propanol and 2% (w/v) dithiothreitol (DTT) in an 80 mM Tris–HCl (pH 8.0) solution. This separation step was followed by the addition of acetone to the solubilized glutenins at a concentration of 40%, which precipitated the HMW subunits. The acetone concentration was increased to 80% to precipitate the LMW subunits (Melas et al., 1994).

2.3.2   Protein identification

For protein analysis, sodium dodecyl sulfate–polyacrylamide gel electrophoresis (SDS–PAGE) was performed to identify the extracted proteins at 7.5 and 12% acrylamide for better separation of the HMW and LMW glutenin subunits, respectively. SDS–PAGE gel was stained with Coomassie Blue R250 (Hoefer, Inc., Holliston, MA, U.S.A.). Glutenin and HMW and LMW glutenin subunits were analyzed separately. Selected protein bands with the highest amount of protein were excised from the gel at the HMW and LMW levels and were analyzed using MALDI/TOF–MS at Applied Biomics (Hayward, CA, U.S.A.). To confirm the identity of the glutenin subunits in the gel bands, they were digested with trypsin, extracted from the gel bands, desalted, and placed on a MALDI plate and the mass spectra of the peptides were obtained. The most abundant peptides were fragmented and subjected to another round of mass spectra analysis. The data were compared to protein databases by comparing the time of flight of the peptides, and

the found peptides were used to identify the proteins in the submitted gel bands. The gliadin bands for SDS–PAGE were also characterized by mass spectrometry to prove that the antigenic peptides for the glutenin subunits are not present in gliadin.

2.3.3   Antibody development

To develop antibodies for the LMW and HMW glutenin subunits, peptide sequences that are present in each subunit but are not found in the other subunit or gliadin were selected. These peptides needed to be relatively short amino acid sequences (10–20 amino acid residues), so that they are repeatable within the amino acid sequence but long enough to have a strong interaction with the antibody (Janeway et al., 2001; Murphy, 2012). The BLAST and alignment tools of NCBI, UniProt, and ExPASy were used to select the desirable unique and repeatable peptides from the amino acid sequences of the proteins identified by mass spectrometry.

Identified amino acid sequences were sent to NovoPro Bioscience, Inc. (Shanghai, China), where they also independently verified the peptide sequences for antibody development. Peptides were synthesized through a standard Fmoc solid-phase peptide synthesis method, and keyhole limpet hemocyanin (KLH) protein was conjugated to the peptides as a carrier. A 63-day immunization protocol was followed with a primary immunization at 500 μg per rabbit and 5 boosters of 250 μg per rabbit at days 14, 28, 35, 45, 49, and 56. At day 63, the rabbits were terminated and the sera were collected. Antibodies were purified from the rabbit sera with antigen peptide-coupled beads and dissolved in phosphate-buffered saline (PBS, pH 7.4) with 0.02% sodium azide and 50% glycerol solution for long-term storage.

2.3.4   Protein separation and immunoblotting

Western blot assays were performed to determine the specificity of antibodies for glutenin and gliadin. A total of 250 ng/mL of crude glutenin and gliadin was solubilized and reduced using a solvent containing 8 mL of water, 4 mL of 1 M Tris base, 1.6 g of SDS, 8 mL of glycerol, and 14 μL of 2-mercapthoethanol and bringing the solution to a boil for 12 min. The proteins were then separated in SDS–PAGE (7.5 and 12% acrylamide) by adding 12 μL of the protein solution into the gel at 100 V for 1.5 h. Proteins were transferred to hydrophobic polyvinylidene difluoride

(PVDF) membranes using a transfer buffer containing 1400 mL of dd water, 400 mL of methanol, and 200 mL of 10× transfer buffer (60.5 g of Tris base and 288.4 g of glycine and volume adjusted to 2000 mL with pure water) at 100 V for 1.25 h. Milk proteins were used as blocking proteins by soaking the membranes in 5% skim milk. The membranes were then soaked with the solutions of the antibodies at 1 μg/mL to attach the antibodies to the target proteins. Alkaline phosphatase-conjugated anti-rabbit antibodies were applied at 0.5 μg/mL (Thermo Fisher Scientific, Waltham, MA, U.S.A.) to the membrane to conjugate them with the developed antibodies attached to the target proteins. Indicator color was developed by a western blue substrate for alkaline phosphatase (Promega, Madison, WI, U.S.A.) (Bhunia et al., 1991).

2.3.5   Conjugation of antibodies with QDs

Antibodies were conjugated with dibenzocyclooctyne (DIBO)-functionalized QDs using site-click chemistry, the antibodies and the method were obtained from Thermo Fisher Scientific (Waltham, MA, U.S.A.). In this site-click method, the integrity and effectiveness of the antibodies are maintained after the conjugation procedure (Bonilla et al., 2016; Zeglis et al., 2013). This is a brand new technique for QD conjugation to antibodies that has never been used before for detection of gluten proteins. The galactose residues located in the Fc region of the antibodies are removed by applying 10 μL of β-galactosidase to 50 μL of the developed antibodies at 2 μg/μL for 4 h at 37 °C. After galactose is removed, a different galactose molecule with an azide modification is attached to the Fc region of the antibody. This second reaction is catalyzed by the enzyme β-galactosyltransferase, followed by overnight incubation at 30 °C. The antibodies are then washed with Tris buffer at pH 7 and concentrated. Then, 50 μL of the DIBO-functionalized–QDs was added to the solution containing the antibodies and incubated overnight at 25 °C. The DIBO molecules are alkynes, and they bind to the azide-modified galactose at the Fc region of the antibodies through a copper-free azide–alkyne cycloaddition (Zeglis et al., 2013). QDs with emissions of 585 and 525 nm were conjugated to the anti-HMW antibodies and anti-LMW antibodies, respectively.

2.3.6 Fluorescence-link immunosorbent assay (FLISA)

A direct FLISA was performed to test the successful conjugation of the QDs to the antibodies. A total of 2 mg/mL of crude glutenin and gliadin was dissolved in a 70% aqueous ethanol solution with 0.2% DTT. The solubilized proteins were diluted to a concentration of 1 mg/mL with citrate buffer at pH 9.6. A total of 100 µL of the solution was placed into an opaque 96 well plate and left overnight at 4 °C for protein deposition. The plate was washed 3 times with PBST (0.05% Tween 20), followed by a blocking step with 1% bovine serum albumin (BSA) in PBS at room temperature for 1 h. A total of 100 µL of both QD-conjugated antibodies was applied to the glutenins and gliadins in the plate at a 1:250 dilution with a 1% BSA solution and incubated for 1.5 h at room temperature. The plate was excited with ultraviolet (UV) light at 300 nm, and the fluorescent emissions from the 585 nm QDs (conjugated to the HMW antibody) and the 525 nm QDs (conjugated to the LMW antibody) were recorded in arbitrary units (a.u.) using a Synergy H1 microplate reader (Biotek Instruments, Inc., Winooski, VT, U.S.A.).

2.3.7 Fluorescent imaging

Following previous procedures developed in our laboratory (Ansari et al., 2015; Bozkurt et al., 2014), dough samples were sliced to a 10 µm thickness and fixed onto microscope slides with 4% paraformaldehyde. The QD-conjugated antibody solution was applied to the slides after a dilution of 1:100 with PBS and then incubated at room temperature for 1 h. The samples were washed with PBS 3 times. The number of washing repetitions was determined after the PBS solution used for washing showed no QD-induced emission. The slices of dough were then analyzed with an A1R multiphoton confocal laser scanning microscope (Nikon Instruments, Inc., Melville, NY, U.S.A.).

2.4 Results and Discussion

2.4.1 Protein extraction and identification

After the crude glutenin and gliadin extraction step, 4 g of gliadin and 6 g of crude glutenin were obtained from 458.3 g of wheat dough, which represent a yield of 1.4 and 2.14% based on 279.95 g of initial flour. A total of 4.66 g of gliadin was extracted during the gliadin extraction with 1-propanol. From the pure glutenin extraction method, 380 mg of pure glutenin was obtained, in

which LMW glutenin subunits make up a higher fraction (320 mg) than HMW glutenin subunits (60 mg). This can be seen in SDS–PAGE, where the LMW subunit bands show much darker and thicker bands compared to the HMW glutenin subunits (Figure 1A). Separation of HMW from LMW glutenin subunit acetone precipitation leads to a small amount of cross-contamination between LMW and HMW glutenin subunits observed in SDS–PAGE. In the HMW region, three bands are clearly separated at 100, 80, and 70 kDa regions; however, it is clear that a small amount of LMW glutenin subunits is still present (Figure 1B). Figure 1C shows the LMW glutenin subunits mainly found in the regions around 40 and 30 kDa. It is also possible to observe a small amount of cross-contamination of HMW glutenin subunits in this figure as well. However, because we are only harvesting the bands pertaining to HMW glutenin subunits in Figure 1B and only the bands pertaining to LMW glutenin subunits from Figure 1C, this small cross-contamination did not affect our final outcomes.
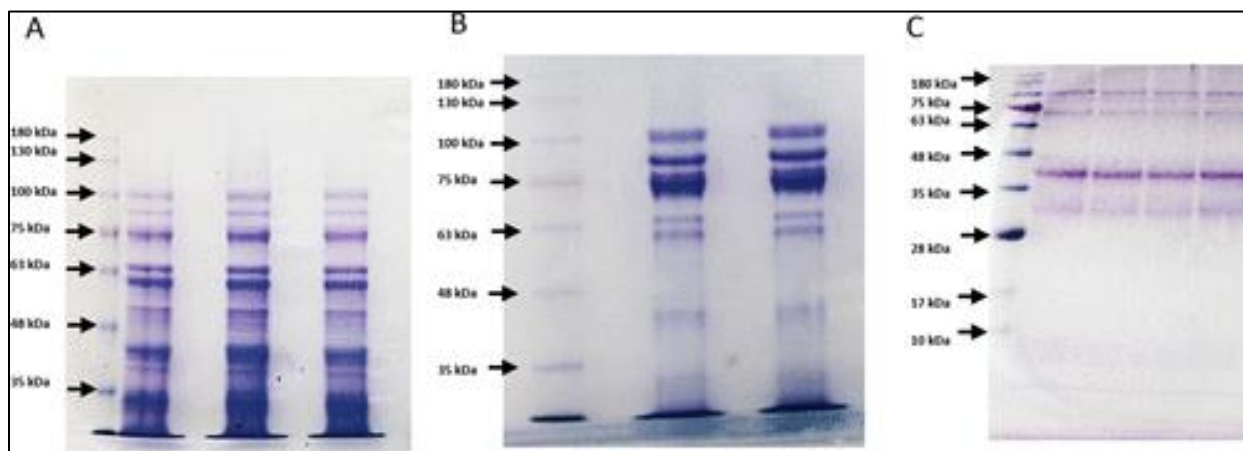
Figure 1. Coomassie Blue stained SDS–PAGE of (A) glutenin subunits in 7.5% acrylamide gel, (B) HMW glutenin subunits in 7.5% acrylamide gel, and (C) LMW glutenin subunits in 12% acrylamide gel.

2.4.2 Antibody development

Table1 shows the results of the mass spectrometry analysis performed on the HMW and LMW glutenin subunits identified by SDS–PAGE. The molecular masses of the harvested gel bands (100, 80, 70, 40, and 30 kDa) correlate with the molecular masses results identified by mass spectrometry. Protein score coefficient intervals (CIs) were reported between 98.68 and 100%, which indicates with high confidence that the peptides found in each gel band belong to each identified protein.

The protein identification match is shown in Table1. The information provided by the mass spectrometry analysis is used to validate the purity of the pure glutenin extraction procedure because no other proteins were found in the gel bands. The accession number in Table1 is the ID number referenced in the NCBI database for the proteins found in the gel bands, and the peptide count indicates the number of peptides found in each gel band used to match each protein subunit within the database. The specific peptides from the gel bands used to identify their proteins are described in Table1 (below each identified protein).

Table 1. Peptides from HMW and LMW glutenins SDS-PAGE bands used to identify the proteins by MALDI-TOF in the NCBI database.

MW on gel	Protein Name					Accession No.	Protein MW	Peptide Count	Protein Score C.I.%
100 kDa	high-molecular-weight glutenin 1Dx2.2 [Triticum aestivum]					gi|399933061	102.94 kDa	7	99.86
	Peptide Information								
	Calc. Mass (Da)	Obsrv. Mass (Da)	± Da	Start seq.	End seq.	Sequence			
	1044.532	1044.5002	-0.0318	34	41	ELQELQER			
	1157.7081	1157.6537	-0.0544	101	110	IFWGIPALLK			
	1313.8093	1313.7546	-0.0547	101	111	IFWGIPALLKR			
	1376.641	1376.5891	-0.0519	45	55	ACQQVMDQQLR			
	1457.7352	1457.6753	-0.0599	948	960	AQQLAAQLPAMCR			
	1990.9618	1990.8794	-0.0824	83	100	GGSFYPGETTPPQQLQQR			
	2972.5188	2972.4026	-0.1162	56	82	DISPECHPVVVSPVAGQYEQQIVVPPK			
80 kDa	high-molecular-weight glutenin subunit Bx17 [Triticum aestivum]					gi|109452233	80.02 kDa	6	98.68
	Peptide Information								
	Calc. Mass (Da)	Obsrv. Mass (Da)	± Da	Start seq.	End seq.	Sequence			
	1048.527	1048.4663	-0.0607	737	746	LEGSDALSTR			
	1302.6688	1302.5853	-0.0835	64	74	QYEQQPVVPSK			
	1457.7352	1457.6449	-0.0903	724	736	AQQLAAQLPAMCR			
	1698.8593	1698.7454	-0.1139	48	63	DVSPGCRPITVSPGTR			
	3166.603	3166.3684	-0.2346	75	102	AGSFYPSETTPSQQLQQMIFWGIPALLR			
	3806.7795	3806.5774	-0.2021	151	185	QQGYYPTSPQQPGQGQQLGQGQPGYYPTSQQPGQK			
70 kDa	high molecular weight glutenin subunit [Triticum aestivum]					gi|162415983	69.71 kDa	13	100
	Peptide Information								
	Calc. Mass (Da)	Obsrv. Mass (Da)	± Da	Start seq.	End seq.	Sequence			
	833.3934	833.362	-0.0314	28	33	QLQCER			
	864.3815	864.3566	-0.0249	65	70	CCQQLR			
	916.5211	916.4957	-0.0254	78	86	SVAVSQVAR			
	1113.6012	1113.5665	-0.0347	45	54	QVVDQQLAGR			
	1204.6144	1204.5693	-0.0451	55	64	LPWSTGLQMR			
	1321.6052	1321.5576	-0.0476	34	44	ELQESSLEACR			
	1469.7529	1469.698	-0.0549	625	637	AQQPATQLPTVCR			
	1992.9565	1992.916	-0.0405	55	70	PWSTGLQMRCCQQLR			
	2135.981	2135.8887	-0.0923	28	44	LQCERELQESSLEACR			
	2288.0691	2287.9685	-0.1006	136	157	QGSYYPGQASPQQPGQGQQPGK			
	2299.1975	2299.1052	-0.0923	45	64	QVVDQQLAGRLPWSTGLQMR			
	3117.4814	3117.363	-0.1184	158	184	QEPGQGQQWYYPTSLQQPGQGQQIGK			
	3453.6208	3453.4543	-0.1665	185	215	GQQGYYPTSLQQPGQGQQGYYPTSLQHTGQR			
40 kDa	low molecular weight glutenin subunit [Triticum aestivum]					gi|109240248	39.02 kDa	5	100
	Peptide Information								
	Calc. Mass (Da)	Obsrv. Mass (Da)	± Da	Start seq.	End seq.	Sequence			
	860.4988	860.4309	-0.0679	321	327	VNVPLYR			
	908.415	908.4288	0.0138	314	320	TLPMMCR			
	1788.0015	1787.8424	-0.1591	239	253	AIIYSIVLQEQQQVR			
	2076.0366	2075.8528	-0.1838	188	205	VFLQQQCSPVAMPQSLAR			
	3443.5493	3443.2043	-0.345	206	233	SQMLQQSSCHVMQQQCCQQLPQIPQQSR			
30 kDa	low molecular weight glutenin subunit, partial [Triticum aestivum]					gi|346229139	30.25 kDa	6	100
	Peptide Information								
	Calc. Mass (Da)	Obsrv. Mass (Da)	± Da	Start seq.	End seq.	Sequence			
	1132.6395	1132.6133	-0.0262	226	235	LEVMTSIALR			
	1267.6907	1267.6608	-0.0299	215	225	GTFLQPHQIAR			
	1361.7172	1361.6831	-0.0341	140	150	IPEQSRYEAIR			
	2110.0686	2110.01	-0.0586	100	117	QQQCSPVAMPQHLAR			
	2723.3743	2723.2925	-0.0818	236	261	TLPTMCSVNVPLYSSITSAPLGVGSR			
	2812.1841	2812.0933	-0.0908	118	139	SQMWQQSSCNVMQQQCCQQLPR			

The antigenic peptides selected for the anti-HMW antibody and anti-LMW antibody production were "QGQSGYYPTSPQ" and "PVLPQQPPFSQQ", respectively, because they contain glutamine (G), serine (S), threonine (T), and tyrosine (Y), which are hydrophilic (G, S, and T) and amphiphilic amino acids (Y). These peptides are partially soluble in water, which allows the antibodies to bind to the native glutenins in wheat because hydrophobic peptides can be surrounded and protected by the lipid fraction in wheat flour. Another important reason for the selection of these two antigens is that the peptide for the anti-HMW antibody was found in the three HMW protein gel bands and was not found in the LMW region and the peptide for the anti-LMW antibody was found in the two LMW protein gel bands and was not found in the HMW region. The results of the protein identification of the gliadin gel bands showed that these two peptides are not present in gliadin. A BLAST search on the online databases showed that these peptides are not found in any other proteins in wheat. Table 2 summarizes the peptides found in each specific protein band that are more than 80% similar to the antigen peptide, which are suitable for antibody detection (Janeway et al., 2001; Murphy, 2012). The peptide count indication in Table 2 indicates how many times each specific peptide is present in the amino acid sequence of that protein band. The identity compares how similar each peptide is to the antigen peptide for each subunit. In addition, total count indicates how many peptides are more than 80% similar to the antigen peptides present in that particular protein band. The frequency of the "QGQSGYYPTSPQ" peptide in the HMW glutenin amino acid sequence is shown in Figure 2A, while the frequency of the "PVLPQQPPFSQQ" peptide in the LMW glutenin amino acid sequence is shown in Figure 2B.

Table 2. Count of Target Antigenic Peptides in the Amino Acid Sequences of HMW and LMW Glutenins

Band MW	Antigen peptide	Maximum identity	Total count
100 kDa (HMW)	QGQSGYYPTSPQ	100%	22
	Found peptide	**Identity**	**Peptide count**
	QGQSGYYPTSPQ	100%	2
	QGQPGYYPTSPQ	91.70%	4
	QGQQGYYPTSPQ	91.70%	2
	QGQHGYYPTSPQ	91.70%	1
	QGQPGYYPTSPL	83.30%	3
	QGQPGYYPTSSQ	83.30%	3
	QGQPGYYPTSLQ	83.30%	1
	QGQPGYYLTSPQ	83.30%	1
	QGQQGYYPTSLQ	83.30%	3
	QGQPGYDPTSPQ	83.30%	1
	QGQPWYYPTSPQ	83.30%	1
85 kDa (HMW)	QGQSGYYPTSPQ	91.7%	15
	Found peptide	**Identity**	**Peptide count**
	QGQPGYYPTSPQ	91.70%	3
	QGQQGYYPTSPQ	91.70%	5
	QGQPGYYPTSQQ	91.70%	2
	QGQQGYYPISPQ	83.30%	2
	QGQSGYFPTSRQ	83.30%	1
	QGQQGYYPTSSQ	83.30%	1
	QGQQGYYPTSLQ	83.30%	1
70 kDa (HMW)	QGQSGYYPTSPQ	91.7%	7
	Found peptide	**Identity**	**Peptide count**
	QGQQGYYPTSPQ	91.70%	2
	QGQQGYYPTSVQ	83.30%	1
	QGQQGYYPTSLQ	83.30%	3
	QWQQGYYPTSPQ	83.30%	1
40 kDa (LMW)	PVLPQQPPFSQQ	100.0%	2
	Found peptide	**Identity**	**Peptide count**
	PVLPQQPPFSQQ	100.00%	1
	PVLPQQPSFSQQ	91.70%	1
30 kDa (LMW)	PVLPQQPPFSQQ	91.7%	2
	Found peptide	**Identity**	**Peptide count**
	PVLPQQPAFSQQ	91.70%	1
	TVLPQQPAFSQQ	83.30%	1

Figure 2. Alignment of the identified amino acid sequences from (A) HMW glutenins and (B) LMW glutenins with their possible antibody biding sites (target peptide similarity of >80%) highlighted in black.

2.4.3 Western blot analysis

The anti-HWM glutenin antibody reacted with glutenin proteins with two clear bands around 100 kDa and did not show any reaction with gliadin (Figure 3A). The anti-LMW glutenin antibody reacted with glutenins in two clear bands at 30 and 40 kDa and did not show any reaction with gliadin (Figure 3B). These results show that the antibodies detected the specific peptide that they were made for and bound to it. The results also show that these antibodies do not recognize gliadin or undesired regions of glutenin and that they were successfully developed. The use of this indirect method (western blot) requires the use of smaller concentrations of proteins, making the cross-contamination of LMW glutenin in the gliadin extracted powder non-detectable by the antibodies. The results of the immunoblotting test for the developed antibody results are consistent with antibodies developed for glutenin subunits previously (Denery-Papini et al., 1996; Mills et al., 2000; Sissons et al., 1999).

Figure 3. Western blot results showing reaction of (A) anti-HMW glutenin and (B) anti-LMW glutenin antibodies against gliadin and glutenin performed with secondary alkaline phosphatase anti-rabbit antibodies. Color reaction was performed using western blue substrate.

2.4.4 FLISA

Successful detection of the QD-conjugated antibodies was obtained when testing both QD–antibody complexes against glutenin (Figure 4). Negligible detection was obtained from the anti-HMW antibody with 585 nm QDs when tested against gliadin, as expected (Figure 4A). Some 525 nm QD emissions from the anti-LMW antibody were detected when tested against gliadin (Figure 4B). This is due to the LMW glutenin cross-contamination with gliadin during the extraction of gliadin. When we extract gliadin with aqueous alcohol solvents, a small amount of LMW glutenins is also extracted (Tatham et al., 1987). In contrast with the western blot result shown before, this experiment is a direct experiment, in which the signal is not enhanced by multiple secondary antibodies. Therefore, a higher concentration of extracted proteins is used, leading to the detection of some LMW fractions in the extracted gliadin powder. These results prove that our developed antibodies have been successfully cross-linked with the QDs.
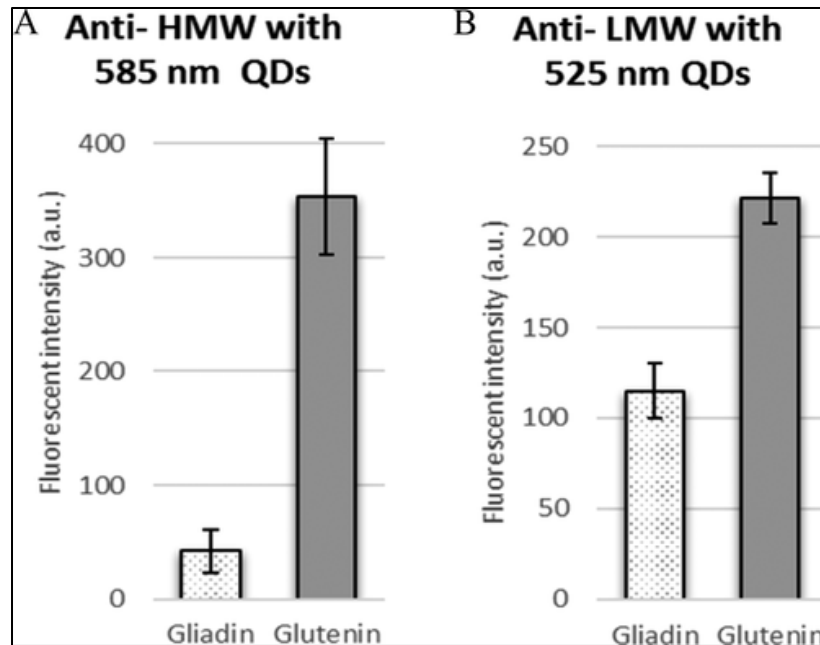
Figure 4. FLISA showing (A) detection of anti-HMW glutenin conjugated with 585 nm QDs in gliadin and glutenin and (B) detection of anti-LMW glutenin conjugated with 525 nm QDs in gliadin and glutenin.

2.4.5 Fluorescent imaging

QD emission was visualized from a dough sample when both antibodies were applied on the samples analyzed in a confocal laser scanning microscope. The emission comes from both antibodies, mostly at similar locations, where gluten is aggregated. We also detected just LMW glutenins and HMW glutenins by themselves in certain specific areas (Figure 5). These results show as a proof of concept that these developed antibodies can be conjugated with QDs for specific glutenin subunits imaging in the dough matrix. With the development of these antibodies, specific glutenin subunits are detected "in situ", and they can be applied to advance the current understanding of these glutenin subunit functions in dough.
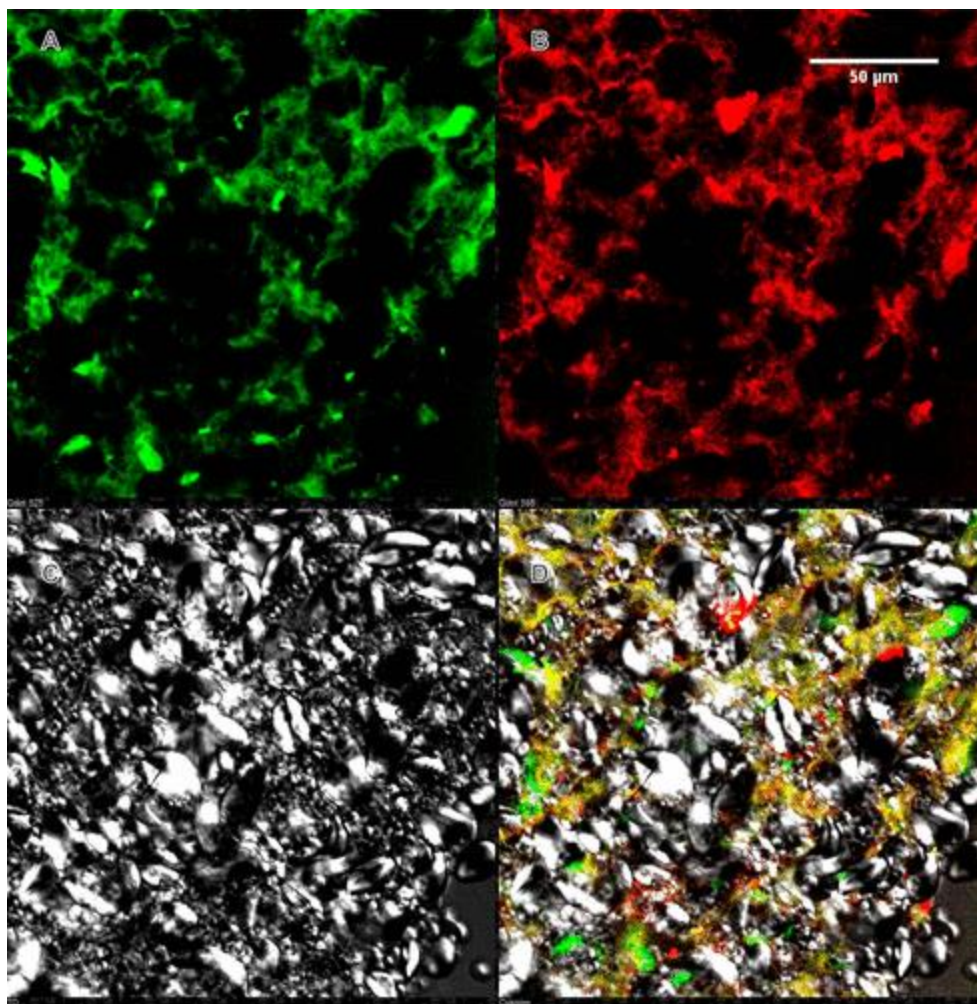
Figure 5. (A) Localization of LMW glutenins in wheat dough stained with the anti-LMW antibody conjugated with 525 nm QDs. (B) Localization of HMW glutenins in wheat dough stained with the anti-HMW antibody conjugated with 585 nm QDs. (C) Starch matrix detection

This technique of antibody-conjugated QDs to detect proteins may be suitable for performing several studies on wheat flours. The distribution of glutenins can be compared between different types of wheat flour doughs with different bread-making quality; also, the behavior of glutenins during different dough processes, such as mixing dough sheeting and others, can be studied. On the basis of previously published work (Ansari et al., 2015), the antibodies would also be applicable to study glutenin and gliadin distribution in baked bread and to study their mobility during baking.

2.5   References

Ansari, S., Bozkurt, F., Yazar, G., Ryan, V., Bhunia, A., Kokini, J., 2015. Probing the distribution of gliadin proteins in dough and baked bread using conjugated quantum dots as a labeling tool. J. Cereal Sci. 63, 41–48. https://doi.org/10.1016/j.jcs.2014.12.001

Bhunia, A.K., Ball, P.H., Fuad, A.T., Kurz, B.W., Emerson, J.W., Johnson, M.G., 1991. Development and characterization of a monoclonal antibody specific for Listeria monocytogenes and Listeria innocua. Infect. Immun. 59, 3176–3184.

Bonafede, M.D., Tranquilli, G., Pflüger, L.A., Peña, R.J., Dubcovsky, J., 2015. Effect of allelic variation at the Glu-3/Gli-1 loci on breadmaking quality parameters in hexaploid wheat (Triticum aestivum L.). J. Cereal Sci. 62, 143–150. https://doi.org/10.1016/j.jcs.2015.02.001

Bonilla, J.C., Bozkurt, F., Ansari, S., Sozer, N., Kokini, J.L., 2016. Applications of quantum dots in Food Science and biology. Trends Food Sci. Technol. 53, 75–89. https://doi.org/10.1016/j.tifs.2016.04.006

Bozkurt, F., Ansari, S., Yau, P., Yazar, G., Ryan, V., Kokini, J., 2014. Distribution and location of ethanol soluble proteins (Osborne gliadin) as a function of mixing time in strong wheat flour dough using quantum dots as a labeling tool with confocal laser scanning microscopy. Food Res. Int. 66, 279–288. https://doi.org/10.1016/j.foodres.2014.09.028

Clarke, B.C., Phongkham, T., Gianibelli, M., Beasley, H., Bekes, F., 2003. The characterisation and mapping of a family of LMW-gliadin genes: effects on dough properties and bread volume. Theor. Appl. Genet. 106, 629–635. https://doi.org/10.1007/s00122-002-1091-1

Clauser, K., Baker, P., Burlingame, A., 1999. Role of Accurate Mass Measurement (±10 ppm) in Protein Identification Strategies Employing MS or MS/MS and Database Searching. Anal. Chem. 71, 2871–2882. https://doi.org/10.1021/ac9810516

Delcour, J.A., Hoseney, R.C., 2010. Proteins of Cereals, in: Principles of Cereal Science and Technology. American Association of Cereal Chemists, St. Paul, Minnesota USA.

Denery-Papini, S., Popineau, Y., Quillien, L., Van Regenmortel, M.H.V., 1996. Specificity of antisera raised against synthetic peptide fragments of highMrglutenin subunits. J. Cereal Sci. 23, 133–144. https://doi.org/10.1006/jcrs.1996.0013

Gasteiger, E., Hoogland, C., Gattiker, A., Duvaud, S., Wilkins, M., Appel, R., Bairoch, A., 2005. Protein Identification and Analysis Tools on the ExPASy Server, in: Walker, J. (Ed.), The Proteomics Protocols Handbook. Humana Press, pp. 571–607. https://doi.org/10.1385/1-59259-890-0:571

Gupta, R.B., MacRitchie, F., 1994. Allelic Variation at Glutenin Subunit and Gliadin Loci, Glu-1, Glu-3 and Gli-1 of Common Wheats. II. Biochemical Basis of the Allelic Effects on Dough Properties. J. Cereal Sci. 19, 19–29. https://doi.org/10.1006/jcrs.1994.1004

Gupta, R.B., MacRitchie, F., Shepherd, K.W., Ellison, F., 1991. Relative Contributions of LMW and HMW Glutenin Subunits to Dough Strengh and Dough Stickness of Bread Wheat, in: Gluten Proteins 1990. American Association of Cereal Chemists, St. Paul, Minnesota USA.

He, H., Hoseney, R.C., 1991. Gluten, a Theory of How it Controls Breadmaking, in: Gluten Proteins 1990. American Association of Cereal Chemists, St. Paul, Minnesota USA, pp. 1–10.

Hoseney, R.C., 1994. Proteins of Cereals, in: Principles of Cereal Science and Technology. American Association of Cereal Chemists, St. Paul, Minnesota USA.

Huang, H., Kokini, J.L., 1993. Measurement of biaxial extensional viscosity of wheat flour doughs. J. Rheol. 37, 879–891. https://doi.org/10.1122/1.550400

Janeway, C., Travers, P., Walport, M., Shlomchik, M., 2001. Immunobiology: The immune System in Health and Disease, 5th ed. Garland Science, New York.

Janssen, A., Vereijken, J., Beintema, J., Witholt, B., 1991. Rheological Studies on Gluten, in: Gluten Proteins 1990. American Association of Cereal Chemists, St. Paul, Minnesota USA.

Kokini, J.L., Cocero, A.M., Madeka, H., de Graaf, E., 1994. The development of state diagrams for cereal proteins. Trends Food Sci. Technol. 5, 281–288. https://doi.org/10.1016/0924-2244(94)90136-8

Melas, V., Morel, M.H., Autran, J.C., Feillet, P., 1994. Simple and Rapid Method for Purifying Low Molecular Weight subunits of glutenin from wheat. Cereal Chem. J. 3, 234–237.

Micard, V., Guilbert, S., 2000. Thermal Behavior of Native and Hydrophobized Wheat Gluten, Gliadin and Glutenin-Rich Fractions by Modulated DSC. Int. J. Biol. Macromol. 27, 229–236.

Mills, E.N.C., Field, J.M., Kauffman, J.A., Tatham, A.S., Shewry, P.R., Morgan, M.R.A., 2000. Characterization of a Monoclonal Antibody Specific for HMW Subunits of Glutenin and Its Use To Investigate Glutenin Polymers. J. Agric. Food Chem. 48, 611–617. https://doi.org/10.1021/jf9909499

Murphy, K., 2012. Janeway's Immunobiology, 8th ed. Garland Science, Taylor and Francis group, LLC., London and New York.

Nieto-Taladriz, M.T., Perretant, M.R., Rousset, M., 1994. Effect of gliadins and HMW and LMW subunits of glutenin on dough properties in the F6 recombinant inbred lines from a bread wheat cross. Theor. Appl. Genet. 88, 81–88. https://doi.org/10.1007/BF00222398

Payne, P.I., Nightingale, M.A., Krattiger, A.F., Holt, L.M., 1987. The relationship between HMW glutenin subunit composition and the bread-making quality of British-grown wheat varieties. J. Sci. Food Agric. 40, 51–65. https://doi.org/10.1002/jsfa.2740400108

Perkins, D., Pappin, D., Creasy, D., Cottrell, J., 1999. Probability-based protein identification by searching sequence databases unsing mass spectrometry data. Electrophoresis 20, 3551–3567.

Sapirstein, H.D., Fu, B.X., 2000. Evidence for variying interaction of gliadin and glutenin proteins as an explanation for differences in dough strength of different wheats. Wheat Gluten 425–428.

Shewry, P.R., Tatham, A.S., 1990. The prolamin storage proteins of cereal seeds: structure and evolution. Biochem. J. 267, 1–12.

Singh, N.K., Shepherd, K.W., 1988. Linkage mapping of genes controlling endosperm storage proteins in wheat. Theor. Appl. Genet. 75, 628–641. https://doi.org/10.1007/BF00289132

Sissons, M.J., Blundell, M.J., Hill, A.S., Skerritt, J.H., 1999. Antibodies to N-terminal Peptides of Low MrSubunits of Wheat Glutenin. I. Characterisation of the Antibody Response. J. Cereal Sci. 30, 267–281. https://doi.org/10.1006/jcrs.1999.0275

Tatham, A., Gilbert, S., Fido, R., Shewry, P., 2000. Extraction, Separation, and Purification of Wheat Gluten Proteins and Related Proteins of Barley, Rye, and Oats, in: Marsh, M., FRCP, M.N.M.M., DSc (Eds.), Celiac Disease, Methods in Molecular Medicine. Humana Press, pp. 55–73. https://doi.org/10.1385/1-59259-082-9:055

Tatham, A.S., Field, J.M., Smith, S.J., Shewry, P.R., 1987. The conformations of wheat gluten proteins, II, aggregated gliadins and low molecular weight subunits of glutenin. J. Cereal Sci. 5, 203–214. https://doi.org/10.1016/S0733-5210(87)80023-1

Tatham, A.S., Miflin, B.J., Shewry, P.R., 1985. The Beta-Turn Conformation in Wheat Gluten Proteins: Relationship to Gluten Elasticity. Cereal Chem. 62, 405–412.

Zeglis, B.M., Davis, C.B., Aggeler, R., Kang, H.C., Chen, A., Agnew, B.J., Lewis, J.S., 2013. Enzyme-Mediated Methodology for the Site-Specific Radiolabeling of Antibodies Based on Catalyst-Free Click Chemistry. Bioconjug. Chem. 24, 1057–1067. https://doi.org/10.1021/bc400122c

CHAPTER 3.   SIMULTANEOUS IMMUNOFLUORESCENT IMAGING OF GLIADINS, LOW MOLECULAR WEIGHT GLUTENINS, AND HIGH MOLECULAR WEIGHT GLUTENINS IN WHEAT FLOUR DOUGH WITH ANTIBODY-QUANTUM DOT COMPLEXES

3.1   Abstract

Gluten proteins and their impact in the quality of wheat-based food products is well known. In order visualize the 'in situ' distribution of low molecular weight glutenins, high molecular weight glutenins, and gliadins simultaneously in wheat doughs we needed to overcome and eliminate dough auto-fluorescence, and to develop a reliable immunostaining procedure for their simultaneous detection in wheat doughs. We are studying different auto-fluorescence quenchers used in biological fluorescent imaging and their effect on dough auto-fluorescence removal, and the effect of different fixative mediums on the adhesion of wheat flours doughs onto microscope slides. We found that the best method to remove dough auto-fluorescence is removing it as background in the microscope detection system. We also found methanol to be the best fixative medium for dough samples. In this research, we are showing the first 'in situ' localization of these gluten subunits simultaneously in wheat flour dough.

3.2   Introduction

Gluten is described as a viscoelastic protein network that develops during dough mixing. In this network, gliadin proteins are known to contribute to its flowability, while glutenins add stiffness/elasticity to the network (Delcour & Hoseney, 2010). The gluten network is responsible for the ability of wheat doughs to retain gases and create the amazing foam-like texture in cereal products that are part of the daily diet. Based on their functionality, glutenins can be divided into High Molecular Weight glutenins (HMW) and Low Molecular Weight glutenins (LMW) (Delcour & Hoseney, 2010). Gluten protein content, gliadin to glutenin ratio, and LMW glutenin to HMW

glutenin ratio have been shown to be key factors influencing dough strength, dough mixing profiles, and final product characteristics (Clarke, Phongkham, Gianibelli, Beasley, & Bekes, 2003; Gupta & MacRitchie, 1994; Nieto-Taladriz, Perretant, & Rousset, 1994; Payne, Nightingale, Krattiger, & Holt, 1987; Singh & Shepherd, 1988; Tatham, Miflin, & Shewry, 1985; Uthayakumaran, Gras, Stoddard, & Bekes, 1999).

In recent research, the 'in situ' distribution of gliadin at different mixing times in a Brabender farinograph has been studied by immunofluorescence using gliadin antibodies coupled with nano-fluorescent quantum dots (QDs) (Bozkurt et al., 2014). A similar immunofluorescence method was used to study the distribution of gliadins in baked bread (Ansari et al., 2015). The breakthrough findings from these studies show the distribution of gliadin proteins influenced by their mobility and flowability inside the dough matrix during the dough mixing and baking processes. Specific antibodies for high molecular weight and low molecular weight glutenins were developed and conjugated to nano-fluorescent QDs (Bonilla, Ryan, Yazar, Kokini, & Bhunia, 2018). The use of these antibodies enables the study and visualization 'in situ' of the distribution of HMW glutenins and LMW glutenins simultaneously with gliadins during different dough processes for the first time.

Fluorescent imaging is a useful method to study food matrices from cereal grains (Ansari et al., 2015; Bonilla et al., 2018; Bozkurt et al., 2014; Bugusu, Hamaker, & Rajwa, 2002; Li, Dobraszczyk, & Wilde, 2004; Zweifel, Handschin, Escher, & Conde-Petit, 2003). These matrices consist of a hydrated starch matrix, which is distributed, in a protein and lipid network, and the behavior of this network is very important in the final quality of food products. When studying starch, proteins, and lipids by fluorescent imaging there are considerable challenges to overcome and ensure that false positives and false negatives do not cloud the findings related to them. Factors including sample collection, fixation medium, tissue auto-fluorescence, staining procedure, and microscope set up can affect the quality of the data collected (Pawley, 2006). Dough auto-fluorescence is generated by the aromatic amino acids tryptophan, tyrosine, and phenylalanine in the amino acid sequences of gluten sub-fractions (Roth & Hampaǐ, 1973; Sozer & Kokini, 2014; Timperman, Oldenburg, & Sweedler, 1995) and has been used to study the interaction of gluten proteins with zein in model cereal products for celiacs in previous studies with the goal of replacing

gliadin with zein (Bugusu et al., 2002). Auto-fluorescence can be used to study organisms as an effective non-labeling detection tool however; there are other situations where auto-fluorescence leads to significant challenges when studying organisms due to low signals when using labeling methods with low expression or low specificity. During simultaneous multi-fluorescent detection of cereal components, it is critical to discriminate between the emissions generated by the different fluorescent dyes. For example, auto-fluorescence results in false positive emission that confuses fluorescent signals from specific fluorescent dye emissions (Sozer & Kokini, 2014).

The fixation medium also plays a key role in the immunostaining procedure and fluorescent detection. Dough and bread samples from wheat gluten and zein-enriched sorghum have been fixed to microscope slides with 4% paraformaldehyde (a crosslinking agent) and then hydrated with ethanol (Bugusu et al., 2002). Bozkurt (2013) fixed wheat dough samples to microscope slides with acetone or 4% paraformaldehyde when measuring immunofluorescence in dough samples. He reported that 4% paraformaldehyde enhances the fixation process of the dough to the slide and causes less artifacts on the component's morphology, while acetone is a better medium for immunostaining and imaging. Sozer and Kokini (2014) used 10% formalin to fix flat bread samples to microscope slides. Chemical fixatives can be divided into coagulating fixatives or crosslinking fixatives (Pawley, 2006). The coagulating fixatives, such as ethanol, methanol or acetone, fix the specimen by rapidly dissolving some of the soluble components in the specimen and gluing the specimen to the slide as the solvent evaporates. Proteins either coagulate or are partially extracted during the solvation process; this is followed by drying of the solvent that fixes the sample on the slide. Coagulating fixatives tend to preserve the antigen recognition sites for immunolabeling very well (Bacallao, Sohrab, & Phillips, 2006). On the other hand, crosslinking fixatives which include formalin or paraformaldehyde, create covalent crosslinks by forming methylene bridges between reactive amino groups, and they bind the specimen more strongly to the slide; however, this chemical crosslinking reaction induces changes in the sample, and the recognition sites may be somewhat altered (Hayat, 2000).

In this study, we are aiming to stain HMW glutenins, LMW glutenins, and gliadins simultaneously with three different antibody-QD complexes for the first time in wheat flour dough samples using the HMW and LMW glutenins antibody-QD complexes developed by Bonilla et al. (2018) along

with a third anti-gliadin-QD complex. This will help us achieve a better understanding of the function of these gluten protein sub-fractions in the dough matrix. To accomplish this, we have to overcome and differentiate dough auto-fluorescence from the specific gluten sub-fractions' detection. To that end, we evaluated different auto-fluorescence quenchers. Fluorescence quenching is the process of decreasing the fluorescence intensity of any given substance (Jameson, 2014). We also compared the effect of different microscope slide fixatives on the immunostaining procedures and on the morphology of dough tissues, which help us determine a reliable methodology for simultaneous detection of different protein sub-fraction in cereal based food matrices. We focused on simultaneous visualization of the distribution of gliadins, LMW, and HMW glutenins with their proper controls using antibody-QD conjugates.

3.3   Materials and Methods

3.3.1   Antibodies conjugation with quantum dots

Anti-gliadin 4F3 antibodies (Thermo Fisher Scientific, Waltham, MA, U.S.A.) were conjugated with dibenzocyclooctyne (DIBO)-functionalized 655 nm QDs (Thermo Fisher Scientific, Waltham, MA, U.S.A.) following previous published procedure used to conjugate QDs to anti-HMW glutenins and anti-LMW glutenins antibodies (Bonilla et al., 2018). This is a site-click method in which the integrity and effectiveness of the antibodies are preserved after the conjugation procedure (Bonilla, Bozkurt, Ansari, Sozer, & Kokini, 2016; Zeglis et al., 2013). The preservation is achieved because galactose sugars located in the tail of the antibodies are removed with β-galactosidase for 4 h at 37 °C and then a different galactose molecule with an azide modification is attached to the tail of the antibodies catalyzed by β-galactosyltransferase overnight at 30 °C. The antibodies are then washed with Tris buffer at pH 7 and concentrated. The solution of DIBO-functionalized 655 nm QDs was added to the solution containing the antibodies and kept overnight at 25 °C. The DIBO molecules attached to the QDs are alkynes, and through an azide−alkyne cycloaddition the QDs were conjugated to the azide-modified galactoses in the tails of the antibodies (Zeglis et al., 2013). The method reported previously to conjugate antibodies to quantum dots for detection of gluten protein and gliadins uses a reducing agent to crosslink the functionalized QDs to thiol groups on the antibodies (Ansari et al., 2015; Bozkurt et al., 2014). The use of the reducing agents may distort the antigen recognition sites in the antibodies since they

41

are constituted of several disulfide groups. The use of a method in which no reducing agent is used and the QDs are attached to the tail of the antibodies leaves the antigen recognition sides intact.

3.3.2   Fluorescent linked immunosorbent assay (FLISA)

The successful conjugation of QDs to the anti-gliadin antibodies and the specificity of the anti-gliadin 4F3 antibody were tested using a Fluorescent Linked Immunosorbent Assay (FLISA) (Bonilla et al., 2018). Glutenin and gliadin were deposited in an opaque 96-wells plate and were then blocked with 1% BSA. The 1% BSA solution blocks the areas not covered by glutenins or gliadins in the plate wells. The anti-gliadin-QDs solution was deposited in the wells where the proteins were fixed at a 1:250 dilution. The excess solution was washed away. The 96 well plate was excited with ultraviolet light at 300 nm, and the fluorescent emissions from the 655 nm QDs were recorded in arbitrary units (a.u.) using a Synergy H1 microplate reader (Biotek Instruments, Inc., Winooski, VT, U.S.A.)

3.3.3   Sectioning and fixation

Small pieces of dough, with a volume approximately of 0.5 cm3, made from a 2:1 mixture of wheat flour and water were placed into disposable plastic Tissue-Tek cryomolds. Optimum cutting temperature (O.C.T.) tissue freezing medium (Thermo Fisher Scientific, Waltham, MA, U.S.A.) was deposited around each sample to entirely cover the samples. O.C.T. is used to avoid dehydration of samples and also to give a suitable specimen medium for cryostat sectioning at $-10\,°C$. The samples were rapidly frozen at $-80\,°C$ and then sectioned using a LEICA CM 1860 Cryostat (Leica Biosystems, Wetzlar, Germany). The samples were longitudinally cut to a thickness of 10 µm. The sections were then placed onto special hydrophilic adhesive microscope slides and immersed in a staining dish containing reagent grade acetone, 4% paraformaldehyde/PBS, or methanol for ten minutes and air-dried overnight at room temperature. For troublesome samples, pipetting the fixatives onto the slides in a fume hood reduced the changes of wash offs.

3.3.4 Quenching of auto-fluorescence in the dough sample

Samples were treated with a 500 I.U./ml heparin solution (Thermo Fisher Scientific, Waltham, MA, U.S.A.), a 0.1% Sudan Black B (Thermo Fisher Scientific, Waltham, MA, U.S.A.) in 70% ethanol solution, or a well-known commercial auto-fluorescence quencher kit, trueVIEW™ (Vector® Laboratories, Burlingame, CA, U.S.A.). The control sample was not treated with any auto-fluorescence quencher for comparison and establishing the effectiveness of the auto-fluorescence quenchers. The dough samples were deposited into a beaker with the heparin solution for 10 min and then rinsed with water before sectioning as described by Bozkurt et al. (2014) and Zweifel et al. (2003). The 0.1% Sudan Black B solution was applied onto a slide containing a piece of 10 μm-sectioned dough and incubated for 30 min at room temperature (Baschong, Suetterlin, & Laeng, 2001; Neumann & Gabel, 2002; Romijn et al., 1999). The trueVIEW™ kit reagents A, B and C were mixed together following the instructions provided by Vector® Laboratories and applied over a piece of 10 μm-sectioned dough, allowed to incubate for 5 min and then was washed away with PBS. In the dough samples with no auto-fluorescence quencher, auto-florescence was reduced by reducing the laser power in the microscope and the gain (magnitude of amplification) in the photomultiplier detector to a point where no background emission (auto-fluorescence) was detected in a dough sample with no QDs treatment.

3.3.5 Staining of dough samples with antibodies conjugated QDs complexes

100 μL of each antibody-QD complex, anti-gliadin antibody conjugated with 655 nm QDs, anti-HMW glutenins antibody conjugated with 585 nm QDs, and anti-LMW glutenin antibody conjugated with 525 nm QDs were all mixed together in a 2 mL tube. A hydrophobic barrier around the samples on each slide was created by encircling each section using a special aqua-hold pap pen (Thermo Fisher Scientific, Waltham, MA, USA). An aliquot of 30 μL of the antibody-QD mixture was deposited on top of the samples for 30 min at room temperature to let the antibodies bind to their target gluten proteins sub-fraction in the wheat dough. The aqua-hold pen prevents the antibody-quantum dots mixture from spreading over the entire surface of the slide. Unbound antibody-QD were washed away from the samples with PBS buffer three times.

3.3.6 Non-specific binding control

A control with no protein content was used in order to prove that the antibody-QD complexes are binding to their specific proteins sub-fractions and they do not stay trapped with the matrix giving false positive detection. For that purpose, a no-protein starch matrix was used, which was prepared in a 2:1 ratio of starch and 3% carboxymehtylcellulose (CMC) in PBS solution. The 3% CMC was used since the hydrated starch by itself was not able to stay fixed onto the microscope slides after the staining and washing procedures. The cross-linking with CMC helped the starch matrix stay fixed to the slide during the staining and washing procedures.

3.3.7 Confocal laser scanning microscope analysis

A Nikon A1R MP confocal laser scanning microscope (Nikon Instruments, Tokyo, Japan) and a Zeiss LSM 880 confocal laser scanning microscope (Carl Zeiss Microscopy, Oberkochen, Germany) were used to visualize dough samples structure by measuring the fluorescent intensity of the antibody conjugated quantum dots. Starch granules suspended in the dough matrix were identified by Differential Interference Contrast (DIC) microscopy. The excitation wavelengths for the QDs were 405 nm and 488 nm. The peak emission filters were set up at 525 nm, 585 nm, and 655 nm. Dough samples were visualized using 20× objectives on both systems, Nikon Plan Apo VC 20×./0.75NA, Zeiss Plan Apo 20×/0.8NA. Digital image files were recorded with the NIS elements software (Nikon Instruments, Tokyo, Japan) and the Zen BLACK software (Carl Zeiss imaging, Oberkochen, Germany). The intensity profiles of the samples were recorded and compared.

3.4 Results and Discussion

3.4.1 Specificity of the gliadin antibody conjugated with 655 nm QDs using fluorescent linked immunosorbent assay (FLISA)

The conjugates of commercial anti-gliadin 4F3 antibodies with 655 nm QDs showed reaction with gliadin and did not show any reaction with glutenins in the FLISA (Figure 6), confirming the specificity of the commercial anti-gliadin antibodies and the successful conjugation of 655 nm QDs to the antibodies as well.
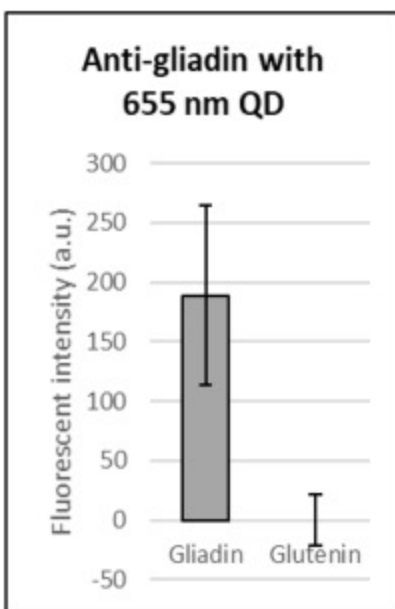
Figure 6. FLISA testing anti-gliadin-QDs 655 nm against gliadin and glutenin

3.4.2   Heparin treatment to reduce auto-fluorescence in wheat dough

Unfortunately, insignificant reduction of dough auto-fluorescence was observed after treatment with the heparin solution. Figure 7 shows four images of emission intensities at 1) 525 nm (green), 2) 585 nm (red), 3) 655 nm (purple), and 4) DIC from the Nikon confocal system. These are presented side by side for clarity. In Figure 7b we have substantial emission intensity in all three channels (525 nm, 585 nm, and 655 nm), caused by the presence of the antibody-QD complexes. Figure 7a shows the dough auto-fluorescence in an untreated dough sample. The emission in Figure 7a and c is caused by dough auto-fluorescence since no QDs or other staining dye is applied to the dough. They both show considerable emission at the 525 nm channel, because the emission for the aromatic amino acids is registered at small wavelengths (200–300 nm) (Held, 2003). The challenge with the fluorescent detection from the QDs in Figure 7b is how to differentiate the emission from dough auto-fluorescence from the emission caused by QDs.
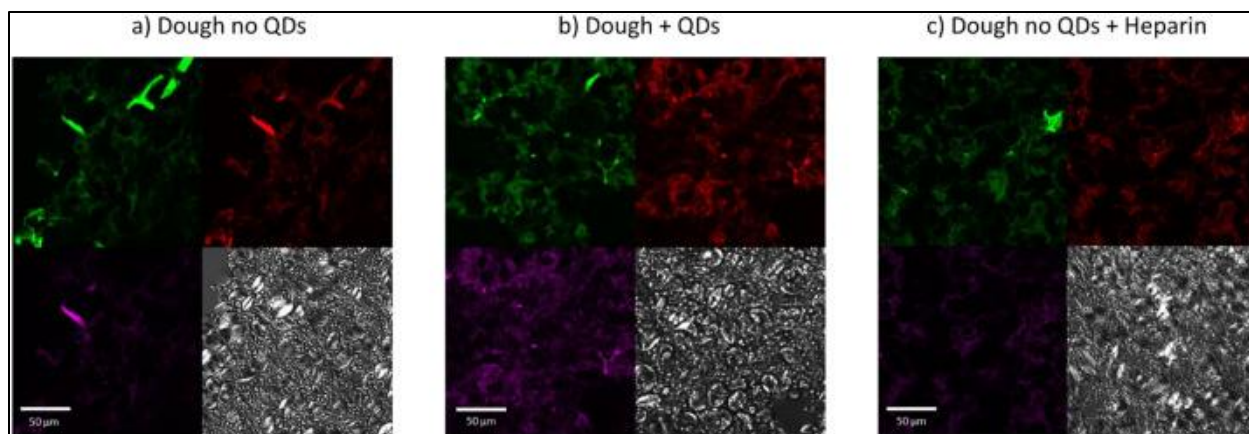
Figure 7. Fluorescent detection of dough in the 525 (green), 585 (red), 655 (purple), and DIC channels. (a) Dough stained with antibody-QD complexes. (b) Unstained dough. (c) Unstained dough treated with heparin solution. Bar: 50 µm

3.4.3 Auto-fluorescence quenching using Sudan black B treatment

Insignificant elimination of dough auto-fluorescence was observed with the Sudan Black B treatment either as shown in Figure 8. Similar emission intensities in the 525 nm (green) and 585 nm (red) channels for the untreated dough (Figure 8a) and the dough treated with Sudan Black B (Figure 8b) were observed. In the 655 nm channel (purple), a significant increase in the emission intensity in the Sudan Black B treated sample is observed. This emission would interfere with the emission from the anti-gliadin-QD 655 nm complex in an antibody-QD stained sample. The Sudan Black B has been reported to quench auto-fluorescence generated by proteins in other biological samples (Oliveira et al., 2010). Sun et al. (2011) reported that it was impossible to distinguish specific immunofluorescence emission from background auto-fluorescence in their 488 nm channel without the use of Sudan Black B. However, they also reported emission from Sudan Black B in far-red channels. Sudan Black B has been used as a lipid fraction dye by Haimovici, Gantz, Rumelt, Freddo, & Small, (2001) and Sabnis (2010) with emission in far-red channels. In the current study fluorescent detection in the 655 nm channel when Sudan Black B is applied can be attributed to the lipid fraction in dough samples, making Sudan Black B not a suitable auto-fluorescent quencher for the purpose of detecting gliadins, LMW glutenins, HMW glutenins simultaneously with three different antibody-QD complexes in dough samples.
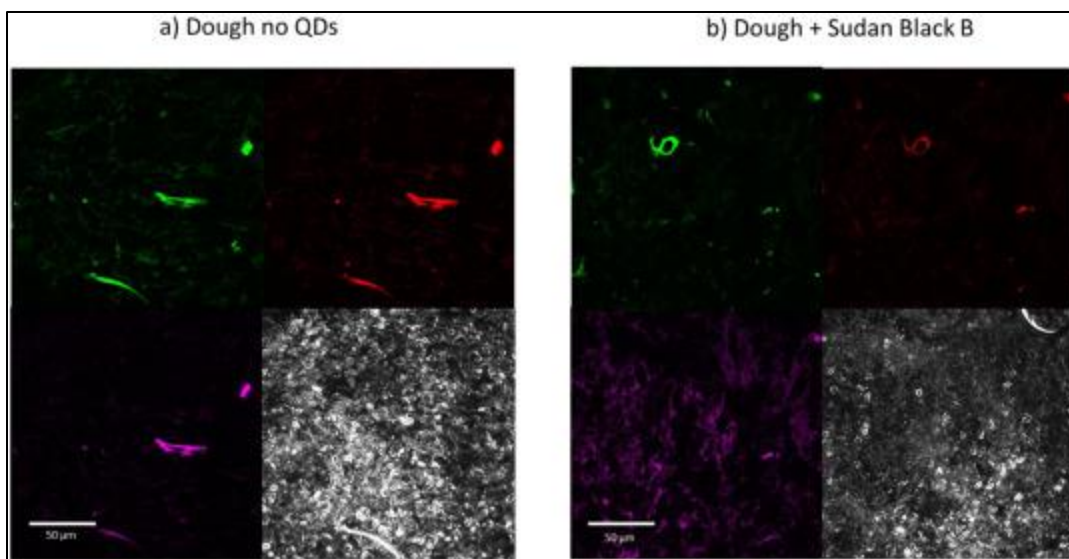
Figure 8. Detection of dough in the 525 (green), 585 (red), 655 (purple), and DIC channels. (a) Unstained dough. (b) Dough treat with 0.1% Sudan Black B. Bar: 50 μm

3.4.4 Auto fluorescent quenching using TrueVIEW™ treatment

No reduction in auto-fluorescence was observed either when the dough samples were treated with the trueVIEW™ auto-fluorescence quencher (Figure 9). In fact, the addition of TrueVIEW intensifies the 525 nm emission. Paraformaldehyde as a fixation medium has been reported to enhance auto-fluorescence in biological tissues before (Baschong et al., 2001). TrueVIEW™ removes background auto-fluorescence coming from aldehydes ("Vector TrueVIEW; Autofluorescence Quenching Kit," 2018). These results indicate that the auto-fluorescence detected in the wheat dough samples studied here is not induced or enhanced by fixation with 4% paraformaldehyde.
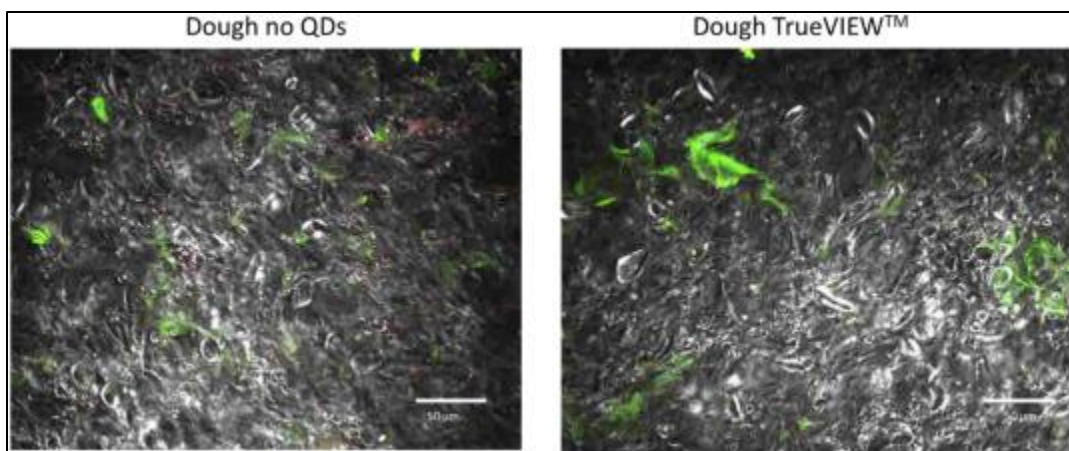
Figure 9. Merged image of the DIC channel and the fluorescent channels of wheat dough fixed with 4% paraformaldehyde. (a) Unstained dough. (b) Dough treat with trueVIEW™ auto fluorescent quencher. Bar: 50 μm

3.4.5 Auto-fluorescence removal using microscope settings

Auto-fluorescence in a wheat dough samples was successfully eliminated after adjusting the laser energy in the microscope and the gain in the photomultiplier detector. The fluorescence in the dough without staining was removed as a background in the Zeiss confocal system (Figure 10a). Samples treated with Antibody-QD complexes presented observable fluorescence signals above control (no Antibody-QD staining) using the same acquisition settings. (Figure 10b). Since the background auto-fluorescent emission does not interfere with the observed emission the difference between Figure 10a and Figure 10b is the presence of QD-antibody complexes. Figs. 10c-e show the particular emission from gliadin, HMW glutenin, and LMW glutenin respectively. These images show the relative spatial distribution of the specific gluten protein sub-fractions, the height of the peak indicates the relative density/concentration of the protein sub-fraction in a specific area. Dough auto-fluorescence removal through this method can be done when the fluorescence emission by QDs is much more intense than the intrinsic auto-fluorescence emission from the dough. The laser power and the gain in the detector system were adjusted to a point where the fluorescent amino acids in the gluten proteins are negligibly excited and the photons emitted by auto-fluorescence are not readable by the detector but the QDs are clearly excitable and their emitted photons are captured by the detector, as shown in Figure 10.
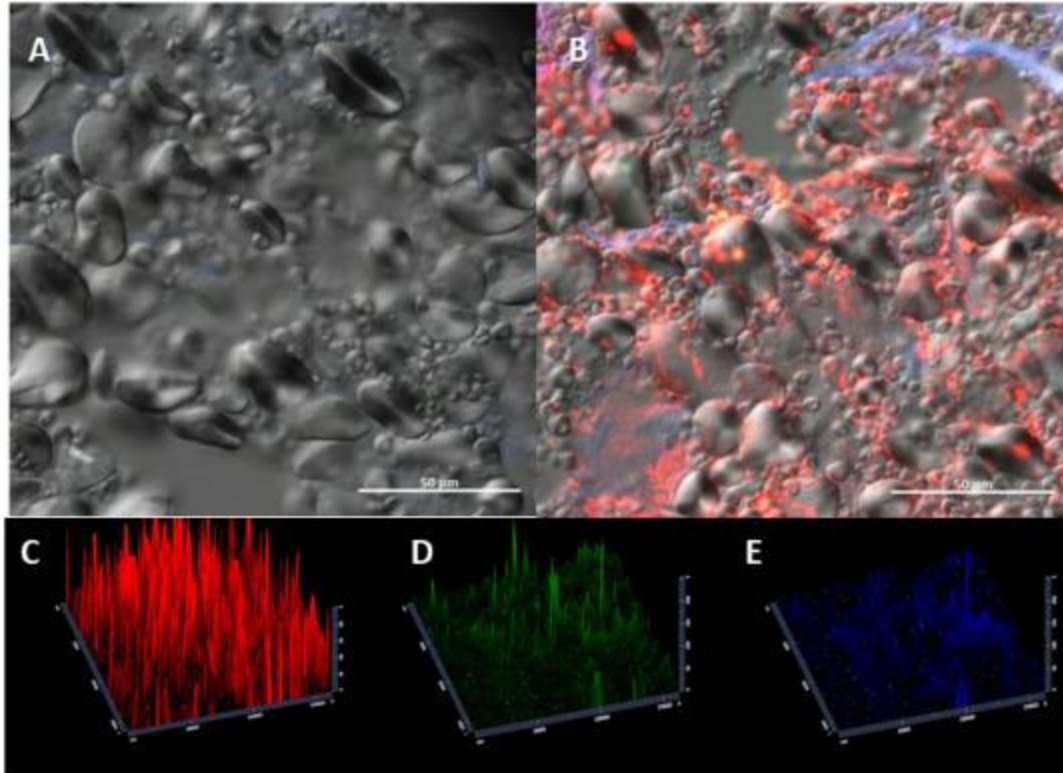
Figure 10. (A) Control, wheat dough without staining, (B) QDs stained wheat dough, (C) gliadin detection in QDs stained wheat dough, (D) HMW glutenins detection in QDs stained wheat dough, (E) LMW glutenins detection in QDs stained wheat dough. Bar: 50 μm

3.4.6 Detection of non-specific QD binding in a no-protein matrix

Figure 11a shows emission intensity in a starch/CMC matrix used as the staining control using Antibody-QD complexes; the starch/CMC control does not have any wheat proteins. Figure 11b shows a sample of wheat dough stained with Antibody-QD complexes. As expected, negligible fluorescence was detected from the no-protein starch/CMC matrix when compared to the wheat dough samples. The blue, green, and red channels represent LMW glutenins stained with 525 nm QDs, HMW glutenins stained with 585 nm QDs, and gliadins stained with 685 nm QDs respectively. Both the starch and the wheat dough samples were stained and washed to remove the excess unbound quantum dots following the same procedure. The starch sample presents negligible fluorescent intensity showing that non-specific binding QDs to the samples is not occurring. These results with the no-protein starch/CMC samples show that fluorescent detection originated from QDs attached to the antibodies are recognizing their specific gluten protein sub-fractions in the wheat dough sample.

49
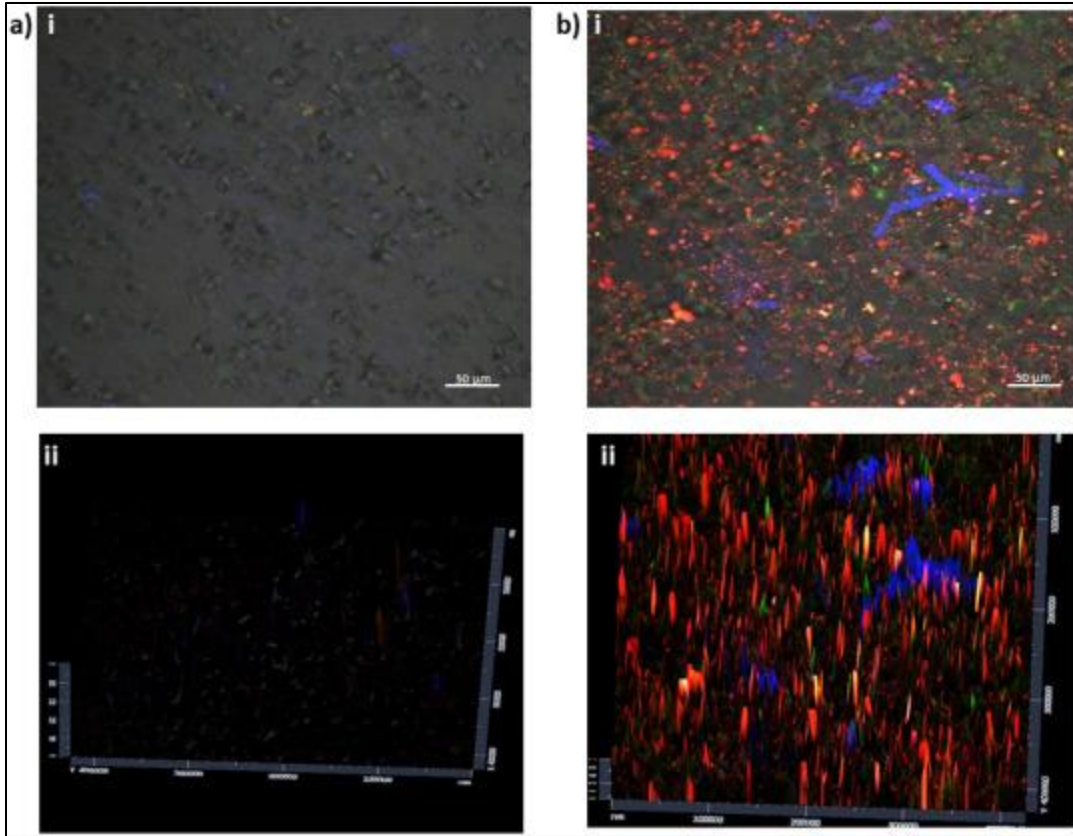
Figure 11. Samples stained with Antibody-QD complexes, (a) Starch/CMC control, (a) Wheat flour dough. Two-dimensional top view (i). Peak intensities profiles for the three different Antibody-QD complexes (ii). Bar: 50 μm

3.4.7 Evaluation of the effect of different slide fixatives on dough fixation and dough fluorescent imaging

The first of three slide fixatives, 4% paraformaldehyde, forms a thick layer that keeps the dough in place and no loss of tissue morphology and sample integrity is observed (Figure 12). With the second fixative, acetone, the dough tissue sample loses morphology easily (Figure 12). The loss of morphology can interfere with the distribution of gluten protein sub-fractions. The results using 4% paraformaldehyde and acetone fixation on dough samples are consistent with the data reported by Bozkurt (2013); where he reported that 4% paraformaldehyde resulted in better tissue morphology for wheat dough compared to acetone, but on the other hand a cleaner signal is obtained with acetone at the expense of keeping the specimen's morphology and integrity intact during the staining procedure. The third fixative method tested, use of methanol, does not cause layer formation or loss of morphology and integrity (Figure 12).
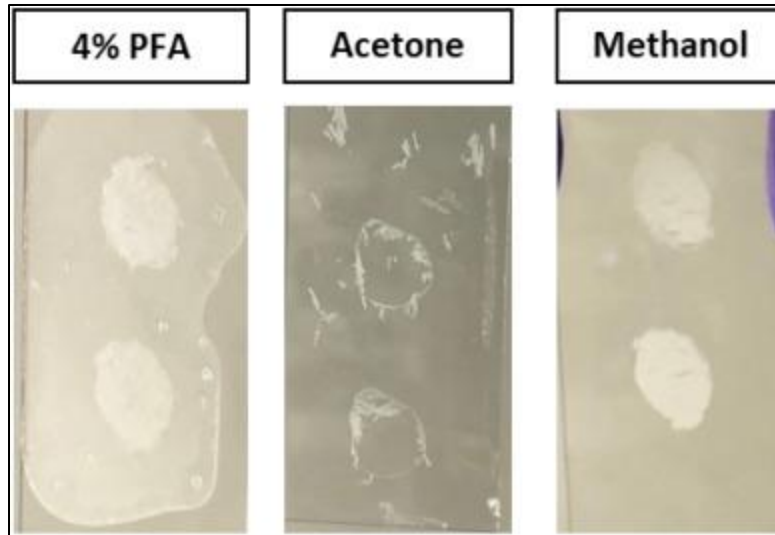
Figure 12. Wheat dough fixation with 4% PFA, acetone, methanol

During imaging analysis of antibody-QD stained dough fixed with 4% PFA some morphology is lost (Figure 13b-i) due to degradation during the staining/washing procedures. This is the thick layer of 4% PFA observed in Figure 12 being washed away. HMW glutenins were clearly detected when fixing dough with 4% PFA; the other two gluten proteins sub-fractions remain undetected (Figure 13b). The antibodies recognition segments in the amino acid sequences of the proteins (antigenic epitopes) can get distorted in this approach, making them unrecognizable by the antibodies since paraformaldehyde has the ability to crosslink proteins residues (Hayat, 2000) affecting the immunofluorescent detection properties of the samples.
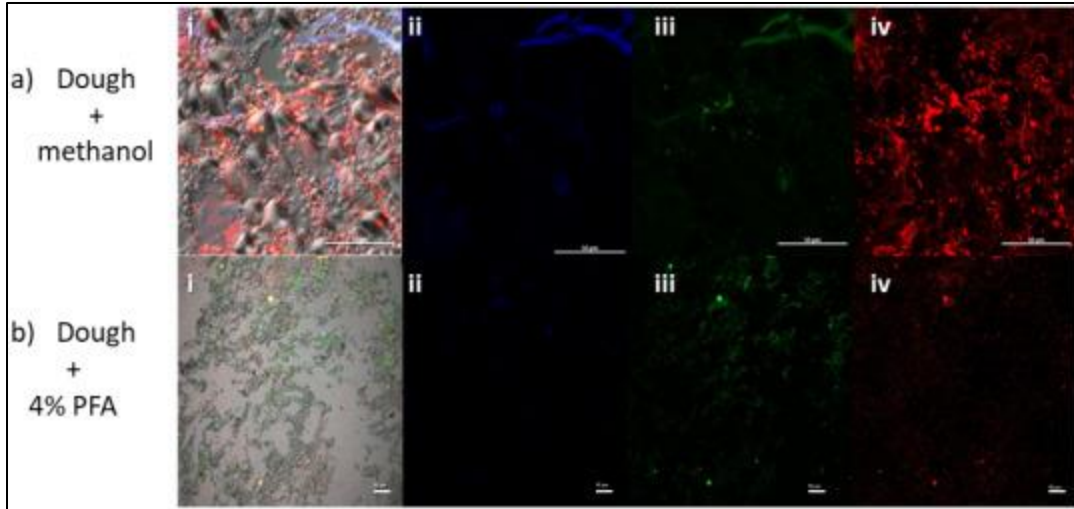
Figure 13. Imaging of wheat dough stained with antibody-QD complexes. (a) Dough fixated with methanol. (b) Dough fixated with 4% PFA. (i) DIC channel merged with fluorescent channels, (ii) 525 channel (LMW glutenins), (iii) 585 channel (HMW glutenins), (iv) 655 channel (gliadins). Bar: 50μm

When the dough tissue is fixed to the slide with methanol, the morphology of the dough sample remains almost intact after staining/washing procedures (Figure 13a-i). Detection of the three-gluten protein sub-fractions was successfully achieved using the three different fluorescence detection channels (525 nm, 585 nm, 655 nm) when wheat dough was fixed with methanol. The methanol fixed dough samples preserved their morphology and integrity, and were suitable for the simultaneous immunofluorescent detection of gliadin, LMW glutenin, and HMW glutenin, demonstrating that methanol as fixative maintains the recognition epitopes available for the antibodies to bind. The methanol fixed dough outcomes are consistent with the literature where methanol as fixation method has been shown to preserve well the antigen recognition sites during immunostaining in other biological samples (Bacallao et al., 2006). Acetone fixed dough samples could not be analyzed under the confocal microscopy system since their integrity was totally lost during the immunostaining procedure.

Comparison between an unstained specimen of wheat dough fixed with methanol (Figure 14a), a specimen of wheat dough fixed with methanol and stained with the three antibody-QD complexes (Figure 14b), and a starch/CMC specimen (no protein control) fixed with methanol and stained with the three antibody-QD complexes (Figure 14c) are shown side by side in Figure 14. The

intensity of the peaks represents the relative spatial distribution/concentration of gliadins (red), HMW glutenins (green), and LMW glutenins (blue) in the sample. All images were obtained under the same microscope and detector configurations. The unstained dough control shows no fluorescence emission and proves that the detected fluorescent emission is not generated by dough intrinsic auto-fluorescence. The stained starch/CMC matrix proves that the detected fluorescent emission is not coming from trapped antibody-QD complexes and that the washing steps after staining removes all unbound antibody-QD.
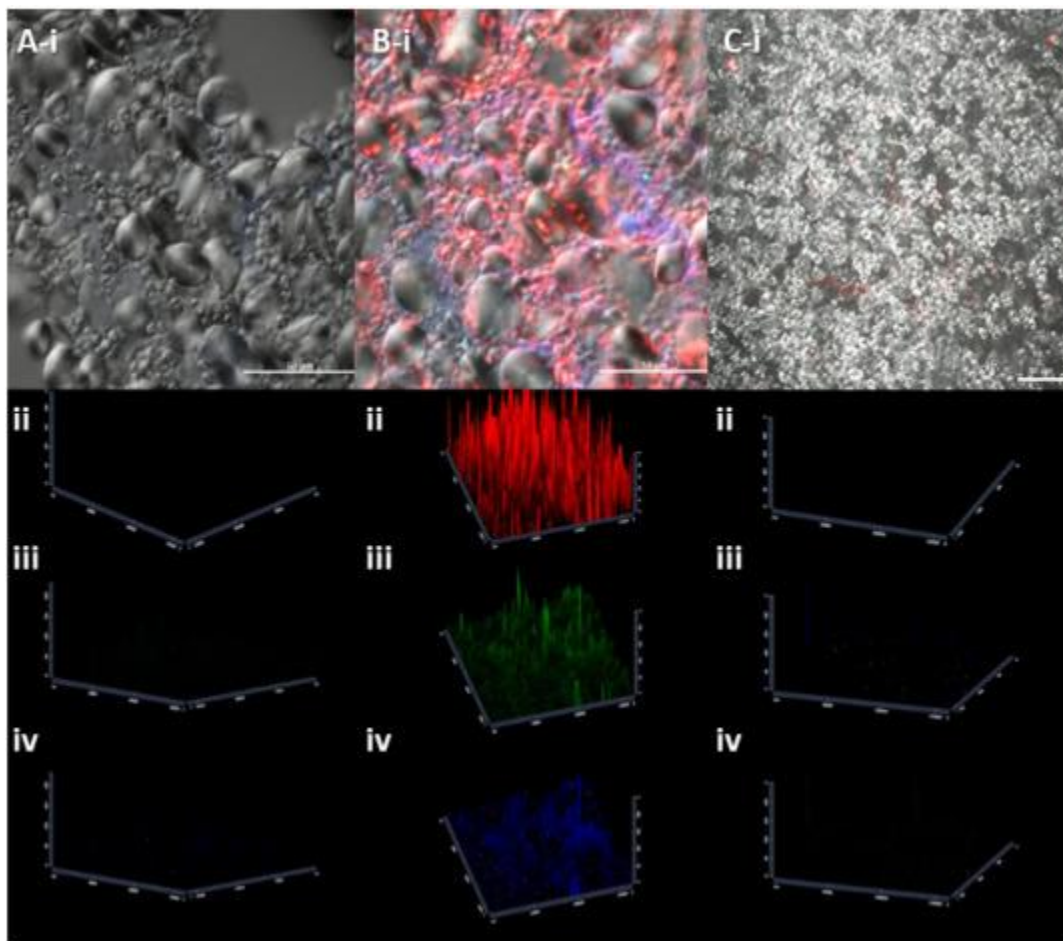
Figure 14. (a) Methanol fixed - unstained wheat dough. (b) Methanol fixed - wheat dough stained with antibody-QD complexes. (c) Methanol fixed - starch/CMC matrix stained with antibody-QD complexes. (i) DIC channel merged with fluorescent detection channels. (ii) 655 nm channel intensity profile(gliadins). (iii) 585 nm channel intensity profile(HMW glutenins). (iv) 525 nm channel intensityprofile (LMW glutenins). Bar: 50μm

The main advantage of this simultaneous detection of gliadins, LMW glutenins, and HMW glutenins is the opportunity to study the three different gluten sub-factions in the same dough area at the same time, this opens the possibility to study the interactions of different gluten sub-fractions 'in situ' by fluorescent imaging. The advantage of this methodology can be easily understood when we look at some its potential applications. The first proposed application is the investigation of the gluten sub-fractions at different mixing times in a Farinograph, following AACCI method 54–21.02. This application might be able to explain the individual contribution and role of each protein sub-fraction in the gluten network development and disruption during dough mixing. Other potential applications can be the study of the gluten sub-fractions under different rheological measurements, and their detection during baking. Some of the limitations of this technique are that pure quantitative analysis are not possible, although semi-quantitative and qualitative analysis are possible. The semi-quantitative analysis includes comparison of relative fluorescent intensities of each protein sub-fraction in different dough areas, and comparison of the localization of different proteins sub-fractions in the same dough areas. Other limitations would be the current cost of the materials, mostly, developed antibodies and quantum dots, and the accessibility to a Confocal Laser Scanning Microscope system.

3.5 Conclusion

We successfully conducted simultaneous 'in situ' fluorescent imaging of gliadin, LMW glutenin and HMW glutenin in wheat dough for the first-time using antibody-QD complexes specific to each sub protein fraction with their respective auto-fluorescence and no-protein controls. This has not been done before and is a first in dough/cereal science. In order to achieve this outcome, we tested several procedures and fixation media. When comparing the effectiveness of 4% PFA, acetone, and methanol as fixative agents we found that methanol is the most suitable fixation medium for dough because it maintains tissue morphology and integrity during the entire immunostaining and washing procedure, keeping the antigenic epitopes available for the antibodies to bind to the respective proteins, which is crucial when doing specific immunofluorescent detection. We also found that dough auto-fluorescence can be masked using the proper microscope/detector settings when the emission signal emitted by the fluorescent dyes is strong enough. We found that heparin, Sudan black B and TrueVIEW™ auto-fluorescence blocking agents were not effective with the wheat dough studied here. We have developed a

reliable protocol for performing successful immunofluorescent imaging of gliadin, LMW and HMW glutenin sub fractions in wheat flour dough systems. We have proven that the antibody-QD complexes bind to their specific proteins in an intact dough matrix, and the imaging results are not the product of dough auto-fluorescence or non-specific binding of Antibody-QD trapped non-specifically in the dough matrix. All these findings combined were used to obtain for the first time fluorescent images capable of detecting the distribution of LMW glutenins, HMW glutenins, and gliadins in dough. In future work we will compare different dough processes and the resulting distribution of these proteins as a function of processing parameters. We are also aiming to compare differences in the quantity and distribution of wheat flour proteins between different types of wheat flour doughs with different bread-making quality.

3.6 References

Ansari, S., Bozkurt, F., Yazar, G., Ryan, V., Bhunia, A., & Kokini, J. (2015). Probing the distribution of gliadin proteins in dough and baked bread using conjugated quantum dots as a labeling tool. *Journal of Cereal Science*, *63*, 41–48. https://doi.org/10.1016/j.jcs.2014.12.001

Bacallao, R., Sohrab, S., & Phillips, C. (2006). Guiding Principles of Specimen Preservation for Confocal Fluorescence Microscopy. In *Handbook Of Biological Confocal Microscopy* (pp. 368–380). Springer, Boston, MA. Retrieved from https://link-springer-com.ezproxy.lib.purdue.edu/chapter/10.1007/978-0-387-45524-2_18

Baschong, W., Suetterlin, R., & Laeng, R. H. (2001). Control of Autofluorescence of Archival Formaldehyde-fixed, Paraffin-embedded Tissue in Confocal Laser Scanning Microscopy (CLSM). *Journal of Histochemistry & Cytochemistry*, *49*(12), 1565–1571. https://doi.org/10.1177/002215540104901210

Bonilla, J. C., Bozkurt, F., Ansari, S., Sozer, N., & Kokini, J. L. (2016). Applications of quantum dots in Food Science and biology. *Trends in Food Science & Technology*, *53*, 75–89. https://doi.org/10.1016/j.tifs.2016.04.006

Bonilla, J. C., Ryan, V., Yazar, G., Kokini, J. L., & Bhunia, A. K. (2018). Conjugation of Specifically Developed Antibodies for High- and Low-Molecular-Weight Glutenins with Fluorescent Quantum Dots as a Tool for Their Detection in Wheat Flour Dough. *Journal of Agricultural and Food Chemistry*, *66*(16), 4259–4266. https://doi.org/10.1021/acs.jafc.7b05711

Bozkurt, F. (2013). *In situ observation of the distribution and location of gliadin as a function of mixing time in wheat flour dough using quantum dots*. University of Illinois at Urbana-Champaign, Urbana, Illinois.

Bozkurt, F., Ansari, S., Yau, P., Yazar, G., Ryan, V., & Kokini, J. (2014). Distribution and location of ethanol soluble proteins (Osborne gliadin) as a function of mixing time in strong wheat flour dough using quantum dots as a labeling tool with confocal laser scanning microscopy. *Food Research International*, *66*, 279–288. https://doi.org/10.1016/j.foodres.2014.09.028

Bugusu, B. A., Hamaker, B. R., & Rajwa, B. (2002). Interaction of maize zein with wheat gluten in composite dough and bread as determined by confocal laser scanning microscopy. *Scanning*, *24*(1), 1–5. https://doi.org/10.1002/sca.4950240101

Clarke, B. C., Phongkham, T., Gianibelli, M., Beasley, H., & Bekes, F. (2003). The characterisation and mapping of a family of LMW-gliadin genes: effects on dough properties and bread volume. *Theoretical and Applied Genetics*, *106*(4), 629–635. https://doi.org/10.1007/s00122-002-1091-1

Delcour, J. A., & Hoseney, R. C. (2010). Proteins of Cereals. In *Principles of Cereal Science and Technology* (3rd ed.). St. Paul, Minnesota USA: American Association of Cereal Chemists.

Gupta, R. B., & MacRitchie, F. (1994). Allelic Variation at Glutenin Subunit and Gliadin Loci, Glu-1, Glu-3 and Gli-1 of Common Wheats. II. Biochemical Basis of the Allelic Effects on Dough Properties. *Journal of Cereal Science*, *19*(1), 19–29. https://doi.org/10.1006/jcrs.1994.1004

Haimovici, R., Gantz, D. L., Rumelt, S., Freddo, T. F., & Small, D. M. (2001). The Lipid Composition of Drusen, Bruch's Membrane, and Sclera by Hot Stage Polarizing Light Microscopy. *Investigative Ophthalmology & Visual Science*, *42*(7), 1592–1599.

Hayat, M. A. (2000). *Principles and techniques of electron microscopy: biological applications* (4th ed..). Cambridge, UK ; New York: Cambridge University Press.

Held, P. (2003, April 18). Peptide and Amino Acid Quantification Using UV Fluorescence in Synergy HT Multi-Mode Microplate Reader | April 18, 2003. Retrieved July 8, 2018, from https://www.biotek.com/resources/application-notes/peptide-and-amino-acid-quantification-using-uv-fluorescence-in-synergy-ht-multi-mode-microplate-reader/

Jameson, D. M. (2014). *Introduction to Fluorescence*. Taylor & Francis.

Li, W., Dobraszczyk, B., & Wilde, P. (2004). Surface properties and locations of gluten proteins and lipids revealed using confocal scanning laser microscopy in bread dough. *Journal of Cereal Science*, *39*(3), 403–411. https://doi.org/10.1016/j.jcs.2004.02.004

Neumann, M., & Gabel, D. (2002). Simple Method for Reduction of Autofluorescence in Fluorescence Microscopy. *Journal of Histochemistry & Cytochemistry*, *50*(3), 437–439. https://doi.org/10.1177/002215540205000315

Nieto-Taladriz, M. T., Perretant, M. R., & Rousset, M. (1994). Effect of gliadins and HMW and LMW subunits of glutenin on dough properties in the F6 recombinant inbred lines from a bread wheat cross. *Theoretical and Applied Genetics*, *88*(1), 81–88. https://doi.org/10.1007/BF00222398

Oliveira, V. C., Carrara, R. C. V., Simoes, D. L. C., Saggioro, F. P., Carlotti Jr., C. G., Covas, D. T., & Neder, L. (2010). Sudan Black B treatment reduces autofluorescence and improves resolution of in situ hybridization specific fluorescent signals of brain sections. *Histology and Histopathology*, *25*(8), 1017–1024.

Pawley, J. B. (2006). *Handbook Of Biological Confocal Microscopy* (Third Edition). Springer.

Payne, P. I., Nightingale, M. A., Krattiger, A. F., & Holt, L. M. (1987). The relationship between HMW glutenin subunit composition and the bread-making quality of British-grown wheat varieties. *Journal of the Science of Food and Agriculture*, *40*(1), 51–65. https://doi.org/10.1002/jsfa.2740400108

Romijn, H. J., van Uum, J. F. M., Breedijk, I., Emmering, J., Radu, I., & Pool, C. W. (1999). Double Immunolabeling of Neuropeptides in the Human Hypothalamus as Analyzed by Confocal Laser Scanning Fluorescence Microscopy. *Journal of Histochemistry & Cytochemistry*, *47*(2), 229–235. https://doi.org/10.1177/002215549904700211

Roth, M., & Hampaǐ, A. (1973). Column chromatography of amino acids with fluorescence detection. *Journal of Chromatography A*, *83*, 353–356. https://doi.org/10.1016/S0021-9673(00)97051-1

Sabnis, R. W. (2010). *Handbook of biological dyes and stains synthesis and industrial applications*. Hoboken, NJ: Wiley-Blackwell.

Singh, N. K., & Shepherd, K. W. (1988). Linkage mapping of genes controlling endosperm storage proteins in wheat. *Theoretical and Applied Genetics*, *75*(4), 628–641. https://doi.org/10.1007/BF00289132

Sozer, N., & Kokini, J. L. (2014). Use of quantum nanodot crystals as imaging probes for cereal proteins. *Food Research International*, *57*, 142–151. https://doi.org/10.1016/j.foodres.2013.12.031

Sun, Y., Yu, H., Zheng, D., Cao, Q., Wang, Y., Harris, D., & Wang, Y. (2011). Sudan Black B Reduces Autofluorescence in Murine Renal Tissue. *Archives of Pathology & Laboratory Medicine*, *135*(10), 1335–1342. https://doi.org/10.5858/arpa.2010-0549-OA

Tatham, A. S., Miflin, B. J., & Shewry, P. R. (1985). The Beta-Turn Conformation in Wheat Gluten Proteins: Relationship to Gluten Elasticity. *Cereal Chemistry*, *62*(5), 405–412.

Timperman, A., Oldenburg, K., & Sweedler, J. (1995). Native Fluorescence Detection and Spectral Differentiation of Peptides Containing Tryptophan and Tyrosine in Capillary Electrophoresis. *Analytical Chemistry*, *67*(19), 3421–3426.

Uthayakumaran, S., Gras, P. W., Stoddard, F. L., & Bekes, F. (1999). Effect of Varying Protein Content and Glutenin-to-Gliadin Ratio on the Functional Properties of Wheat Dough. *Cereal Chemistry*, *76*(3), 389–394. https://doi.org/10.1094/CCHEM.1999.76.3.389

Vector TrueVIEW; Autofluorescence Quenching Kit. (2018). Retrieved July 8, 2018, from https://vectorlabs.com/vector-reg-trueview-trade-autofluorescence-quenching-kit.html

Zeglis, B. M., Davis, C. B., Aggeler, R., Kang, H. C., Chen, A., Agnew, B. J., & Lewis, J. S. (2013). Enzyme-Mediated Methodology for the Site-Specific Radiolabeling of Antibodies Based on Catalyst-Free Click Chemistry. *Bioconjugate Chemistry*, *24*(6), 1057–1067. https://doi.org/10.1021/bc400122c

Zweifel, C., Handschin, S., Escher, F., & Conde-Petit, B. (2003). Influence of High-Temperature Drying on Structural and Textural Properties of Durum Wheat Pasta. *Cereal Chemistry*, *80*(2), 159–167. https://doi.org/10.1094/CCHEM.2003.80.2.159

CHAPTER 4. MIXING DYNAMICS AND MOLECULAR INTERACTIONS OF HMW GLUTENINS, LMW GLUTENINS, AND GLIADINS ANALYZED VY FLUORESCENT CO-LOCALIZATION AND PROTEIN NETWORK QUANTIFICATION

4.1 Abstract

Gluten proteins and their impact affecting the texture and rheology of wheat-based food products is well-known. We are now using newly developed antibodies for LMW and HMW glutenins along with gliadin antibodies, all of them conjugated with Quantum Dots to visualize these gluten subunits in wheat dough during dough mixing. We are also using Confocal Laser Scanning Microscopy and image analysis software from to obtain quantitative analysis regarding the degree of co-localization of the different gluten subunits in the same dough area and the quantification of the gluten network branches. The co-localization coefficient is shown as a promising technique to evaluate the interaction between different components in dough samples. We are linking the qualitative observations and quantitative data of gliadins, LMW glutenins, and HMW glutenins to dough physical characteristics at different stages of mixing in a Brabender farinograph. During dough mixing the three gluten subunits associate together to form a strong gluten network however, with continuous mixing, LMW glutenins dissociate from the network first, followed by a later dissociation of the HMW glutenins. Visualizing the distribution of the gluten subunits during mixing is helping us advance our understanding of the mechanism of dough development.

4.2 Introduction

The gluten protein subunits are responsible for network formation during hydration and mixing in wheat flour dough. This network provides unique properties to the dough, like air retention through the formation of an impermeable membrane around gas cells that results in a foam like baked final product (Delcour and Hoseney, 2010). Based on their extractability in different solvents, gluten

proteins are divided into gliadins, soluble in aqueous alcohol solutions, and glutenins, soluble in acids and bases (Osborne, 1907). The entire gluten network, gliadins and glutenins together, has been described as a viscoelastic network, in which the viscosity is given by gliadins, while the elasticity is contributed by glutenins (Xu et al., 2007).

Glutenins have been classified into high molecular weight glutenins (HMW) and low molecular weight glutenins (LMW) based on their molecular mass and functionality. HMW glutenins have been shown to have a higher impact on dough elasticity than LMW glutenins (Gupta et al., 1991). LMW glutenins have also been shown to have some contribution, but to a lesser extent, to dough strength (Gupta and MacRitchie, 1994). However, the contribution of LMW glutenins to rheology has been found to be of the same order as the contribution of gliadins (Clarke et al., 2003). This has been supported by the finding that their genetic encoding loci are very closely located and they are believed to come from the same group of ancestral genes (Singh and Shepherd, 1988).

All these previously mentioned studies on the influence of gliadin, HMW glutenins, and LMW glutenins on viscoelasticity have been performed by extraction and/or reconstitution techniques. A great deal of information about the gluten protein subunits has been learned with these early and elegant chemistry techniques, however these extraction/reconstitution techniques change the protein secondary structure and configuration, which potentially may distort the results and interpretations. This potential limitation, has led investigators in this field of research to conclude that the precise changes in the gluten network occurring during dough development/mixing are not completely understood, however these network changes are generally attributed to protein-protein interactions within the gluten protein subunits including gliadins and glutenins (Shewry et al., 2002).

Fluorescent imaging has been used to study gluten in dough by staining gluten with amine reactive dyes in several studies (Newberry et al., 2004, Sozer and Kokini, 2014). The visualizations of gluten proteins by fluorescent microscopy by these studies have shown the location of gluten only qualitatively. More recently multiple quantitative studies of gluten network characteristics together with visual qualitative descriptions of fluorescent detections of gluten using a 'protein network analysis' have been conducted (Bernklau et al., 2016, Hackenberg et al., 2018, Lucas et al., 2018). This analysis showed promising quantification of the gluten network characteristics. Its limitation

is that it has been performed in gluten as a whole with amine-reactive dyes, which does not provide specific information about the individual contribution of gluten subunits to the gluten network. Recently, a new highly specific approach was used to study only the distribution of gliadin subunits in wheat dough and bread, by using gliadin antibodies conjugated to quantum dots (QDs) (nano-fluorescent dyes) (Ansari et al., 2015, Bozkurt et al., 2014). Gliadin antibodies are commercially available for detection of gluten in gluten-free tests, and antibody-QDs conjugation methods are available (Bonilla et al., 2016). More recently, antibodies for HMW glutenins and LMW glutenins have been developed using specific and unique peptides from the amino acid sequences of HMW glutenins and LMW glutenins as targets (Bonilla et al., 2018). The antibodies were conjugated with different color quantum dots with a new available site-click method for antibody-QDs conjugation enabling the simultaneous fluorescent detection of HMW and LMW glutenins in wheat dough, followed by simultaneous staining and multi-spectral imaging of gliadins, HMW glutenins, and LMW glutenins (Bonilla et al., 2019).

In the current study we are using the developed antibodies for HMW glutenins and LMW glutenins, with gliadin antibodies, together with the recently published multi-spectral imaging protocol to study the gluten proteins subunits during dough mixing following the official AACCI 54-21.02 (AACCI, 1995) method for rheological dough testing. A protein network analysis is used to obtain quantitative data on network characteristics of each protein subunit. In addition the relative location of each gluten subunit is compared with the location of each of the other two gluten subunits. These comparisons are obtained through fluorescent co-localization coefficients. The co-localization coefficients method is an established pairwise comparison technique measuring the locations of fluorescent emission from two different channels in a specific image area (Dunn et al., 2011). In this case, the co-localization coefficients explain the relationship between the location of two different gluten subunits in the same dough area at a specific mixing time, and serves as an indicator of co-existence and possible interactions between the different gluten subunits.

This is the first time that the fluorescent co-localization analysis has been reported to study possible interactions between different gluten proteins subunits in dough based on quantitative fluorescent microscopy. In this study quantitative protein network analysis and co-localization coefficients are used to gain a better understanding of the behavior and interactions of gluten subunits and their function during dough mixing in a Brabender Farinograph.

4.3 Materials and Methods

4.3.1 Antibodies conjugation with quantum dots

Anti-LMW glutenins, anti-HMW glutenins (Bonilla et al., 2018), and the anti-gliadin 4F3 antibodies (Thermo Fisher Scientific, Waltham, MA, U.S.A.) were conjugated with 525 nm, 585 nm, and 655 nm dibenzocyclooctyne (DIBO)-functionalized QDs (Thermo Fisher Scientific, Waltham, MA, U.S.A.), respectively using a site-click procedure (Bonilla et al., 2019). By using this site-click method the integrity and effectiveness of the antibodies are conserved after the conjugation procedure. Antibodies maintain their effectiveness since the conjugation process does not disturb the antigen binding sites in the antibodies. Galactose sugars situated on the tail of the antibodies are removed with β-galactosidase. A different azide-modified galactose molecule is attached to the tail of the antibodies catalyzed by β-galactosyltransferas. DIBO-functionalized QDs in solution are then added to the solution containing the antibodies. The DIBO molecules functionalized to the QDs are alkynes, and QDs are conjugated to the antibodies through an azide-alkyne cycloaddition to the azide-modified galactoses in the tails of the antibodies.

4.3.2 Wheat dough preparation

Wheat flour dough was prepared using hard wheat flour from hard red winter wheat generously provided by Siemer milling company (Teutopolis, IL) following the AACCI method 54-21.02 (AACCI, 1995). The water absorption level of the flour was obtained following the same method. The moisture of the hard wheat flour was determined using a rapid moisture analyzer (Mettler Toledo, Columbus, OH). The official method requires 300 g of flour with an ideal moisture of 14%; once the real moisture of the flour is determined, the amount of flour to be used in the test is adjusted in order to have the same amount of dry matter as in ideal conditions (14% moisture). The hard wheat flour had 12.90% moisture, therefore; 296.20 g, hard wheat flour, was used for determining the water absorption levels. The water absorption level is the percentage of water volume added to the flour to reach a consistency of 500 Brabender units (BU) in a Brabender Farinograph. The dough's arrival time, peak time, and departure time to the 500 BU line were recorded. The arrival time, peak time, and departure time, are characteristics times in the wheat flour Farinogram, they are used to determine dough development and stability. Dough was kept mixing 10 min after departure in order to collect a sample of an over-mixed dough.

4.3.3 Sample collection, sectioning, and fixation

Small samples, around 0.5 cm3 pieces of dough were collected from the Farinograph mixing bowl by means of forceps at the specific arrival time, peak time, departure time, and 10 min after departure. In order to keep the dough components undamaged, the collected samples were placed on tissue-tek cryomolds (Fisher Scientific, Hamptom, NH) and embedded with Optimum Cutting Temperature (OCT) compound (Fisher Scientific, Hamptom, NH), covered with aluminum foils and directly immersed liquid nitrogen. OCT gives a suitable medium for cryostat sectioning and avoids dehydration of dough samples. Samples were kept at $-80\,°C$. They were transferred to the cryostat in liquid nitrogen and aluminum foil packs were removed inside the cryostat. Dough samples were then sectioned using a LEICA CM 1860 Cryostat (Leica Biosystems, Wetzlar, Germany). The samples were longitudinally cut to a thickness of $10\,\mu m$ in the cryostat. The 10-μm wheat dough sections were placed onto hydrophilic adhesive microscope slides and then immersed for ten minutes in a staining dish containing methanol and air-dried. Methanol has been found to be the most suitable fixative for wheat dough samples when performing multispectral imaging of gliadins HMW glutenins, and LMW glutenins (Bonilla et al., 2019).

4.3.4 Confocal Laser Scanning Microscopy analysis

A Zeiss LSM 880 Confocal Laser Scanning Microscope (Carl Zeiss Microscopy, Oberkochen, Germany) was used to visualize the hard wheat dough samples' structure by detecting the fluorescent intensity of the 525 nm, 585 nm, and 655 nm QDs conjugated to the anti-LMW, anti-HMW, and anti-gliadin antibodies respectively. The fluorescence intensity is a measure of the local concentration of the protein subunit. A 405 nm laser was used in the confocal system to excite the QDs in the samples. Dough samples were visualized using a $20 \times$ objective, Zeiss Plan Apo $20 \times /0.8NA$. The collected images consist of 512×512 pixels with a resolution of $0.35\,\mu m$/pixel. Digital image files were recorded using the Zen BLACK software and analyzed with the Zen BLUE software (Carl Zeiss imaging, Oberkochen, Germany). Contrast/LUTs settings were determined with the brightness of the samples and all images were set based upon those calibration settings. Three dough samples were collected at each specific mixing time (arrival, peak, departure, and 10 min after). These samples were organized into thin specimens of $10\,\mu m$. In addition, three different random areas far apart from one another in each dough sample were imaged, for a total

of nine images from nine different areas. Subsequently, each image is split into three separate images, one for each of the three detected channels, 'channel A' at 525 nm, 'channel B' 585 nm, and 'channel C' at 655 nm channels representing LMW glutenins, HMW glutenins, and gliadins respectively for a total of 27 images.

4.3.5 Protein network analysis

The nine fluorescent images at the four different mixing times were analyzed using AngioTool64 software. Angiotool64 has been found to be useful to quantify network characteristics in fluorescent imaging of gluten in dough samples (Bernklau et al., 2016). The protein network analysis draws lines where the 'protein filaments' of the network are located in the fluorescent image and offers information on the protein area, protein percentage area, number of protein junctions, number of protein end points, and mean Lacunarity. Lacunarity is used as a metric for the shape, uniformity, and structural variance of the gluten network (Bernklau et al., 2016). All the parameters are important for the quantitative description of the network. For example, a higher protein area, protein percentage area, number of network junctions, network end points and a lower mean Lacunarity values are indicatives of a uniform network formed. In order to determine the individual contribution of gliadins, LMW glutenins, and HMW glutenins, the protein network parameters were analyzed individually for the emission channel of each protein subunit in all nine samples from all four mixing times.

4.3.6 Analysis of protein subunits co-localization

The co-localization analysis from the Zen BLUE software gives a coefficient which indicates the 'degree of co-localization' between the emissions of two different channels corresponding to two different quantum dots bound to two different protein subunits in the same image (Manders et al., 1993). The "Manders' co-localization coefficient" is a measure of the co-existence and possible interactions between two different gluten subunits. The co-localization coefficient measures the fraction of pixels with positive emission values in both channels in the same area (Dunn et al., 2011). The analysis is done pixel by pixel in the 262,144 pixels (512×512 pixels per image) in the image captured by the CLSM system. Three analyses are run per image, 1) a comparison between the emission of HMW glutenins with gliadins, 2) LMW glutenins with gliadins, and 3)

HMW glutenins with LMW glutenins. The results for each analysis is a number between '0' and '1'. A value of '0' indicates that the pixels showing emission for the protein subunit 'a' are not the same pixels showing emission for the protein subunit 'b'. This means that the proteins are not present in the same location and therefore may not be interacting with one another at those locations. A value of '0.5' indicates that the fluorescent emission of protein subunit 'a' and protein subunit 'b' overlap in locations in 50% of the total area of emission. This indicates that the proteins interact with one another at 50% of the available area. A value of '1' indicates that all the pixels showing emission for protein subunit 'a' are exactly in the same location that the pixels where protein subunit 'b' shows emission. A high co-localization factor is indicative that the likelihood of interaction at these locations is very high, co-localization is used to determine structural associations of two molecules such as potential protein-protein interactions (Dunn et al., 2011). The co-localization coefficients enable us to link the individual qualitative description and quantitative network analysis of each gluten subunit with those of a different gluten subunit, giving a better understanding of how the different gluten subunits interact with each other at different dough mixing times.

4.3.7   HMW/LMW glutenin ratio determination

Wheat flour dough was mixed and frozen at each mixing time (arrival, peak, departure, 10 min after departure). Each dough was freeze dried, glutenins were extracted from each freeze-dried flour in a 50% propan-2-ol. 0.08 M Tris–HCl (pH 8.0) and 1% (w/v) dithiothreitol. (Dhaka and Khatkar, 2015). The glutenin extracts were run in a 7.5% acrylamide SDS-PAGE gel after dissolving in an SDS sample solvent following a previously published SDS-PAGE method for glutenins (Bonilla et al., 2018). The HMW/LMW glutenin ratios of the doughs at each mixing time were determined using the gel analysis tool in Image J, which compares the intestines of the HMW band with the intensities of the HMW bands.

4.3.8   Viscosity of the 1.5% SDS-soluble protein

Dough was mixed and stopped at arrival, peak, departure, and 10 min after departure times. Each one of the four doughs were freeze dried. 1.4g of freeze-dried dough was solubilize in 28 ml of

1.5% SDS solution and centrifuged at 20,000xG for 2 h in order to separate the 1.5% soluble proteins from the flour (Don et al., 2005).

4.4   Results and Discussion

4.4.1   Dough mixing profile

The water absorption level for the hard wheat flour with 11% protein and an equilibrium moisture content of 12.9% was 58.8%. The hard wheat flour was found to have arrival time of 1:17 min, peak time of 6:34 min, and departure time of 14:02 min. The stability of the hard wheat flour was 12:45 min. The distribution and organization of gliadins, HMW glutenins, and LMW glutenins is being analyzed 1) at arrival time 2) peak time, 3) departure time, and 4) ten minutes after departure. The averaged dough strengths at these times were 465 BU, 510 BU, 480 BU, and 450 BU respectively. We are focused on determining the changes which occur in the distribution of proteins when the dough is mixed more and more up to 10 min after departure.

4.4.2   Analysis of the changes in the distribution of LMW glutenins, HMW glutenins, and gliadins from arrival time to peak time

The distributions of gliadins, LMW glutenins, and HMW glutenins in the hard wheat flour dough at arrival time (1:17 min of mixing) and peak time (6:34 min of mixing) are shown in Figure 15. The nine different dough areas imaged at arrival time (images i-ix), and at peak time (images x-xviii) are shown side by side. Each of the nine images is analyzed through the three different detection channels; channel A (blue) represents LMW glutenins, channel B (green) represents HMW glutenins, and channel C (red) represent gliadins.
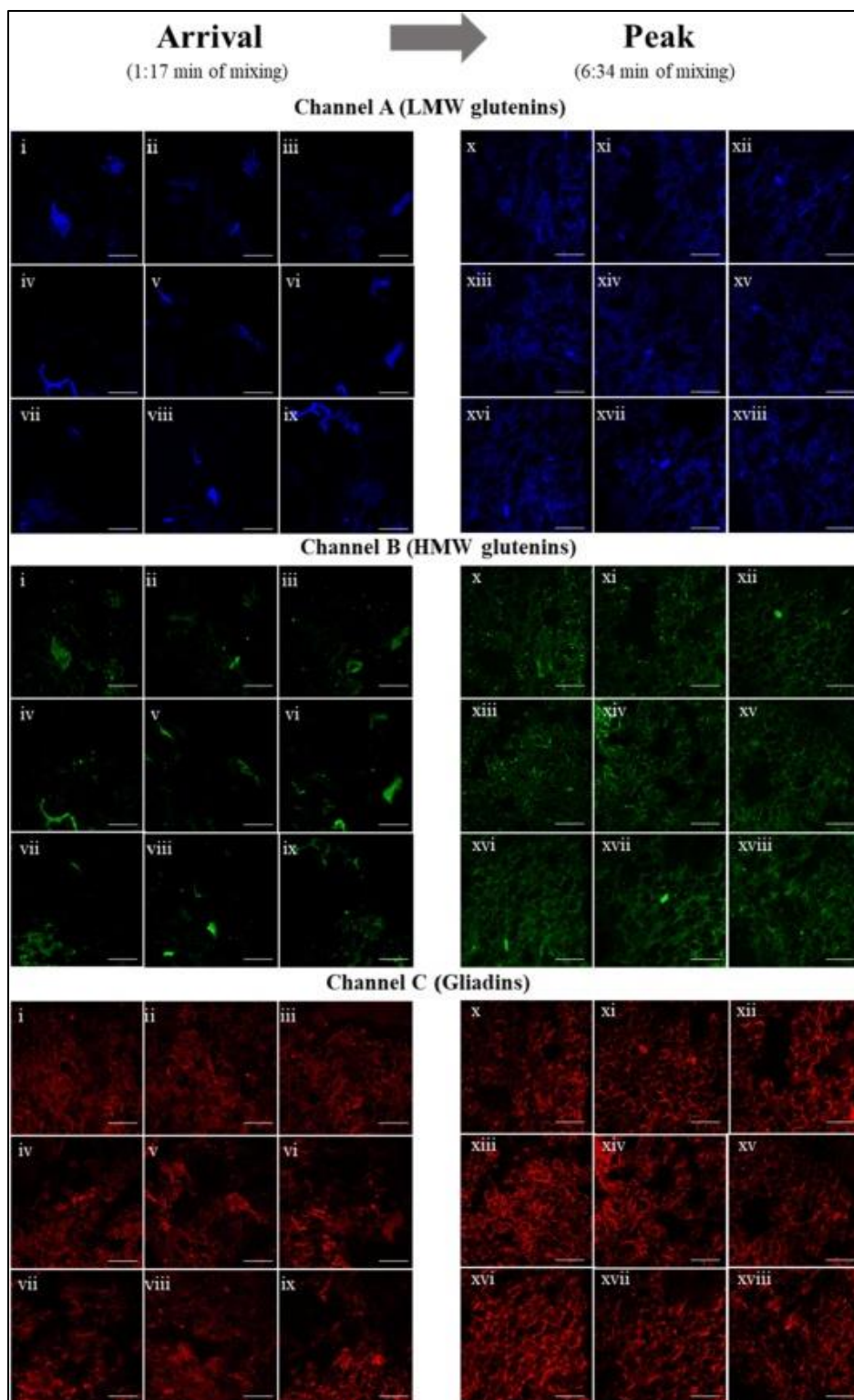
Figure 15. Distribution of LMW glutenins (Channel A), HMW glutenins (Channel B), and Gliadins (Channel C) from nine different areas of wheat dough at arrival time (i-ix) and peak time (x-xviii) in the farinograph. Bar 50 μm

At arrival time, LMW glutenins and HMW glutenins form agglomerates only in a few spots as can be seen in the channels A and B of images i-ix (Figure 15). This is supported with the network quantitative analysis data showed in Table 3, where the averaged area covered by LMW and HMW glutenins is 3.43%, and 4.40% of the imaged dough area respectively. The high brightness in the few agglomerates where LMW and HMW are located indicates that very few aggregates are accumulated in those areas. The images i-ix in their channels A and B (Figure 15) show that the areas of accumulation of LMW match the spatial location of the areas of accumulations of HMW glutenins. This is in accordance with the co-localization analysis data reported in Table 3, in which a high co-localization factor (0.81) exists between LMW-HMW glutenins at arrival mixing time. Even though the areas where interaction occurs is low the degree of interaction at these locations between LMW and HMW is high. The low degree of distribution of LMW and HMW glutenins is due to the stiff and strong networks generated by a large number of both intermolecular and intramolecular disulfide bonds in these protein subunits preventing significant movement of these proteins during the early stages of mixing. It may also be possible that the LMW and HMW subunits are bonded with hydrophobic interactions and move together as a result of these interactions (Lindsay and Skerritt, 1999, Orsi et al., 2001).

Table 3. Network analysis and co-localization analysis on the fluorescent detection HMW glutenins, LMW glutenins, and Gliadins at arrival and peak times in the farinograph

Protein subunit	Protein area		Protein percentage area		Network junctions		Network end points		Mean Lacunarity		Co-localization coefficients		
	Arrival	Peak	Arrival	Peak	Arrival	Peak	Arrival	Peak	Arrival	Peak	Protein subunits	Arrival	Peak
LMW	$7778^{b,y}$	$50954^{a,y}$	$4.40^{b,y}$	$20.32^{a,y}$	$45.00^{b,y}$	$468.33^{a,y}$	$168^{b,y}$	$541^{a,y}$	$2.275^{a,x}$	$0.263^{b,x}$	LMW-Gliadin	$0.42^{b,z}$	$0.62^{a,y}$
HMW	$6104^{b,y}$	$36979^{a,z}$	$3.43^{b,y}$	$14.64^{a,z}$	$27.22^{b,y}$	$258.33^{a,z}$	$184^{b,y}$	$739^{a,x}$	$2.232^{a,x}$	$0.270^{b,x}$	HMW-Gliadin	$0.53^{b,y}$	$0.84^{a,x}$
Gliadin	$44055^{b,x}$	$79981^{a,x}$	$17.55^{b,x}$	$30.93^{a,x}$	$367.6^{b,x}$	$675.33^{a,x}$	$689^{a,x}$	$693^{a,x}$	$0.363^{a,y}$	$0.105^{b,y}$	LMW-HMW	$0.81^{a,x}$	$0.79^{a,x}$

[a, b] Numbers with different letters show significant difference between the mixing times (arrival time and peak time) ($p < 0.05$). Statistical analyses were conducted separately for each protein and for each parameter, for instance the protein area of HMW glutenins at arrival time was statistically compared to the protein area of HMW glutenins at peak time only.

[x, y] Numbers with different letters show significant differences between the three different protein subunits (LMW, HMW, and gliadin) ($p < 0.05$). Statistical analyses were conducted separately for

each mixing time and for each parameter, for instance the protein area of HMW glutenins at arrival time was statistically compared to the protein area of LMW glutenins and gliadins at arrival time only.

Gliadins cover more area as seen in channel C of images i-ix (Figure 15). Their more extensive visual distribution over larger areas at arrival time is also corroborated by the quantitative network analysis (Table 3). At arrival time, gliadins show significantly higher protein area, protein percentage area, network junctions, and network end points; and a significantly lower Lacunarity (a measure of the uniformity of the network) than LMW and HMW glutenins (Table 3). For example, gliadins cover 17.55% of the dough area, compared to the 3.43% and 4.40% reported for LMW and HMW glutenins respectively. This is due to the higher mobility of gliadin because of its lower molecular size and the absence of intermolecular disulfide bonds (Bozkurt et al., 2014). As mixing time increases and dough keeps mixing for an additional 5:17 min from arrival to peak time the images displaying LMW and HMW glutenins (Channels A and B) show fewer and less bright points (protein agglomerates) and a more network-like structure. These observations are corroborated with the network analysis data in Table 3, where significant increases in the protein area, protein area percentage, network junctions, network end points; and a decrease in Lacunarity are observed for LMW and HMW glutenins when comparing peak time images to arrival time images. All these changes in the network analysis parameters indicate network development throughout dough mixing from arrival time to peak time. Gliadins also showed a more even and increased distribution at peak time than at arrival time. Significant increases in protein area, protein percentage area, and network junctions; and a significantly lower Lacunarity are all indication of further network development. These results are in accordance with the qualitative description in our earlier study by Bozkurt et al. (2014), where gliadin was found to be more evenly distributed at peak time when compared with other mixing times. The network quantitative analysis of LMW and HMW glutenins show major increases when compared with the change from arrival time to peak time that gliadins undergo. The protein percentage area covered by the LMW and HMW increases from 4.40% to 3.43% at arrival to 20.32% and 14.64% at peak. It is interesting to note that the LMW glutenins are able to spread further compared to HMW glutenins because the LMW glutenins are more mobile compared to the HMW glutenins since their molecular size is considerably smaller than HMW glutenins (~30–50 kDa vs. ~70–100 kDa) and HMW also have

69

a much higher density of intermolecular disulfide bonds (Delcour and Hoseney, 2010). The area covered by gliadin at peak is (30.93%) compared to (17.55%) at arrival time. As indicated above and consistent with our earlier study this is because gliadins are smaller and more mobile and do not have any intermolecular disulfide bonds to prevent their diffusion/distribution.

The visualization of network formation at peak time from the gluten subunit aggregates at arrival time is consistent with Newberry et al. (2004) who imaged aggregates of gluten in under-mixed dough when tagging gluten with an amine-reactive dye; a more even distribution of gluten was detected with optimally mixed dough. We have obtained similar results when gluten was conjugated to quantum dots beautifully imaging the distribution of gluten around starch granules (Sozer and Kokini, 2014). In the current study the network formation process as a function of mixing time of the dough matrix from arrival time (under-mix) to peak time (optimally mixed dough) was visualized by looking at the movement of the 3 subunits forming gluten and offer a more detailed understanding of the molecular behavior of the 3 subunits during mixing. Our results are also consistent with Don et al. (2005) who found a significant amount of glutenin macro polymer in under-mixed doughs, and did not find glutenin macro polymer in optimally mixed doughs. Glutenin macro-polymer is defined as aggregates of LMW and HMW glutenins in wheat dough which are non-extractable with an SDS solution.

The individual qualitative description of the images and the quantitative protein network analysis describe how each gluten protein subunits, especially LMW and HMW glutenins, become more distributed with mixing from arrival time to peak time. Using the co-localization analysis, it is possible to quantitatively link network distribution between the different gluten subunits. In Table 3, the co-localization of LMW with gliadin increases from 0.42 at arrival time to 0.62 at peak time, and the co-localization of HMW with gliadin increases from 0.53 at arrival time to 0.84 at peak time. This indicates that LMW and HMW glutenins not only increase their spatial distribution and form a network-like structure independently but they also co-assemble with gliadin to form one gluten network by interacting through non-covalent bonds such as hydrogen bonds, ionic bonds and hydrophobic bonds (Wieser, 2007). The co-localization analysis data provides molecular insights and understanding of farinograph data of dough strength as a function of dough-mixing time. At arrival time, the dough's mean consistency was 465 BU while at peak, with all three

70

subunits more evenly distributed and highly co-localized the mean consistency goes up to 510 BU. This increase in the strength of the dough is due to this more even distribution of glutenins and their integration with gliadin during dough mixing and are responsible for the gluten network formation, leading to an increased dough strength from arrival time to peak time.

From the co-localization data on Table 3, we can also can see that at the peak time (higher dough strength) the co-localization of HMW glutenin with gliadin (0.84) is significantly higher than the co-localization of LMW glutenin with gliadin (0.62). While they both significantly increased their values from arrival to peak, they were not significantly different at arrival time. The statistically significant higher co-localization between HMW glutenins and gliadins, compared to LMW glutenins and gliadins at peak time is indicative that HMW have a more impactful contribution to the increased distribution in HMW glutenin subunits leading to a high dough strength at peak time compared to the contribution of the LMW subunits. The preferential co-assembly of gliadin with HMW glutenin in comparison with LMW glutenin shows the synergistic interaction between the two, lubricating the movement of HMW glutenin and its help in distributing it throughout the dough matrix. Larger glutenin polymers are more responsible for dough elasticity, due to a higher amount of disulfide bonds formation (Gupta et al., 1991) and the synergistic interaction with gliadin helps the high elasticity glutenin distribute better in the dough making the dough highly viscoelastic. However, this is the first time that the higher impact of HMW glutenins on the gluten network strength has been carefully visualized and measured with direct proof from inside the dough.

4.4.3 Analysis of the distribution of LMW glutenins, HMW glutenins, and gliadins from peak time to departure time

The distribution of LMW glutenins, HMW glutenins, and gliadins in the hard wheat flour dough at peak time (6:34 min of mixing) and departure time (14:02 min mixing) is shown in Figure 16. The nine different dough areas imaged at peak time (images i-ix), and at departure time (images x-xviii) are shown side by side. Each of the nine images is subdivided and displayed in the three different detection channels; The images from channel A (blue) in Figure 16 show that the LMW glutenins that were found evenly distributed at peak time (i-ix), are now aggregated in a few spots with bright emission at departure time (x-xviii). HMW glutenins (channel B) and gliadins (channel C) seem to still have a uniform distribution at departure time. These observations are also

confirmed by the quantitative network analysis in Table 4. In general, we see reduction of the network quantitative parameters as expected since the dough strength is reduced from 510 BU to 480 BU. The HMW glutenins reduced their protein percentage area from 14.6% to 9.1%, and gliadins reduced their protein area from 30.9% to 18.1%. However, the LMW glutenins reduced their protein percentage area from 20.3% at peak time to 7.3% at departure time, showing a much more significant reduction. The protein area was reduced 40% and 42% for HMW glutenins and gliadins respectively, while it was reduced in 67% for LMW glutenins. The decreases in other quantitative network parameters like, network junctions and network end points are also of a larger magnitude for LMW than those of HMW and gliadins from peak time to departure time. For instance, the average number of network junctions is reduced from 468 to 99 for the LMW glutenins; while, the number of network junctions in glutenins and gliadins is reduced from 258 to 130, and from 675 to 333 respectively.
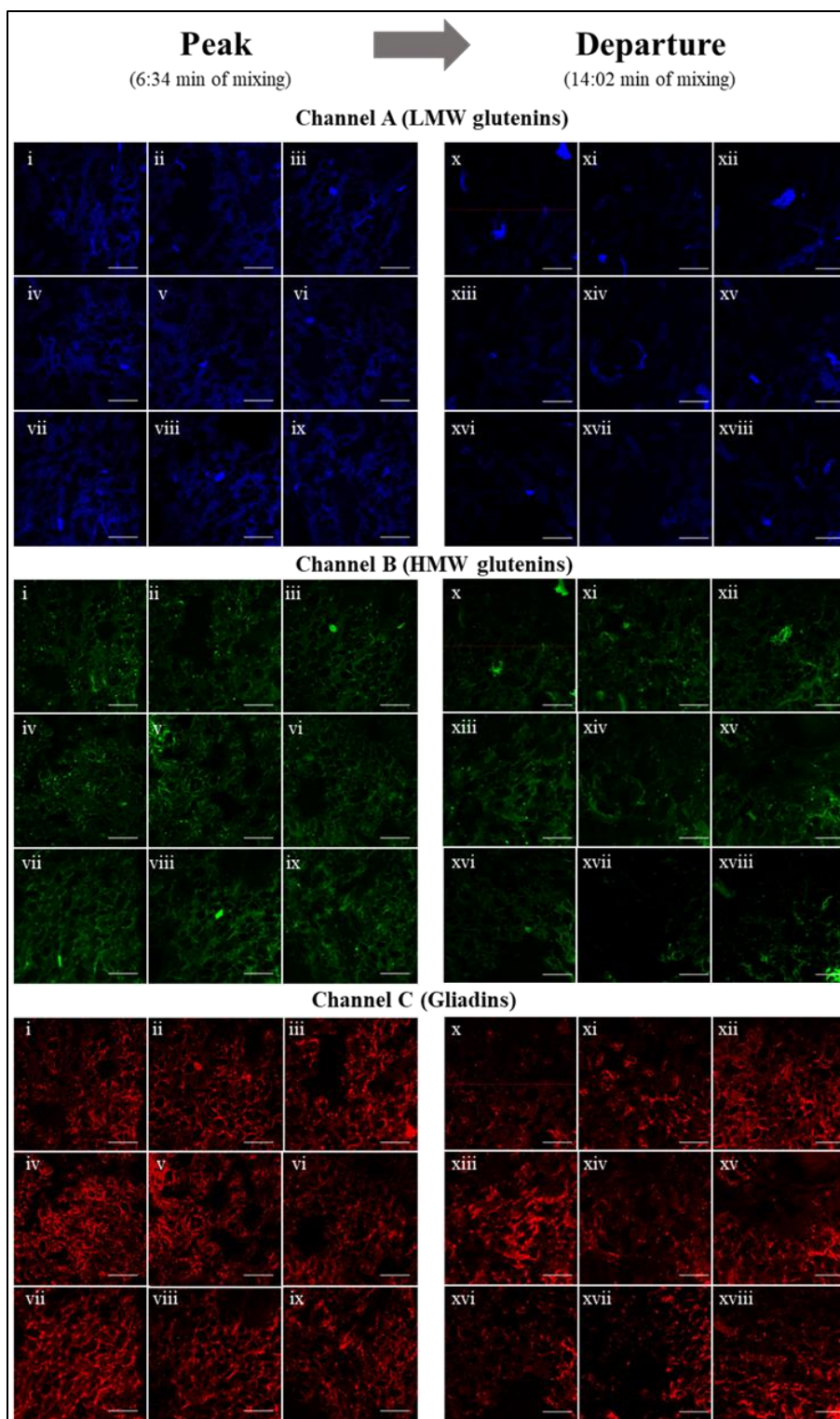
Figure 16. Distribution of LMW glutenins (Channel A), HMW glutenins (Channel B), and Gliadins (Channel C) from nine different areas of wheat dough at peak (i-ix) and departure time (x-xviii) in the farinograph. Bar 50 μm

73

Table 4. Network analysis and co-localization analysis on the fluorescent detection HMW glutenins, LMW glutenins, and Gliadins at peak and departure times in the farinograph

Protein subunit	Protein area		Protein percentage area		Network junctions		Network end points		Mean Lacunarity		Co-localization coefficients		
	Arrival	Departure	Arrival	Departure	Arrival	Departure	Arrival	Departure	Arrival	Departure	Protein subunits	Arrival	Departure
LMW	50954[a,y]	16988[b,y]	20.3[a,y]	7.3[b,y]	468[a,y]	99[b,y]	541[a,y]	367[b,y]	0.26[b,x]	0.99[a,x]	*LMW-Gliadin*	0.62[a,y]	0.53[b,y]
HMW	36978[a,z]	2229[b,y]	14.6[a,z]	9.1[b,y]	258[a,z]	130[b,xy]	738[a,x]	522[b,z]	0.27[b,x]	0.77[a,x]	*HMW-Gliadin*	0.84[a,x]	0.80[a,x]
Gliadin	79981[a,x]	46664[b,x]	30.9[a,x]	18.1[b,x]	675[a,x]	333[b,x]	693[a,x]	770[a,x]	0.10[b,y]	0.28[a,y]	*LMW-HMW*	0.79[a,x]	0.79[a,x]

[a, b] Numbers with different letters show significant difference between the mixing times (peak time and departure time) ($p < 0.05$). Statistical analyses were conducted separately for each protein and for each parameter, for instance the protein area of HMW glutenins at peak time was statistically compared to the protein area of HMW glutenins at departure time only.

[x, y] Numbers with different letters show significant differences between the three different protein subunits (LMW, HMW, and gliadin) ($p < 0.05$). Statistical analyses were conducted separately for each mixing time and for each parameter, for instance the protein area of HMW glutenins at peak time was statistically compared to the protein area of LMW glutenins and gliadins at peak time only.

In this stage of mixing, reduction of network matrices for all gluten subunits are observed, with reductions of higher magnitude for LMW glutenins. This is also attributed to the higher mobility of LMW compared with HMW and the increased aggregation by LMW compared to HMW. Moreover, the co-localization explains how LMW and HMW glutenins interact differently with gliadin from peak time to departure time. In this case, the co-localization of LMW glutenins with gliadin shows a statistically significant reduction from 0.62 at peak time to 0.53 at departure time (Table 4). In addition, the co-localization of HMW glutenins with gliadins does not show a significant reduction from peak time (0.84) to departure time (0.80), which remains significantly higher than the co-localization of LMW glutenins with gliadins. This data shows that LMW glutenins dissociate first from the gluten network formed at peak time by gliadins, LMW glutenins, and HMW.

This information, together with the observations and the protein network analysis, indicate that LMW glutenins tend to agglomerate between peak and departure time much more than HMW glutenins and gliadins. The dissociation of LMW glutenins from gliadins reported by the co-localization factor indicates that they are more responsible for the initial network breakdown and dough strength reduction occurring between peak and departure time. This confirms that HMW

glutenin play a major role in the gluten and dough strength. The LMW glutenins have less intermolecular and intramolecular disulfide bonds, which are broken down more easily by the mechanical energy during mixing and they aggregate together in few areas.

4.4.4 Analysis of the distribution of LMW glutenins, HMW glutenins, and gliadins from departure time to 10 min after departure

The distributions of LMW glutenins, HMW glutenins, and gliadins in the hard wheat flour dough at the departure (14:02 min) and ten minutes after departure time (24:02) are shown in Figure 17. The nine different dough areas imaged at departure time (images i-ix), and at ten min after departure time (images x-xviii) are shown side by side. In this stage the HMW glutenins agglomerate into small areas with very bright emission (channel B, Figure 17). This behavior of HMW glutenins is similar to the behavior of the LMW glutenins from peak time to departure time. The quantitative network analysis shows that the LMW glutenins do not have significant reduction in the quantitative network parameters (Table 5) indicating that LMW glutenins which agglomerated from peak to departure remained agglomerated during the following 10 min of mixing. In the case of HMW glutenins, which did not show aggregation of the same level as LMW glutenins from peak time to departure time, show significant reductions in this stage, in the quantitative network parameters like, protein area, protein percentage area, network junctions, and network end-points; and higher Lacunarity. The protein percentage area decreases from 9.1% at departure to 5.64% at ten minutes after departure. The network junctions reduce from 130 at departure time to 57 ten minutes after departure, the network end-points decrease from 552 to 207 and the Lacunarity increases from 0.77 to 2.11. The data pertaining to all these parameters are in accordance with the few and bright accumulation points of protein that we see in images x-xvii at channel B (Figure 17). These observations can be explained by considering the probability that intermolecular disulfide bonds are ruptured during this stage of mixing reducing the network junctions that were formed in prior stages of mixing consistent with prior observations using SE-HPLC (Haraszi et al., 2008).
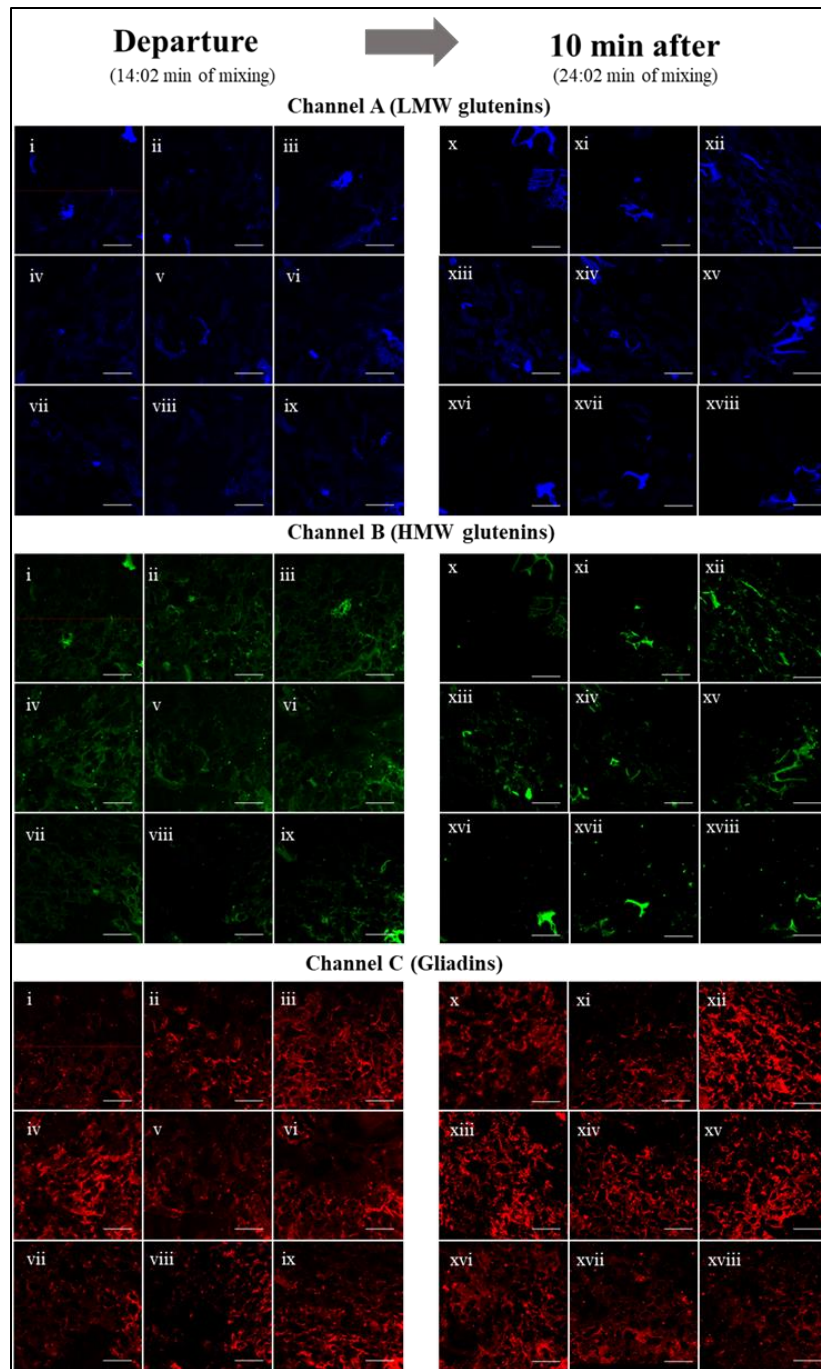
Figure 17. Distribution of LMW glutenins (Channel A), HMW glutenins (Channel B), and Gliadins (Channel C) from nine different areas of wheat dough at departure time (i-ix) and ten minutes after departure time (x-xviii) in the farinograph. Bar 50 µm

Table 5. Network analysis on the fluorescent detection HMW glutenins, LMW glutenins, and Gliadins at peak and departure times in the farinograph

Protein subunit	Protein area		Protein percentage area		Network junctions		Network end points		Mean Lacunarity		Co-localization coefficients		
	Departure	10 min	Departure	10 min	Departure	10 min	Departure	10 min	Departure	10 min	Protein subunits	Departure	10 min
LMW	16988[a,y]	16035[a,x]	7.3[a,y]	7.78[a,y]	99[a,y]	98[a,y]	367[a,y]	270[a,y]	0.99[a,x]	1.87[a,x]	LMW-Gliadin	0.53[a,y]	0.42[b,y]
HMW	22294[a,y]	11995[b,x]	9.1[a,y]	5.64[b,y]	130[a,xy]	57[b,y]	522[a,z]	207[b,y]	0.77[b,x]	2.11[a,x]	HMW-Gliadin	0.80[a,x]	0.41[b,y]
Gliadin	46664[b,x]	71008[a,x]	18.1[b,x]	27.7[a,x]	333[b,x]	587[a,x]	770[a,x]	617[b,x]	0.28[a,y]	0.17[a,y]	LMW-HMW	0.79[a,x]	0.79[a,x]

[a, b] Numbers with different letters show significant difference between the mixing times (departure time and 10 min after departure) (p < 0.05). Statistical analyses were conducted separately for each protein and for each parameter, for instance the protein area of HMW glutenins at arrival time was statistically compared to the protein area of HMW glutenins at peak time only.

[x, y] Numbers with different letters show significant differences between the three different protein subunits (LMW, HMW, and gliadin) (p < 0.05). Statistical analyses were conducted separately for each mixing time and for each parameter, for instance the protein area of HMW glutenins at departure time was statistically compared to the protein area of LMW glutenins and gliadins at departure time only.

Co-localization between LMW glutenins and gliadin decreased from departure (0.53) to ten minutes after departure (0.42) following similar observations from peak to departure (Table 5). More importantly, the co-localization of the HMW glutenins with gliadins is reduced by half, from 0.80 at departure to 0.41 ten minutes after departure. The co-localizations of LMW glutenins with gliadins and HMW with gliadin do not show statistical difference again, same as seen just at arrival time (1:17 min of mixing). This evidence indicates that the agglomeration of HMW glutenins and their dissociation from gliadin are now responsible for the later decay in dough strength from 480 BU to 450 BU. These results in later stages of mixing are also in accordance with Don et al. (2005), they report that the glutenins particles are dissociated in smaller fragments in overmixed doughs. They report that the changes in rheological properties when dough is over-mixed are due to changes in internal structures of the proteins in gluten network. This is consistent with the results of this research, in which the dissociation of LMW glutenins is noticed from peak o departure, and the later dissociation of HMW glutenins is seen after departure time.

4.4.5 Overall observations throughout the dough mixing process

At arrival time, the accumulations of HMW glutenins and LMW glutenins are detected with high intensity in few areas in the sample, at the same locations forming the glutenin macro polymer complex in which HMW glutenins have been described to form a backbone where the LMW glutenins cluster (Lindsay and Skerritt, 1999). In this early stage of mixing gliadins are found to be more distributed among the same sample due to their higher mobility. At peak time both, LMW glutenins, and HMW glutenins distribute more evenly in the sample and significant increases in the protein network analysis for both gluten subunits are detected. The increase in the co-localization factor is related to the increase in the dough resistance to mix from arrival to peak, which is due to the complete protein hydration. Water acts as a plasticizer increasing the proteins' mobility and allowing them to interact through non-covalent bonds such as hydrogen bonds, ionic bonds and hydrophobic bonds, and covalent disulfide bonds, forming the strong gluten network. (Wieser, 2007, Wrigley et al., 2006). At departure time, LMW glutenins are agglomerated in a few spots with high intensity, while gliadins and HMW glutenins are still evenly distributed and highly co-localized. The co-localization factor of LMW glutenins with gliadin decreases, and the protein network parameters decrease in higher magnitude for LMW glutenins. This is due to the higher mobility of LMW glutenins compared to HMW glutenins and the minor amount of disulfide bonds. After departure, the HMW glutenins aggregate in few areas with high intensities coinciding again with the areas of aggregation of LMW glutenins and its co-localization with gliadins and protein network parameters decreases. This is due the continued energy input from the mixing blades which distorts the proteins conformation breaking the numerous disulfide bonds from HMW glutenins lowering then the dough strength (Haraszi et al., 2008). Gliadins stays evenly distributed throughout the entire mixing process when compared to LMW and HMW glutenins, with a better distribution at peak time. Even though LMW glutenins and gliadins are related in their amino acid compositions (Wieser and Kieffer, 2001) they have shown different behavior during dough mixing. The co-localization coefficient of HMW glutenin with LMW glutenin does not present significant changes throughout mixing (~0.80), this result was expected since both subunits have a known affinity, with HMW glutenins serving as a backbone of the glutenin polymer (Lindsay and Skerritt, 1999). Is therefore the difference in the evolution of the co-localization coefficients of gliadin with LMW glutenins, and with HMW glutenins supported by the individual protein network analysis, which serve as evidence of the different behavior of each subunit after peak time mixing time. The

viscosity of the 1.5% SDS-soluble proteins was 1.7 ± 0.08, 2.4 ± 0.18, 2.3 ± 0.19, and 1.9 ± 0.11 mPa s, at arrival, peak, departure, and 10 min after departure respectively. An increase in the viscosity from arrival to peak is attributed do the rupture of the glutenin macro polymer as reported in the literature (Don et al., 2005). The decrease in viscosity after peak is attributed to the LMW glutenins separating from the HMW glutenins in the network, as seen in the co-localization results. This was further demonstrated with the determination of the HMW/LMW throughout the mixing. The HMW/LMW glutenins ratio were 0.72 ± 0.01, 0.72 ± 0.4, 0.71 ± 0.4, and 0.72 ± 0.01 at arrival, peak, departure, and 10 min after departure mixing times respectively. These results serve as additional evidence that the decrease in viscosity after peak is a result of S-S breakdown of the HMW-LMW aggregates and it is not due to molecular breakdown of the proteins during mixing.

4.5 Conclusions

We have successfully applied the multi-spectral fluorescent detection of gliadins, LMW glutenins, and HMW glutenins during dough mixing in a Brabender Farinograph using the official AACCI method 54-21.01 to understand specific changes which occur in the interactions between the key three subfractions (gliadin, LMW and HMW glutenin) of gluten in hard wheat flour dough. The use of co-localization factor has been shown as a useful image analysis technique, which provides significant and reliable data-matrices to measure potential protein-protein interactions in the gluten subunits in dough samples. We have obtained quantitative data and qualitative observations from which we concluded that at early stages of mixing (arrival time) LMW and HMW glutenins form aggregates, which are then distorted to form a uniform network with gliadin when mixed until the dough reaches peak time. The development of this gluten network formed by the assembly of the three gluten subunits is related to the significant increase of dough strength. After additional mixing, the network breakdown and consequent decrease in dough strength occur in two phases; at first, from peak time to departure time, the LMW glutenins dissociate from the network and form aggregates. The second phase comes after departure time when the dough strength keeps decreasing. The HMW glutenins now dissociate from the gliadins and form aggregates, these aggregates are found again in the same locations with the LMW glutenins aggregates. Changes in aggregation of HMW glutenins appear to be the key factor for the continued network disruption and decreased dough strength.

4.6   References

AACC International. Approved Methods of Analysis, 11th Ed. Method 54-21.02. Rheological Behavior of Flour by Farinograph: Constant Flour Weight Procedure. Approved November 8, 1995. AACC International, St. Paul, MN, U.S.A. http://dx.doi.org/10.1094/AACCIntMethod-54-21.02

Ansari, S., Bozkurt, F., Yazar, G., Ryan, V., Bhunia, A., Kokini, J., 2015. Probing the distribution of gliadin proteins in dough and baked bread using conjugated quantum dots as a labeling tool. J. Cereal Sci. 63, 41–48. https://doi.org/10.1016/j.jcs.2014.12.001

Bernklau, I., Lucas, L., Jekle, M., Becker, T., 2016. Protein network analysis — A new approach for quantifying wheat dough microstructure. Food Res. Int. 89, 812–819. https://doi.org/10.1016/j.foodres.2016.10.012

Bonilla, J.C., Bernal-Crespo, V., Schaber, J.A., Bhunia, A.K., Kokini, J.L., 2019. Simultaneous immunofluorescent imaging of gliadins, low molecular weight glutenins, and high molecular weight glutenins in wheat flour dough with antibody-quantum dot complexes. Food Res. Int. 120, 776–783. https://doi.org/10.1016/j.foodres.2018.11.038

Bonilla, J.C., Bozkurt, F., Ansari, S., Sozer, N., Kokini, J.L., 2016. Applications of quantum dots in Food Science and biology. Trends Food Sci. Technol. 53, 75–89. https://doi.org/10.1016/j.tifs.2016.04.006

Bonilla, J.C., Ryan, V., Yazar, G., Kokini, J.L., Bhunia, A.K., 2018. Conjugation of Specifically Developed Antibodies for High- and Low-Molecular-Weight Glutenins with Fluorescent Quantum Dots as a Tool for Their Detection in Wheat Flour Dough. J. Agric. Food Chem. 66, 4259–4266. https://doi.org/10.1021/acs.jafc.7b05711

Bozkurt, F., Ansari, S., Yau, P., Yazar, G., Ryan, V., Kokini, J., 2014. Distribution and location of ethanol soluble proteins (Osborne gliadin) as a function of mixing time in strong wheat flour dough using quantum dots as a labeling tool with confocal laser scanning microscopy. Food Res. Int. 66, 279–288. https://doi.org/10.1016/j.foodres.2014.09.028

Clarke, B.C., Phongkham, T., Gianibelli, M., Beasley, H., Bekes, F., 2003. The characterisation and mapping of a family of LMW-gliadin genes: effects on dough properties and bread volume. Theor. Appl. Genet. 106, 629–635. https://doi.org/10.1007/s00122-002-1091-1

Delcour, J.A., Hoseney, R.C., 2010. Proteins of Cereals, in: Principles of Cereal Science and Technology. American Association of Cereal Chemists, St. Paul, Minnesota USA.

Dhaka, V., Khatkar, B.S., 2015. Effects of Gliadin/Glutenin and HMW-GS/LMW-GS Ratio on Dough Rheological Properties and Bread-Making Potential of Wheat Varieties. J. Food Qual. 38, 71–82. https://doi.org/10.1111/jfq.12122

Don, C., Lichtendonk, W.J., Plijter, J.J., van Vliet, T., Hamer, R.J., 2005. The effect of mixing on glutenin particle properties: aggregation factors that affect gluten function in dough. J. Cereal Sci. 41, 69–83. https://doi.org/10.1016/j.jcs.2004.09.009

Dunn, K.W., Kamocka, M.M., McDonald, J.H., 2011. A practical guide to evaluating colocalization in biological microscopy. Am. J. Physiol. Cell Physiol. 300, C723-742. https://doi.org/10.1152/ajpcell.00462.2010

Gupta, R.B., MacRitchie, F., 1994. Allelic Variation at Glutenin Subunit and Gliadin Loci, Glu-1, Glu-3 and Gli-1 of Common Wheats. II. Biochemical Basis of the Allelic Effects on Dough Properties. J. Cereal Sci. 19, 19–29. https://doi.org/10.1006/jcrs.1994.1004

Gupta, R.B., MacRitchie, F., Shepherd, K.W., Ellison, F., 1991. Relative Contributions of LMW and HMW Glutenin Subunits to Dough Strengh and Dough Stickness of Bread Wheat, in: Gluten Proteins 1990. American Association of Cereal Chemists, St. Paul, Minnesota USA.

Hackenberg, S., Jekle, M., Becker, T., 2018. Mechanical wheat flour modification and its effect on protein network structure and dough rheology. Food Chem. 248, 296–303. https://doi.org/10.1016/j.foodchem.2017.12.054

Haraszi, R., Larroque, O.R., Butow, B.J., Gale, K.R., Bekes, F., 2008. Differential mixing action effects on functional properties and polymeric protein size distribution of wheat dough. J. Cereal Sci. 47, 41–51. https://doi.org/10.1016/j.jcs.2007.01.007

Lindsay, M.P., Skerritt, J.H., 1999. The glutenin macropolymer of wheat flour doughs: structure–function perspectives. Trends Food Sci. Technol. 10, 247–253. https://doi.org/10.1016/S0924-2244(00)00004-2

Lucas, I., Becker, T., Jekle, M., 2018. Gluten Polymer Networks—A Microstructural Classification in Complex Systems. Polymers 10, 617. https://doi.org/10.3390/polym10060617

Manders, E.M.M., Verbeek, F.J., Aten, J.A., 1993. Measurement of co-localization of objects in dual-colour confocal images. J. Microsc. 169, 375–382. https://doi.org/10.1111/j.1365-2818.1993.tb03313.x

Newberry, M.D., Simmons, L.D., Morgenstern, M.P., 2004. Confocal Visualization of MDD dough Development, in: The Gluten Proteins. The Royal Society of Chemistry, Cambridge, UK.

Orsi, A., Sparvoli, F., Ceriotti, A., 2001. Role of Individual Disulfide Bonds in the Structural Maturation of a Low Molecular Weight Glutenin Subunit. J. Biol. Chem. 276, 32322–32329. https://doi.org/10.1074/jbc.M103833200

Osborne, T., 1907. The proteins of the wheat kernel. Carnegie Institution of Washington - Press of Judd and Detweiler, Washington D.C.

Shewry, P.R., Halford, N.G., Belton, P.S., Tatham, A.S., 2002. The structure and properties of gluten: an elastic protein from wheat grain. Philos. Trans. R. Soc. B Biol. Sci. 357, 133–142. https://doi.org/10.1098/rstb.2001.1024

Singh, N.K., Shepherd, K.W., 1988. Linkage mapping of genes controlling endosperm storage proteins in wheat. Theor. Appl. Genet. 75, 628–641. https://doi.org/10.1007/BF00289132

Sozer, N., Kokini, J.L., 2014. Use of quantum nanodot crystals as imaging probes for cereal proteins. Food Res. Int. 57, 142–151. https://doi.org/10.1016/j.foodres.2013.12.031

Wieser, H., 2007. Chemistry of gluten proteins. Food Microbiol., 3rd International Symposium on Sourdough 3rd International Symposium on Sourdough 24, 115–119. https://doi.org/10.1016/j.fm.2006.07.004

Wieser, H., Kieffer, R., 2001. Correlations of the Amount of Gluten Protein Types to the Technological Properties of Wheat Flours Determined on a Micro-scale. J. Cereal Sci. 34, 19–27. https://doi.org/10.1006/jcrs.2000.0385

Wrigley, C., Bekes, F., Bushuk, W., 2006. Gliadin and Glutenin the Unique Balance of Wheat Quality. Presented at the AACC International, St. Paul, Minnesota.

Xu, J., Bietz, J.A., Carriere, C.J., 2007. Viscoelastic properties of wheat gliadin and glutenin suspensions. Food Chem. 101, 1025–1030. https://doi.org/10.1016/j.foodchem.2006.02.057

CHAPTER 5. DISTRIBUTION AND FUNCTION OF LMW GLUTENINS, HMW GLUTENINS, AND GLIADINS IN WHEAT DOUGHS ANALYZED WITH 'IN -SITU' DETECTION AND QUANTITATIVE IMAGING TECHNIQUES

5.1   Abstract

The different gluten subunits, gliadins, LMW glutenins, and HMW glutenins have been reported to play different and key roles in different type of wheat products. This paper studied the interaction between gliadin, LMW and HMW glutenins in soft, hard and durum semolina flour doughs during different stages of mixing. In order to see how do the gluten subunits (gliadin, LMW glutenin and HMW glutenin) redistribute during mixing, dough samples were taken at maximum strength and after 10 minutes of maximum strength. The doughs have been mixed with the same level of added water (55%), therefore they all have different strengths values due to their changes in proteins content. Oscillatory rheological measurements were performed on the doughs. It has been found that HMW glutenins are relatively immobile because of their less molecular mobility and do no redistribute themselves especially at high strength for doughs such as hard wheat flour. LMW glutenins and gliadins on the other hand redistribute themselves at even at high dough strengths forming a more stable network. In weaker doughs such as soft wheat, the breakdown of the three proteins subunits is responsible for the decay in dough strength. We have also visualized how the greater amount of LMW glutenins in semolina is in constant interaction with HMW glutenins and gliadins allowing the dough to maintain a stable strength for an extended mixing time. Finally, we have found the 'in situ' detection and quantitative analysis techniques to be more sensitive to the changes occurring in the gluten network of the dough than the oscillatory rheological analysis.

5.2 Introduction

Wheat is the most important food grain in human diet, it occupies more land area than any other crop for human consumption and it is responsible for the biggest portion of our calorie intake (FAO, 2017). Wheat is consumed all over the world in different products with very different textural properties for example: white bread, donuts, cookies, cakes, crackers, tortillas, chapatis, noodles, and pasta. The main difference between the wheat flour required for the elaboration of this wide variety of products is its gluten content and gluten composition (Finnie and Atwell, 2016). The amount of gluten synthetized by a wheat plant depends on genetics and growing conditions (Delcour and Hosney, 2010). A wheat plant growing under tougher conditions will synthetize more proteins as a mechanism of storing more energy in the seed for its upcoming growing. The storage proteins of wheat kernels are known as gluten proteins.

Gluten proteins are the most studied proteins in food science research. The first classification of wheat protein has been done by Osborne (Osborne, 1907). Wheat proteins are classified by their solubility into non-storage proteins, albumins and globulins, and storage or gluten proteins, gliadins and glutenins. Gliadins are defined as the group of proteins that are soluble in water-alcohol solutions, while glutenins are soluble in diluted acid solutions. When a dough is formed the hydrated gluten proteins, gliadins and glutenins, form a viscoelastic network responsible for the unique rheological properties of wheat doughs. Gliadins have been found to be the major contributor to the viscosity of the gluten viscoelastic network (Xu et al., 2007). The glutenins have been further classified depending on their molecular mobility into high molecular weight (HMW) glutenins and low molecular weight (LMW) glutenins. HMW glutenins have been extensively linked to bakery performance (Branlard and Dardevet, 1985, Gupta et al., 1989, Payne et al., 1988). HMW are especially correlated with dough strength and extensibility due to their intra-molecular and inter-molecular disulfide bonds (Gupta and MacRitchie, 1994). LMW glutenins only form intra-molecular disulfide bonds and more abundant than HMW glutenins. The influence of LMW in quality characteristics of bread making are usually found similar with the influence in quality characteristics of gliadins, contributing on the viscosity of the viscoelastic network (Clarke et al., 2003). However, LMW glutenins have been reported to be the most important gluten subfraction in determining gluten strength and stability in durum wheat (D'Ovidio and Masci, 2004, du Cros, 1987, Sissons et al., 2005). This has been attributed to the greater amount of LMW glutenins

present in durum semolina, allowing more LMW molecules to interact with HMW subunits, keeping the dough strength stable (Edwards et al., 2003).

The majority of the studies investigating the individual contribution of gluten subunits, gliadins, LMW glutenins, and HMW glutenins have been performed through extraction and reconstitution methods. A great deal of information has been gained in the last decades by using these methods, however they present a fundamental disadvantage. The extraction and reconstitution methods have not been able to match the characteristics of a native dough system due to the conformational changes in the proteins during extractions. More recently imaging studies in wheat dough have been achieving the level of specificity necessary to study individual gluten subunits by themselves, for example gliadins have been tracked during different processes (Ansari et al., 2015, Bozkurt et al., 2014, Sozer and Kokini, 2014). Subsequently, Bonilla et al. (2018) developed specific antibodies for HMW glutenins and LMW glutenins and conjugated them with different color quantum dots (QDs). These antibodies-QDs complexes have been used along with gliadin antibodies also coupled with QDs to develop a multispectral simultaneous detection of HMW glutenins, LMW glutenins, and gliadins in wheat doughs (Bonilla et al., 2019a). This methodology was then applied to track how the three different gluten subunits distribute and interact at four characteristics mixing times of hard wheat flour in a Brabender Farinograph (Bonilla et al., 2019b). This latest research provided the first 'in situ' insights of the role of each individual gluten subunit at different levels of dough strength by not only showing descriptive images of the proteins but also introducing the use of a quantitative tool for image analysis called 'co-localization coefficient'. The 'co-localization coefficient' was used to analyze how different proteins subfractions interact during dough mixing.

The objective of this research is to study the mechanism of interaction of LMW glutenins, HMW glutenins, and gliadins in soft, hard and semolina wheat doughs with very different mixing regimes caused by different gluten levels and gluten composition at constant moisture content of 55%. Our goal is to understand how the differences in the type and quantity of gluten subunits contribute use the new available antibodies-QDs complexes, the simultaneous multispectral detection methods, and quantitative image analysis tools to gain more fundamental insights of the role of each gluten units in general, not only for breadmaking or pasta making.

5.3 Materials and Methods

5.3.1 Wheat dough preparation

Wheat flour doughs were prepared using soft red winter wheat flour, hard red winter wheat flour generously provided by Siemer milling company (Teutopolis, IL), and durum semolina from Fowlers milling Co (Chardon, OH). The doughs were prepared following the AACCI method 54-21.02. Water was added to a 55% level; this water level was chosen because it is the middle point between the optimal water absorption levels for the different flours. The moisture of the wheat flours was determined using a rapid moisture analyzer (Mettler Toledo, Columbus, OH). The amount of flour used in each test was adjusted depending on their moisture. The peak time (dough's maximum strength) of each dough was recorded and the doughs were kept mixing for a total of 25 minutes. Three samples were collected at their respective peak time and 10 minutes after their peak time. The strength of the dough is reported in Brabender units (BU). The 500 BU line is used as a quality standard for gluten network development in wheat doughs.

5.3.2 Determination of the Glutenin to Gliadin ratio

Osborne separation method was used to separate gluten from gliadins and glutenins. Gluten was separated from dough by manual washing with 3% NaCl in water. The gluten was then suspended in 1 L of 70% (v/v) ethanol and stirred on magnetic stirrer for 3 h at room temperature followed by centrifugation at 5,000×g for 10 min in cooling centrifuge at 4 °C. The extraction was repeated three times. The precipitant was collected as glutenins and the supernatant was subjected to vacuum oven at 30 ºC to remove ethanol and recover the gliadins.

5.3.3 Extraction and SDS-PAGE characterization of Glutenins

Glutenins were extracted by adding 1g of each flour in a NaCl solution (0.5 M) to remove albumins and globulins (Dhaka and Khatkar, 2015). The flour pellets were washed and resolubilized in 70% ethanol no remove gliadins. The residue was then solubilized in 50% (v/v) propan-2-ol, 0.08 M Tris–HCl (pH 8.0) and 1% (w/v) dithiothreitol (Fisher Scientific, Hamptom, New Hampshire, USA). at 60 °C for 90 min. The samples were centrifuged at 15,000×g for 30 min. Glutenins were solubilized in the supernatant, which was collected. Acetone was added to a final concentration of

(80%) to precipitate the glutenins. The glutenins were collected and oven dried at 60 °C for 10 minutes. Sodium Dodecyl Sulfate–Polyacrylamide Gel Electrophoresis (SDS–PAGE) was performed to characterize the extracted glutenins (Bonilla et al., 2018). The gels were made with 12% acrylamide (Bio-rad, Hercules, California, USA). 10 mg of the purified glutenins samples were dissolved in 1 ml from a sample made of 1.6g SDS in 4ml of dd-water, 4 ml glycerol, 14 um 2-mercaptoethanol, 4 ml Tris (1M).

5.3.4 Determination LMW/HMW ratio

The ratio of LMW glutenins to HMW glutenins was determined using previous a published methodology with some modifications (Dhaka and Khatkar, 2015). The pictures of the gel were taken in a ChemiDoc MO Imaging System (Bio-Rad, Hercules, California, USA). The images were analyzed with the imaging software ImageJ. The ratio of the LMW/HMW glutenins was calculated by plotting the total intensities of the LMW bands divided by the total intensities of the HMW bands. Three replicates were completed for each flour.

5.3.5 Preparation of dough samples for imaging

The sample preparation method was performed following previous published articles (Bonilla et al., 2016, 2019b). In this method, small pieces of dough are taken from the Farinograph mixing bowl at specific mixing times. In this case, the samples were collected at their peak time and 10 minutes after their peak time for each dough. The sample were places on 'tissue-tek' cryomolds (Fisher Scientific, Hamptom, New Hampshire, USA) and covered with Optimum Cutting Temperature (OCT) compound (Fisher Scientific, Hamptom, New Hampshire, USA) The samples were enclosed with aluminum foil and immersed liquid nitrogen. Samples were store in a -80 °C freezer. The samples were then cryo-sectioned using a LEICA CM 1860 Cryostat (Leica Biosystems, Wetzlar, Germany) at -20 °C. The thickness of the cut was set-up to 10 μm in the cryostat. The 10-μm sections of dough were placed on hydrophilic microscope slides and immersed for ten minutes in methanol and then air-dried. The LMW and HMW glutenins antibodies previously developed (Bonilla et al., 2018), along with the 4F3 gliadin antibody (Fisher Scientific, Hamptom, New Hampshire, USA). Were conjugated with 525 nm, 585 nm, 655 nm QDs respectively. The mixture of the three antibodies-QDs complexes were spread over the

different dough samples and incubated for 30 min at room temperature. The samples were washed with Phosphate-Buffered Saline PBS (Fisher Scientific, Hamptom, New Hampshire, USA) three times to remove unbound antibodies-QDs complexes.

5.3.6 Confocal Laser Scanning Microscopy analysis

The stained wheat dough samples were analyzed under a Confocal Laser Scanning Microscope, Zeiss LSM 880 (Carl Zeiss Microscopy, Oberkochen, Germany). The Zeiss LSM 880 is equipped with three adjustable detection filter sets. The filter set were adjusted to 525 nm, 585 nm, and 655 nm in order to detect the anti-LMW, anti- HMW, and anti-gliadin antibodies individually. The samples were excited with a 405 nm laser in the confocal system. The samples were visualized using a Zeiss Plan Apo 20×/0.8NA. Three areas from each of the three different samples for each mixing times were collected. The images consist of 512 x 512 pixels with a resolution of 0.35 μm/pixel. The samples were analyzed using the Zeiss ZEN blue edition software. The software records an overlapped image of the three channels and an image form each channel (525 nm, 585, nm, and 655 nm).

5.3.7 Co-localization quantitative imaging analysis

The co-localization analysis was run in the Zen blue edition software. The co-localization coefficient is used to measure the overlap between the distribution of one gluten subunit relative to a different gluten subunit. In order to perform this analysis, the image of one channel is overlapped with the image from another channel (Manders et al., 1993). In other words, the image of one gluten subunits with the image of another gluten subunits from the same dough area. Based on preliminary data, two co-localization coefficients were collected per image, the co-localization coefficient between the HMW glutenins with gliadins, and the co-localization coefficient between LMW glutenins with gliadins. This co-localization analysis is performed pixel by pixel in the 262,144 pixels of the collected images. The co-localization analysis is a number between '0' and '1', with 0 indicating no overlapping between the distribution of the two gluten subunits, and '1' indicates that all the pixels showing emission for one gluten subunit are exactly in the same location that the pixels for the other gluten subunits. The changes in co-localization of different

gluten subunits have been as an indicative of interactions between different gluten subunits during wheat dough mixing. (Bonilla et al., 2019b).

5.3.8 Quantitative protein network analysis

The images were analyzed using the AngioTool64 software. Angiotool64 is software that gives quantitative parameters of network characteristics from fluorescent imaging of gluten in dough samples (Bernklau et al., 2016). The protein network analysis offers information on, protein percentage area, which in this case, indicates what percentage of the area of the sample is being covered by the network formed by that specific gluten subunits; number of network junctions, number of network end points, and mean lacunarity. Lacunarity is a metric that represents the variance in the size of the gaps of the network. When the gaps in the gluten network are uniform in size, the lacunarity is low, this low value represents a well-formed network, when the gaps have a high variability in size, the lacunarity is high and the proteins are forming a much less even network. All the parameters are important for the quantitative description of the network. The protein network parameters of the image from each channel (each gluten subunit) were analyzed individually in order to capture the changes in network formation of each gluten subunits during the mixing of each of the different doughs.

5.3.9 Oscillatory rheological analysis

Oscillatory measurements were conducted in a Discovery HR-3 Rheometer (TA Instruments, New Castle Delaware, USA). A 40-mm crosshatched parallel plate geometry was used and sand paper placed below the sample to prevent sample slip from the surface of parallel plates. Amplitude sweeps were carried out between 0.01 and 200% strain at 1 rad/s. Frequency sweeps were conducted between 1 and 100 rad/s applying at 0.025% strain. At 0.025% all samples were in their linear region.

5.4 Results and Discussion

5.4.1 Mixing and protein characterization

Farinograph peak times were 1:14 min, 2:47 min, and 5:58 min for soft wheat, hard wheat, and semolina respectively with 55% water added. At their peak the consistency was 450 BU, 650 BU, and 530 BU for soft wheat hard wheat, and semolina flour doughs respectively. The Farinograph consistencies of soft wheat, hard wheat and semolina dropped 100 BU, 80 BU, and 30 BU respectively after 10 minutes of mixing. The complete Farinogram from each flour can be seen in Figure 18. It must be noted that unlike classical Farinograph mixing curves which are obtained at 500 BU water absorption level these farinograms are obtained at constant moisture content in order to focus on the impact of the protein and protein content on the development of the three different flours. The peak times during dough development (DDT) are correlated with the protein level of the flours. Flours with more protein show a prolonged development time and higher stability doughs. Hard wheat flour doughs showed prolonged peak time compared to soft wheat doughs due to higher protein content. Table 6 summarizes the mixing characteristics at 55% moisture content as well as the protein composition of each wheat flour. The ratios of the extracted total glutenins to gliadins was 1.09, 1.00, and 1.64, for soft wheat, hard wheat and semolina respectively. The LMW/HMW ratio analyzed by the SDS-PAGE image analysis were 2.24, 2.08, and 3.46 for soft wheat, hard wheat, and semolina respectively. Interestingly the LMW/HMW ratios also follow the gliadin to glutenin ratios. Soft wheat contains 3.83% gliadins, 2.80% LMW glutenins, and 1.37% HMW glutenins; hard wheat contains 5.5% gliadins, 3.71% LMW glutenins, and 1.79% HMW glutenins; and semolina contains 5% gliadins, 6.36% LMW glutenins, and 1.84% HMW glutenins.
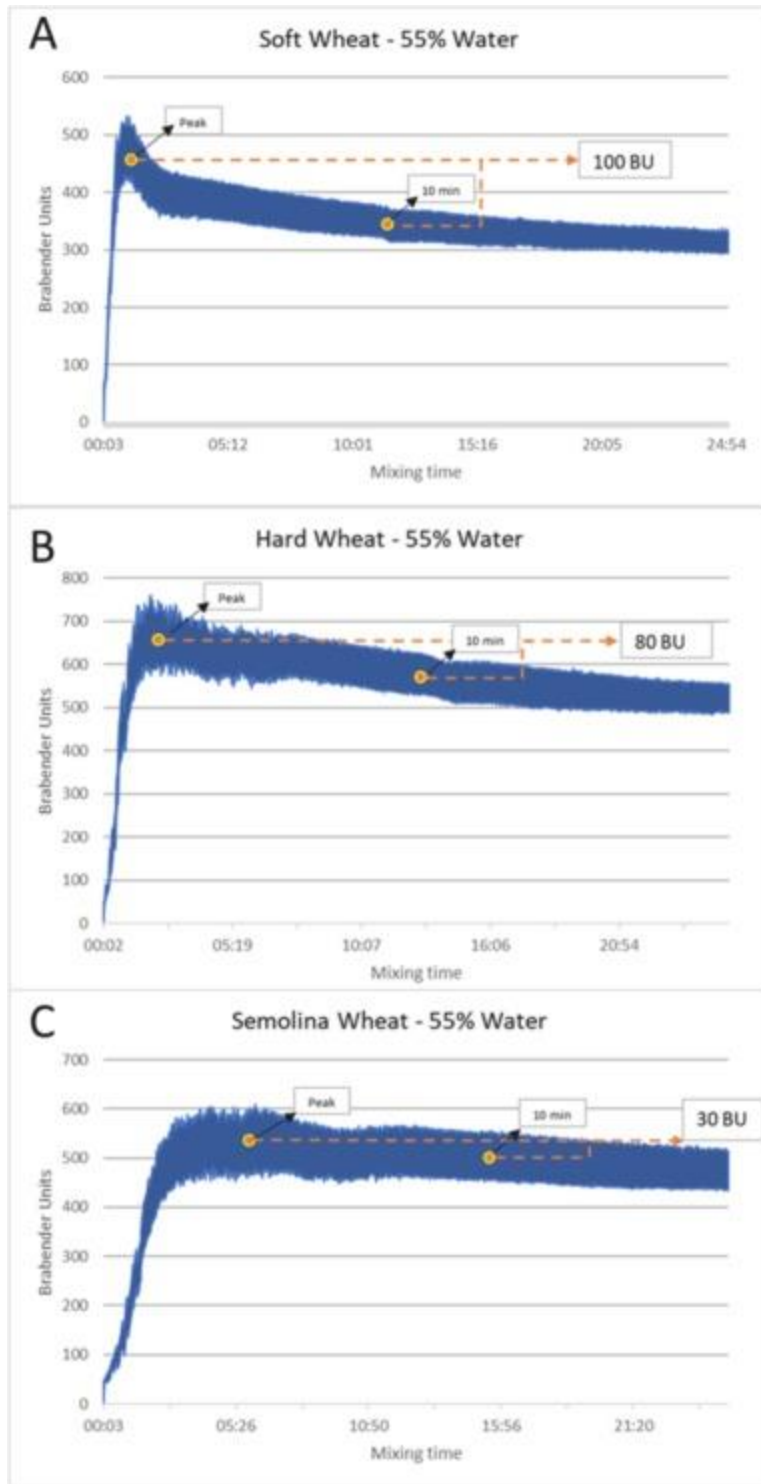
Figure 18. Farinograms of soft wheat (A), hard wheat (B), and semolina (C) with 55% added moisture.

Table 6. Mixing characteristics and protein composition of soft wheat, hard wheat, and semolina.

Flour	Peak time	Protein content (Dry basis)	Glutenin/gliadin ratio	LMW/HMW glutenins ratio	Moisture content
Soft wheat	1:14 min	8.00%	1.09 : 1	2.24 : 1	12.92% ± 0.04%
Hard wheat	2:47 min	11.00%	1 : 1	2.08 : 1	13.02% ± 0.01%
Semolina	5:58 min	13.20%	1.64 : 1	3.46 : 1	12.62% ± 0.02%

5.4.2 Changes in gluten subunits distribution during soft wheat flour mixing

Figure 19 shows a summary of the changes in the spatial distribution using co-localization analysis, protein network analysis and fluorescence imaging of the three protein subunits, gliadins, LMW glutenins, and HMW glutenins, from peak mixing time to mixing 10 minutes after the peak time. At peak time (450 BU) the co-localization coefficients of gliadin with HMW glutenins and gliadin with LMW glutenins are 0.76±0.03 and 0.61±0.04 respectively (Figure 19A). 10 minutes of mixing (350 BU) the co-localization coefficients decreased to 0.75±0.15 and 0.56±0.09. While there is no noticeable change in mean value of the co-localizations, there is a considerable difference in the distribution of the data of the co-localization between gliadin and HMW glutenins. At peak time the co-localization coefficients for gliadin with HMW glutenins from the nine different imaged areas range from 0.72 to 0.81, and 10 minutes after peak time it varies between 0.51 and 0.94. Figure 19B help us visualize this increased in variability of the co-localization of gliadins with HMW glutenins with three different images for each mixing time. At peak time the red channel and green channel representing gliadin and HMW glutenins respectively gave co-localization coefficients of 0.76, 0.77, and 0.74 resulting in an image with an orangish color caused by the overlap between the red and green colors the result of strong co-localization of the protein subunits. On the other hand, 10 minutes after mixing there was a lot of variability in the co-localization coefficients with some at 0.94, an indication of almost perfect mixing and overlay, while others showed much lower co-localization coefficients. These lower co-localization coefficients were the result of only partially mixed gliadin (red network) with separate green agglomerates for HMW glutenins, giving co-localization coefficients of 0.62, and 0.51, much lower than the case where there was efficient mixing with a co-localization coefficient of 0.94. The green agglomerates of HMW glutenins in some areas of the dough samples after 10 minutes of mixing are responsible for the decay in the dough's strength during mixing. These results are consistent with earlier findings that reported that HMW glutenins are the most responsible

subfractions for dough resistance and extensibility (Gupta et al., 1991, Gupta and MacRitchie, 1994). The agglomeration of HMW glutenins played an important role in the advanced stages of network disruption with hard wheat flour with 58.8% added water (Bonilla et al., 2019b). The results from hard wheat dough from Bonilla et al. (2019b) are comparable with these results of soft wheat flours since in they are both looking at the role of HMW glutenins during dough disruption stage (below the 500 BU line).
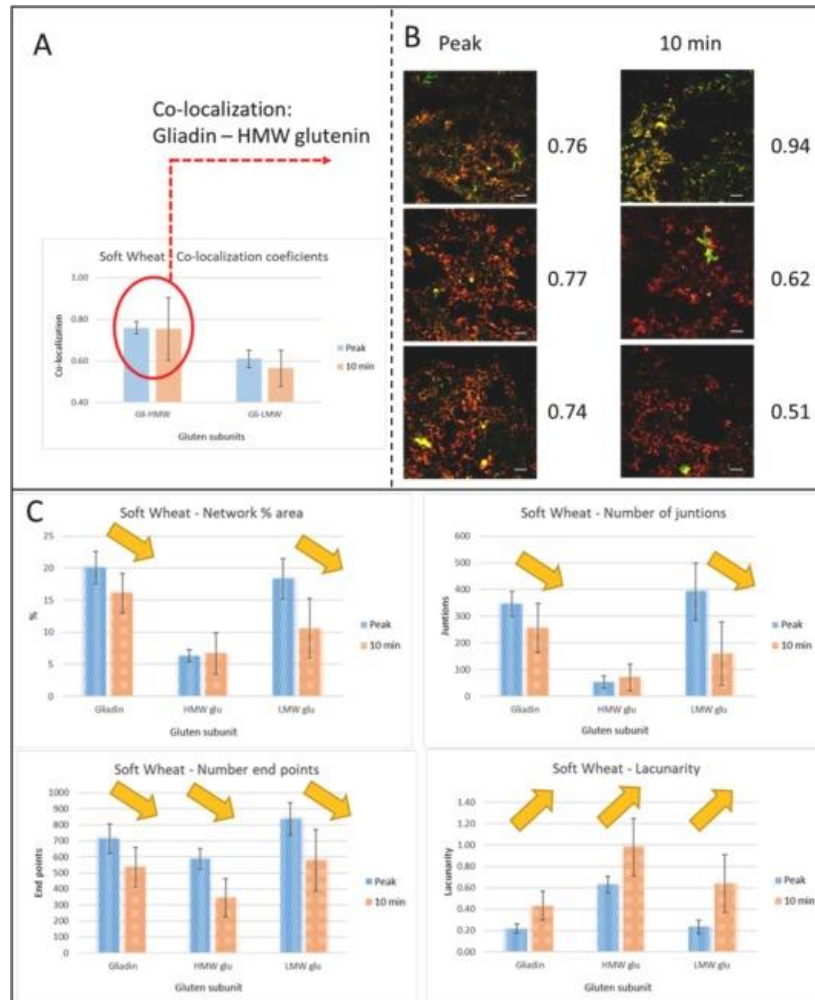
Figure 19. Summary of results in soft wheat flour dough mixing at peak time (blue bars) and 10 min after peak (orange bars). (A) Co-localization coefficients of gliadins-HMW glutenins, and gliadins- LMW glutenins. (B) Images showing the co-localization between gliadin-HMW glutenins. (C) Protein network analysis results for gliadins, HMW glutenins, and LMW glutenins. Scale bar: 50 μm. Error bars: standard deviation. Each column contains nine data points (three measures from three differences pieces of dough)

Figure 19C shows the changes in the protein analysis parameters obtained with the PNA software of the network formed by each protein subunit from peak mixing time to mixing time of 10 minutes after peak. The network formed by gliadins and LMW glutenins individually undergo a decrease in the area they cover and in the number of junctions when mixed for 10 min after peak time. Moreover, the network formed by each of the three gluten subunits presents a reduction in number of end points and an increase in lacunarity a measure of the disruption in the network as a result of mixing. Therefore, the reduction in dough strength during soft wheat flour mixing is also due to the decrease of network characteristics of three different gluten subunits, LMW glutenins, HMW glutenins, and gliadins.

5.4.3   Changes in gluten subunits distribution during hard wheat flour mixing

Figure 20 shows a summary of the changes in the spatial distribution of LMW glutenins, HMW glutenins, and gliadins from peak time to 10 minutes after the peak time for hard flour. During the 10 minutes of mixing after peak time the consistency of the dough decreased from 650 BU to 570 BU. At 650 BU (peak time) the co-localization coefficients of gliadin-HMW glutenins and gliadin-LMW glutenins are 0.82 ± 0.08 and 0.52 ± 0.06 respectively (Figure 20A). At 570 BU (10 minutes of mixing) the co-localization coefficients are 0.82 ± 0.06 and 0.70 ± 0.06. The significant increase in co-localization of gliadins-LMW glutenins from peak to 10 minutes after peak can be visualized in more detail with three images in Figure 20C.
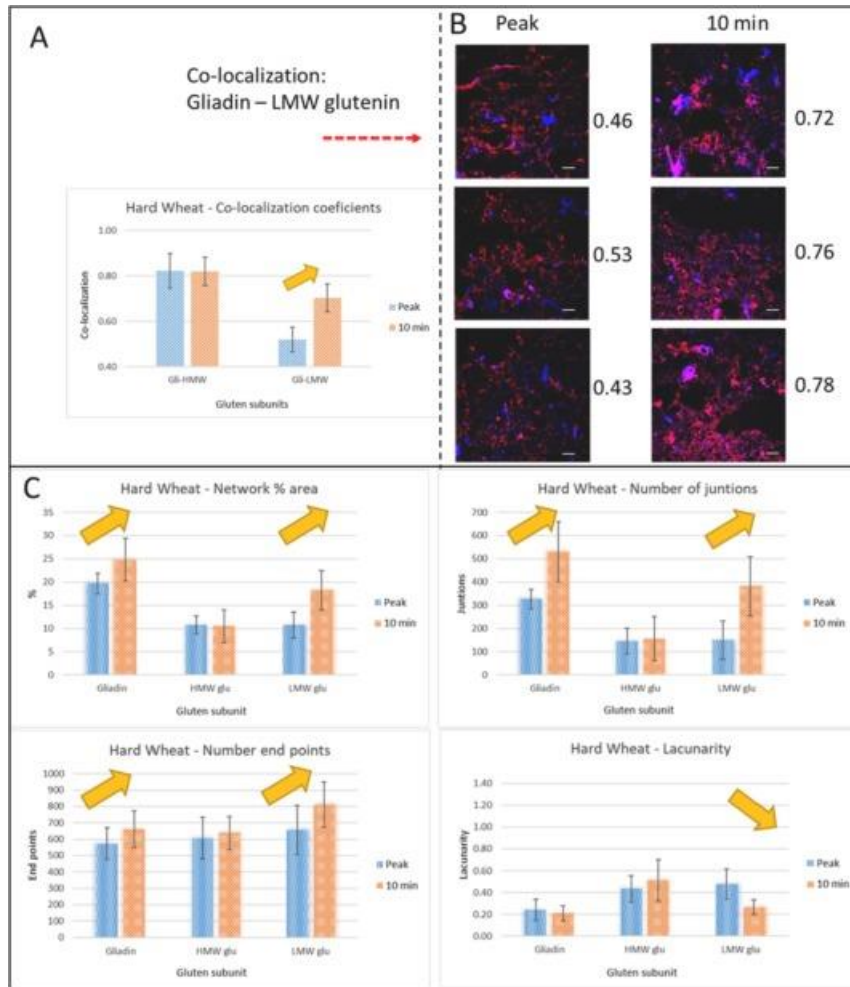
Figure 20. Summary of results in hard wheat flour dough mixing at peak time (blue bars) and 10 min after peak (orange bars). (A) Co-localization coefficients of gliadins-HMW glutenins, and gliadins- LMW glutenins. (B) Images showing the co-localization between gliadin-LMW glutenins. (C) Protein network analysis results for gliadins, HMW glutenins, and LMW glutenins. Scale bar: 50 μm. Error bars: standard deviation. Each column contains nine data points (three measures from three differences pieces of dough)

In the overlay of the images from gliadin (red) and LMW glutenins (blue) at peak time many red-only and blue-only areas can be seen, showing why the co-localization coefficient is so low at peak time. After ten minutes of mixing (570 BU), when the dough is closer to the 500 BU line the increase in the co-localization of the gliadins and LMW glutenins can be overserved with a change in color to purple/violet compared to the red color for gliadins and blue color for LMW glutenins the result of the red and blue channels being overlaid due to the increasing interaction between gliadins and LMW glutenins. The co-localization of gliadin-HMW glutenins does not change

much during this stage of mixing. The network characteristics of HMW glutenins does not change either at 10 minutes of mixing after peak time. Gliadins show an increase in the area covered, an increase in the number of junctions, and an increase in the number of endpoints; LMW glutenins on the other hand show an increase in all networking characteristics including lacunarity, which means that the network formed by the LMW glutenins distributives more uniformly.

Overall, these results show and increase in the gluten network characteristics of the hard wheat dough when mixed for 10 minutes after its peak time with 55% added water. This increase in gluten network despite the 80 BU decrease in dough strength is because during this mixing time the dough is moving towards the 500 BU quality line, doughs above or below that line does not show optimal gluten characteristics (too stiff or too weak). In this case the increase of the gluten network is due to the redistribution and reorganization of LMW glutenins and gliadins specifically, while HMW glutenins do not play a significant role in that specific mixing stage. These results are explained with the significant less molecular mobility of HMW glutenins due to their molecular size and also extensive intermolecular disulfide bond presence which increases molecular binding and dramatically reduces mobility of HMW glutenins. The coupling of the molecular size and S-S bonding with reduction in the optimal level of plasticizer (water) increases the resistance to deformation considerably resulting in higher BUs than observed when the optimal water level is added and the 500 BU line is reached. The LMW glutenins and gliadins as well as the fact that the density of intermolecular S-S bonds is lower in these two fractions results in much greater mobility compared to HMW glutenins.

5.4.4 Changes in gluten subunits distribution during semolina mixing

Figure 21 shows a summary of the changes in the spatial distribution of LMW glutenins, HMW glutenins, and gliadins from peak time to 10 minutes after the peak. During the 10 minutes of mixing after peak, the consistency of the dough decreased from 530 BU to 500 BU. At 530 BU (peak time) the co-localization coefficients of gliadin-HMW glutenins and gliadin- LMW glutenins are 0.90±0.02 and 0.73±0.06 respectively (Figure 21A). At 10 minutes of mixing the co-localization coefficients are 0.90±0.01 and 0.74±0.08. Figure 21B illustrates the similarity in the co-localization coefficients at peak time and 10 minutes after peak. Two images with overlays of gliadin-HMW glutenins and of the gliadin-LMW glutenins with a comparison of networking

behavior at peak time and 10 minutes after peak are shown side by side. No difference in color and/or aggregates its observed. Figure 21C shows no significant changes when analyzing the network parameters of each subunit at peak and ten minutes after peak. These results show that the stability of the semolina during mixing is correlated with the internal distribution of the gluten subunits. The stability of semolina in the faringraph is related to the high amount of LMW glutenins present. In the SDS-PAGE experiments it was found that semolina has an LMW:HMW ratio of 3.76:1, this indicates that the LMW glutenins in semolina are 78% of the total glutenins. This result is consistent with earlier studies where durum glutenin was shown to be composed of~ 80% LMW and 20% HMW (Payne et al., 1984). LMW and HMW subunits are interacting in the gluten network, with a model of large HMW glutenins as a backbone and small LMW glutenins attached to them (Delcour and Hosney, 2010; Lindsay and Skerritt, 1999). In this case, with a significantly larger amount of small LMW molecules the number of associative groups per unit weight increases. The large amount of LMW glutenins bring a large amount of intramolecular disulfide bonds that keep changing during mixing, this leads to the different protein molecules to interact in between them during mixing. Mechanical force from mixing disrupts disulfide bonds, leaving free thiols that can re-associate forming new disulfide bonds. It is because of this reason that the interactions of LMW and HMW glutenins specifically in durum semolina have been described to follow the associative polymer model (Edwards et al., 2003, Payne et al., 1984, Plazek and Frund, 2000)..In this model, the LMW glutenins are being detached from the HMW backbone by mechanical disruption during mixing, however due to the excessive amount of LMW glutenins, all the other unattached LMW glutenins in the system constantly fill the gaps and gluten network does not get disrupted, therefore maintaining the dough strength stable. The dissociation of LMW and HMW in hard wheat was also proven by Bonilla et al. (2019b), where as a function of mixing time LMW started to be less co-localized from the 3-protein network formed at peak with ideal water absorption level. The dissociation seen in the images and measured with the image analyses was also proven by a decrease in the solubility of the 1.5% SDS soluble proteins with no changes in the LMW/HMW ratio, which is an indicator of LMW glutenins being detached from HMW glutenins backbones in hard wheat dough with significantly less amount of LMW glutenins compared to durum semolina. The images from this research in addition to the quantitative image analysis results represent the first 'in situ' visualization and measurements of this associative polymer phenomena in durum semolina during ten minutes of mixing.
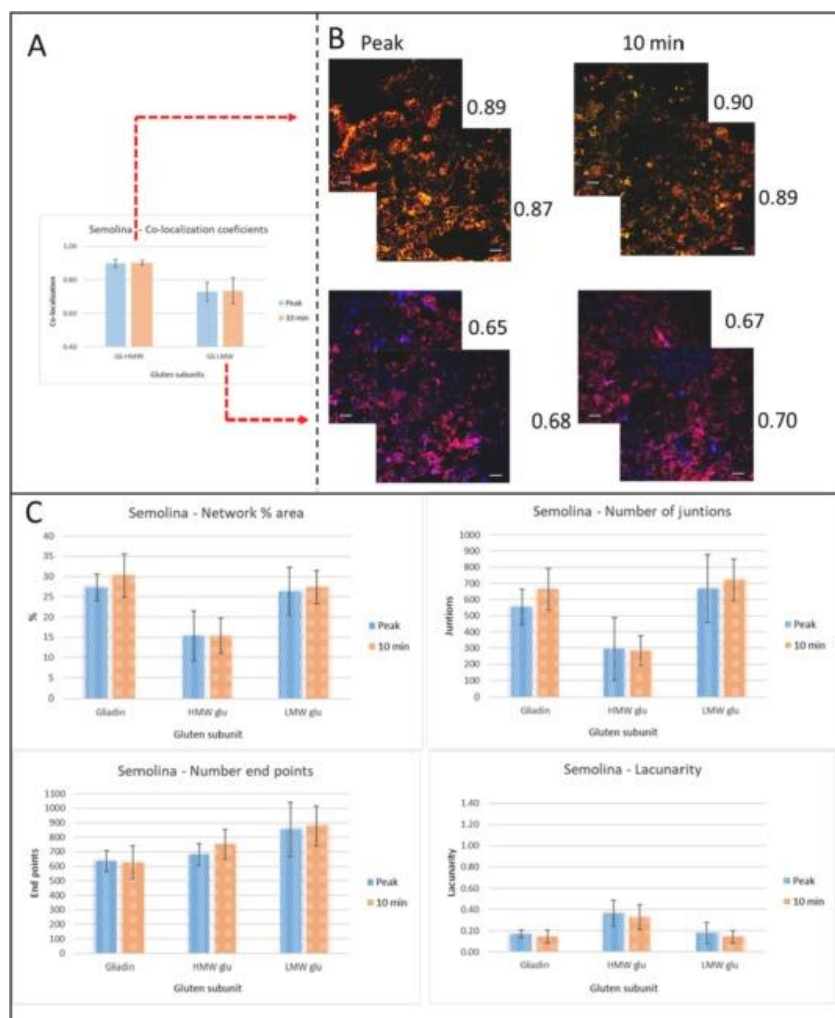
Figure 21. Summary of results in Semolina flour dough mixing at peak time (blue bars) and 10 min after peak (orange bars). (A) Co-localization coefficients of gliadins-HMW glutenins, and gliadins- LMW glutenins. (B) Images showing the co-localization between gliadin-LMW glutenins, and gliadin-HMW. (C) Protein network analysis results for gliadins, HMW glutenins, and LMW glutenins. Scale bar: 50 μm. Error bars: standard deviation. Each column contains nine data points (three measures from three differences pieces of dough)

5.4.5   Comparison between oscillatory rheological data and imaging analyses

Figure 22 shows the frequency sweep and amplitudes sweep for soft wheat, hard wheat, and semolina at their peak time and 10 minutes after peak. In the rheological data, soft wheat shows a higher G' value for the dough mixed until peak time compared with the dough mixes for 10 more minutes. A slight increase in the rate of decay is reported at large deformations in the soft wheat dough mixed 10 minutes after peak, which is an indication of a weaker network. These results are in compliance with the farinograph data (100 BU decay) and network analysis data, where the

subunits (LMW glutenins, HMW glutenins, and gliadins) lose network characteristics. The small changes seen in the soft wheat amplitude sweep graph are also due to the graphs plotted in log' vs log'. For instance, the raw G' values at 0.1% strain are 25193 and 17117 for peak time and 10 minutes after peak time respectively. And, the values at 200% strain are 1002 and 699 for peak time and 10 minutes after peak time respectively. In hard wheat, G' values almost over impose for the dough mixed at peak and the dough mixed 10 minutes after peak despite the fact that the dough mixed for ten minutes after is significantly weaker in the Brabender farinograph. The rheological oscillatory measurements consider the material's strength and the molecular network arrangement, while the farinograph mixer considers only the resistance to mixing of the dough (dough strength). When considering the material's network, this result is in accordance with the increase gluten network development driven by LMW glutenins and gliadins during that mixing time found by the 'in situ' detection and image analysis. Therefore, in the hard wheat flour case, the loss of dough strength during mixing is compensated by the build-up in gluten network, giving similar G' values. In semolina, G' values in the frequency sweep are very close and follow the same trend at peak time and ten minutes after peak times. G' values over impose each other in the amplitude sweeps. This is in accordance with the small 30 BU decay in dough resistance in the farinograph results and the results from the 'in situ' gluten network analysis where no notable changes are detected in the network characteristics of the three different gluten subunits.
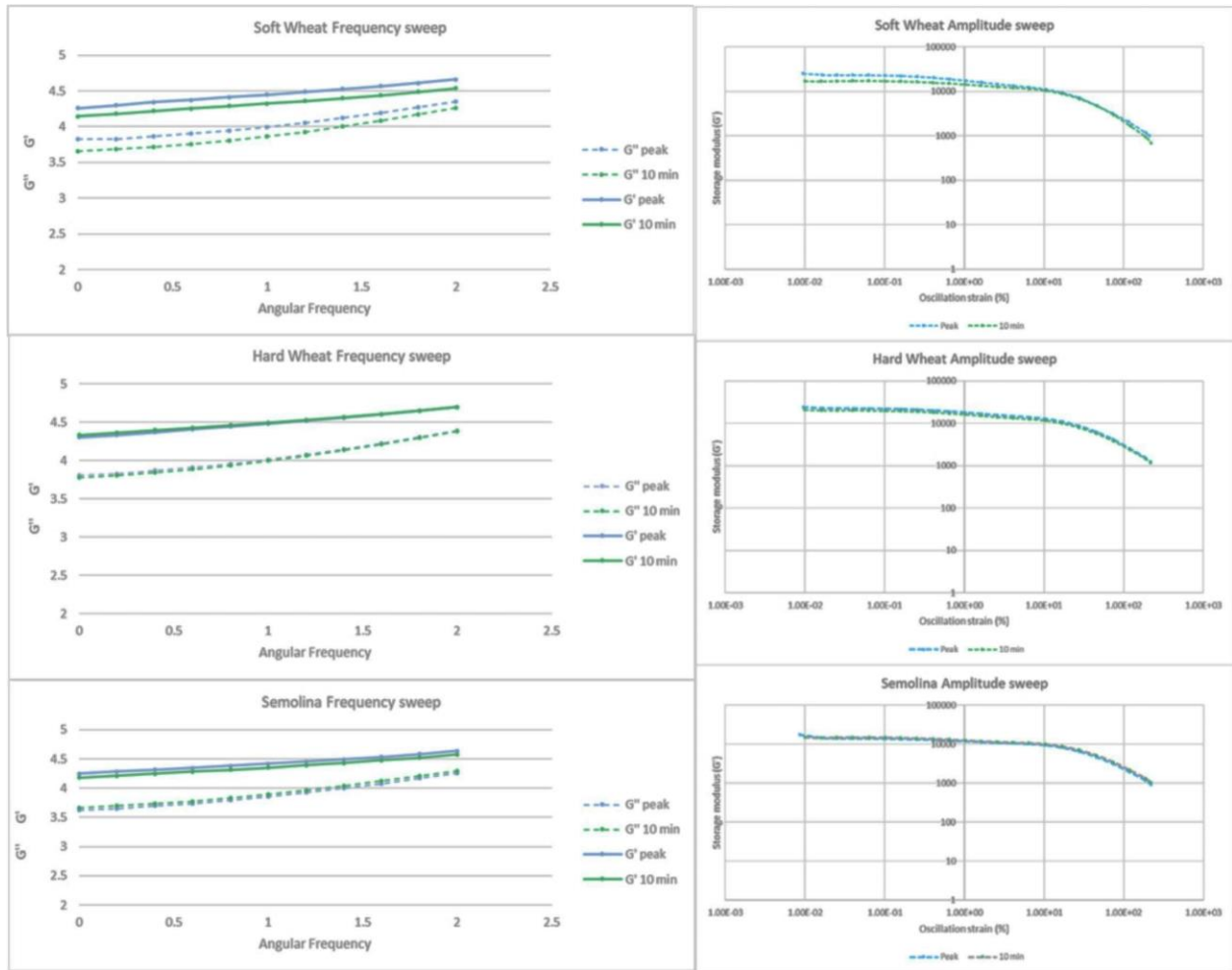
Figure 22. Frequency sweeps and Amplitude sweeps of soft wheat, hard wheat, and semolina at peak time and 10 minutes after peak time with 55% added water.

A complete understanding of the changes occurring in the three different doughs during mixing has been achieved by coupling the rheological data with the 'in situ' detection and image quantitative analyses. The 'in situ' detection and image analyses techniques have proven to be complementary detection methods to rheology. Both together help us explain the changes occurring in the gluten network microstructure more in depth. Moreover, these techniques allow the identification of the individual contribution of each protein subunit to the gluten network microstructure.

5.5 Conclusions

We have gained relevant insights on the role of gliadins, LMW glutenins, and HMW glutenins in dough mixing by using three different dough systems with three different proteins composition. The three gluten subunits (LMW glutenins, HMW glutenins, and gliadins) breakdown during weak soft wheat mixing (from 450 to 350 BU), HMW glutenins agglomerate during this network disruption. LMW glutenins and gliadins are responsible for the gluten network development during stiff hard wheat dough mixing (from 650 to 570 BU), HMW glutenins do not reorganize themselves in the gluten network at that mixing stage. We have been able to visualize and measure the unique internal mobility of each gluten subfraction in a durum semolina dough that undergoes minimal strength loss (530 to 500 BU) due to the associative polymer model of the glutenins. The protein subunits remain co-localized and with the no significant changes network parameters during mixing proving the role that the high amount of LMW glutenins plays in keeping the semolina dough strength stable. The magnitude and specificity of the microstructural changes in the gluten subunits achieved with the 'in situ' detection and quantitative imaging techniques cannot be achieved with oscillatory rheological measurement or other conventional microstructural techniques currently used in dough products.

5.6 References

Ansari, S., Bozkurt, F., Yazar, G., Ryan, V., Bhunia, A., Kokini, J., 2015. Probing the distribution of gliadin proteins in dough and baked bread using conjugated quantum dots as a labeling tool. J. Cereal Sci. 63, 41–48. https://doi.org/10.1016/j.jcs.2014.12.001

Bernklau, I., Lucas, L., Jekle, M., Becker, T., 2016. Protein network analysis — A new approach for quantifying wheat dough microstructure. Food Res. Int. 89, 812–819. https://doi.org/10.1016/j.foodres.2016.10.012

Bonilla, J.C., Bernal-Crespo, V., Schaber, J.A., Bhunia, A.K., Kokini, J.L., 2019a. Simultaneous immunofluorescent imaging of gliadins, low molecular weight glutenins, and high molecular weight glutenins in wheat flour dough with antibody-quantum dot complexes. Food Res. Int. 120, 776–783. https://doi.org/10.1016/j.foodres.2018.11.038

Bonilla, J.C., Bozkurt, F., Ansari, S., Sozer, N., Kokini, J.L., 2016. Applications of quantum dots in food science and biology. Trends Food Sci. Technol. 53, 75–89. https://doi.org/10.1016/j.tifs.2016.04.006

Bonilla, J.C., Ryan, V., Yazar, G., Kokini, J.L., Bhunia, A.K., 2018. Conjugation of specifically developed antibodies for high- and low-molecular-weight glutenins with fluorescent quantum dots as a tool for their detection in wheat flour dough. J. Agric. Food Chem. 66, 4259–4266. https://doi.org/10.1021/acs.jafc.7b05711

Bonilla, J.C., Schaber, J.A., Bhunia, A.K., Kokini, J.L., 2019b. Mixing dynamics and molecular interactions of HMW glutenins, LMW glutenins, and gliadins analyzed by fluorescent co-localization and protein network quantification. J. Cereal Sci. 102792. https://doi.org/10.1016/j.jcs.2019.102792

Bozkurt, F., Ansari, S., Yau, P., Yazar, G., Ryan, V., Kokini, J., 2014. Distribution and location of ethanol soluble proteins (Osborne gliadin) as a function of mixing time in strong wheat flour dough using quantum dots as a labeling tool with confocal laser scanning microscopy. Food Res. Int. 66, 279–288. https://doi.org/10.1016/j.foodres.2014.09.028

Branlard, G., Dardevet, M., 1985. Diversity of grain protein and bread wheat quality: II. Correlation between high molecular weight subunits of glutenin and flour quality characteristics. J. Cereal Sci. 3, 345–354. https://doi.org/10.1016/S0733-5210(85)80007-2

Clarke, B.C., Phongkham, T., Gianibelli, M., Beasley, H., Bekes, F., 2003. The characterisation and mapping of a family of LMW-gliadin genes: effects on dough properties and bread volume. Theor. Appl. Genet. 106, 629–635. https://doi.org/10.1007/s00122-002-1091-1

Delcour, J.A., Hoseney, R.C., 2010. Principles of cereal science and technology authors provide insight into the current state of cereal processing. Cereal Foods World 55(1), 21-22. Cereal Foods World 55, 21–22.

Dhaka, V., Khatkar, B.S., 2015. Effects of gliadin/glutenin and HMW-GS/LMW-GS ratio on dough rheological properties and bread-making potential of wheat varieties. J. Food Qual. 38, 71–82. https://doi.org/10.1111/jfq.12122

D'Ovidio, R., Masci, S., 2004. The low-molecular-weight glutenin subunits of wheat gluten. J. Cereal Sci. 39, 321–339. https://doi.org/10.1016/j.jcs.2003.12.002

du Cros, D.L., 1987. Glutenin proteins and gluten strength in durum wheat. J. Cereal Sci. 5, 3–12. https://doi.org/10.1016/S0733-5210(87)80003-6

Edwards, N.M., Mulvaney, S.J., Scanlon, M.G., Dexter, J.E., 2003. Role of gluten and its components in determining durum semolina dough viscoelastic properties. Cereal Chem. 80, 755–763. https://doi.org/10.1094/CCHEM.2003.80.6.755

FAO, 2017. FAO cereal supply and demand brief | FAO | Food and Agriculture Organization of the United Nations [WWW Document]. URL http://www.fao.org/worldfoodsituation/csdb/en/ (accessed 4.8.17).

Finnie, S.M., Atwell, W.A., 2016. Wheat flour. Elsevier. https://doi.org/10.1016/C2015-0-06189-5

Gupta, R.B., MacRitchie, F., 1994. Allelic Variation at glutenin subunit and gliadin loci, glu-1, glu-3 and gli-1 of common wheats. II. Biochemical basis of the allelic effects on dough properties. J. Cereal Sci. 19, 19–29. https://doi.org/10.1006/jcrs.1994.1004

Gupta, R.B., MacRitchie, F., Shepherd, K.W., Ellison, F., 1991. Relative Contributions of LMW and HMW glutenin subunits to dough strengh and dough stickness of bread wheat, in: Gluten proteins 1990. American Association of Cereal Chemists, St. Paul, Minnesota USA.

Gupta, R.B., Singh, N.K., Shepherd, K.W., 1989. The cumulative effect of allelic variation in LMW and HMW glutenin subunits on dough properties in the progeny of two bread wheats. Theor. Appl. Genet. 77, 57–64. https://doi.org/10.1007/BF00292316

Lindsay, M.P., Skerritt, J.H., 1999. The glutenin macropolymer of wheat flour doughs: structure–function perspectives. Trends Food Sci. Technol. 10, 247–253. https://doi.org/10.1016/S0924-2244(00)00004-2

Manders, E.M.M., Verbeek, F.J., Aten, J.A., 1993. Measurement of co-localization of objects in dual-colour confocal images. J. Microsc. 169, 375–382. https://doi.org/10.1111/j.1365-2818.1993.tb03313.x

Osborne, T.B., 1907. The Proteins of the wheat kernel. Carnegie institution of Washington.

Payne, P.I., Holt, L.M., Krattiger, A.F., Carrillo, J.M., 1988. Relationships between seed quality characteristics and HMW glutenin subunit composition determined using wheats grown in Spain. J. Cereal Sci. 7, 229–235. https://doi.org/10.1016/S0733-5210(88)80004-3

Payne, P.I., Jackson, E.A., Holt, L.M., 1984. The association between γ-gliadin 45 and gluten strength in durum wheat varieties: A direct causal effect or the result of genetic linkage? J. Cereal Sci. 2, 73–81. https://doi.org/10.1016/S0733-5210(84)80020-X

Plazek, D.J., Frund, Z.N., 2000. Recoverable creep compliance properties of associative model polymer and polyoxyethylene solutions. J. Rheol. 44, 929–946. https://doi.org/10.1122/1.551114

Sissons, M.J., Ames, N.P., Hare, R.A., Clarke, J.M., 2005. Relationship between glutenin subunit composition and gluten strength measurements in durum wheat. J. Sci. Food Agric. 85, 2445–2452. https://doi.org/10.1002/jsfa.2272

Sozer, N., Kokini, J.L., 2014. Use of quantum nanodot crystals as imaging probes for cereal proteins. Food Res. Int. 57, 142–151. https://doi.org/10.1016/j.foodres.2013.12.031

Xu, J., Bietz, J.A., Carriere, C.J., 2007. Viscoelastic properties of wheat gliadin and glutenin suspensions. Food Chem. 101, 1025–1030. https://doi.org/10.1016/j.foodchem.2006.02.057

CHAPTER 6.   UNDERSTANDING THE ROLE OF GLUTEN SUBUNITS (LMW, HMW GLUTENINS AND GLIADINS) IN THE NETWORKING BEHAVIOR OF SOFT AND SEMOLINA WHEAT FLOURS DOUGHS AND THE RELATIONSHIP WITH LINEAR AND NON-LINEAR RHEOLOGY

6.1   Abstract

The differences in viscoelastic properties of gluten from two very different wheat flours, a weak soft flour dough and a strong semolina dough, primarily caused by their gliadin and glutenin content including gliadin to glutenin ratio were studied. The doughs where subjected to small and large oscillatory time sweep tests at small and large amplitudes as well as small and large frequencies. The gluten subunits (LMW, HMW glutenins and gliadins) tagged with specific fluorescent quantum dots with a specific excitation wavelength were imaged with confocal laser scanning microscopy and their specific pixel density was measured. The quantitative pixel density data was converted into networking data that included lacunarity, network area and number of network junctions. This networking data was correlated with rheology. The two different dough systems showed different oscillatory behavior during time sweeps. The critical role of LMW glutenins in keeping the structural integrity of semolina doughs was demonstrated by a direct correlation between the non-linear elastic component e3/e1 of the dough and protein network parameters of LMW glutenins. It was also shown that gliadins and HMW glutenins co-localize and associate throughout rheological deformations of the dough. The disruption of the three gluten subunits are responsible for rheological breakdown of soft wheat flour dough, with gliadins influencing the breakdown of the network at higher amplitude deformations. This research presents a new method to analyze the microstructure of wheat doughs and new understanding of how the network structure of the dough subunits contribute and are correlated with fundamental rheological tests.

6.2 Introduction

The importance of gluten proteins in the final quality of wheat products is well-known. The textural differences in the wide variety of wheat products are mostly due to the differences in gluten content and gluten composition and quality in different wheat flours. Gluten is developed during mixing, using water as a plasticizer. Gluten development during mixing has been extensively studied as a function of mixing time, heat, added plasticizer, genetic composition of wheat, etc. (Don et al., 2005; Mohamed and Rayas-Duarte, 2003; Morel et al., 2002; Popineau et al., 2001; Redl et al., 1999). Moreover, oscillatory rheological analysis at small and large amplitude strains, creep-recovery tests, and stress relaxation have been used to gain more fundamental knowledge about the networking and inter-molecular structure of gluten in wheat flour dough (Bohlin and Carlson, 1981; Lefebvre et al., 2003; Li et al., 2003; Onyango et al., 2009). Describing the properties of gluten as one large matrix of proteins presents the challenge of not being able to discriminate between the contributions of individual gluten subunits to the properties of dough especially its rheology. Many studies have also been done using the extracts of the two largest group of gluten proteins, gliadins and glutenins. Those studies have led to the understanding that gliadins, contribute to the viscosity/flowability of the viscoelastic gluten, while glutenins, especially HMW glutenins, contribute to the elasticity of gluten (He and Hoseney, 1991; Hoseney et al., 1970; Orth and Bushuk, 1972). The glutenins and gliadins have also been characterized by rheological experiments in the linear (SAOS) and non-linear (LAOS) regions (Khatkar et al., 2002, 1995; Yazar et al., 2017). The information obtained from the isolated gluten factions has helped researchers understand better how gluten behaves in a dough matrix. However, the material studied is not the gluten in the dough, but the isolated gluten proteins, which have gone through irreversible conformational changes in their structure due the use of solvents during extraction.

New image analysis and gluten subunit staining techniques have become available and have been used to describe microstructural changes in gluten proteins in dough (Bernklau et al., 2016; Bonilla et al., 2019b, 2016). The protein network analysis software and the co-localization techniques provide data about the structural imaged gluten network and about the interaction between the different subunits. The individual visualization of each individual gluten subunit was possible with the use of specifically-developed antibodies for the main glutenins subunits, HMW glutenins, and LMW glutenins (Bonilla et al., 2018), and commercially available gliadin antibodies coupled with

the developed new staining and imaging procedures for wheat doughs (Bonilla et al., 2019a). With the use of these individual protein staining and image processing techniques, new insights about the role of LMW glutenins, HMW glutenins, and gliadins in dough during mixing of wheat flour has been obtained. One of these studies shows how interact together during the mixing process of hard wheat dough (Bonilla et al., 2019b). It was shown how the three gluten protein subunits come together at peak time (dough maximum strength), and then how LMW glutenins separate from three-gluten subunits network first, being responsible for the initial decay in dough strength, while HMW glutenins agglomerate later in the mixing, being more responsible for the long-term decay in dough strength. A different study analyzed the differences of the behavior and interactions of LMW glutenins, HMW glutenins, and gliadins during mixing in three different wheat flours. This study shows how HMW glutenins do not re-distribute at high dough strengths, how the three gluten subunits breakdown in weak soft wheat flours mixing, and showing no changes in the structural distribution and interaction of the gluten subunits in the stable semolina dough (Bonilla et al., 2020). The use of these novel staining and image processing techniques has helped researchers to measure gluten and its subunits 'in-situ' in a quantitative way, where the material analyzed is the gluten protein subunits in their native unmodified state inside the dough and not an extracted and modified agglomerate of proteins. These recent studies resulted in ground-breaking information about the role of the gluten subunits during mixing, where the doughs are subjected to very large and intense deformations, which are often hard to quantify so the results are presented as a function of mixing time.

The objective of this research is to study the networking parameters of each individual gluten subunits and their interactions under controlled and very-well defined small and large amplitude oscillatory rheological deformations of wheat dough. The goal is to determine the individual contribution of each gluten subunit to the structural integrity of the doughs by deforming the doughs to different amplitudes in the linear and non-linear region and measuring their stress response. To this end, a weak soft wheat flour dough and a strong and stable semolina flour are being used for comparison in this study. The three gluten subunits, LMW glutenins, HMW glutenins, and gliadins have been stained in the dough samples, after freezing them 'on-site' immediately after the rheological experiments are finished. The protein network analysis and co-localization tools have been used to obtain data about each individual protein subunit and their

interactions with the other two subunits. This allows us to directly correlate quantitative measures of changes in networking behavior to the rheology of the dough and to help understand the role and interactions between gliadins, LMW glutenins, and HMW glutenins in the dynamic change in the network as a function of extent of deformation.

6.3   Materials and methods

6.3.1   Wheat dough preparation

The doughs were prepared following the AACCI method 54-21.02 with the modification of adding a constant 55% water (Bonilla et al., 2020). Keeping a constant added water level is key to clearly demonstrate the impact of the differences in protein composition of each flour in affecting dough rheology and dough strength.   Soft red winter wheat flour was provided by Siemer milling company (Teutopolis, IL, USA), and durum semolina from Fowlers milling Co (Chardon, OH, USA). The initial moisture of the flours was determined using a rapid moisture analyzer (Mettler Toledo, Columbus, OH, USA). The amount of flour used in each test was adjusted to 300 g dry basis considering differences in their moisture. The doughs were mixed until they reached their unique peak time (dough's maximum strength); three samples were collected once the dough reached this time. The soft wheat flour and semolina used in this study had 8% and 13.20% protein content respectively. The glutenin to gliadin ratio was 1.09:1 for soft wheat flour, and 1.64:1 for semolina. They also had an LMW glutenin /HMW glutenin ratio of 2.24:1 for soft wheat, and 3.46:1 for semolina as determined before (Bonilla et al., 2020)

6.3.2   Small and large strain Oscillatory rheological analysis

Each sample taken from the faringraph bowl was placed directly between the parallel plate geometry of the TA HR3. The top plate was a 20-mm crosshatched plate and the bottom plate was coated with sand paper to prevent slip. Vacuum grease (Fisher scientific, Hampton, NH, USA) was applied around the edge of the sample in order to prevent dehydration during the rheological measurements. Amplitude sweeps were performed from 0.01% strain amplitude to 200% in order to observe both the linear and non-linear region of the doughs. The amplitude sweeps were done at three different frequencies, 1 rad/sec, 10 rad/sec, and 100 rad/sec. Oscillatory time sweeps were performed at 0.025, 10, 100% strain amplitudes at a frequency of 10 rad/sec for 100 seconds. The

outcome of this latter test was used to develop correlations between the structural behavior of the two doughs. The rate of decay of G'in the non-linear region was used a measure of structure breakdown in the doughs as a function of strain coupled with frequency. The data selected was the region where a sharp decay was observed in the G' vs. strain curves. The oscillatory response of stress during the 100 seconds of time sweep experiment was recorded and was used as another structure of dough strength and dough structure decay during oscillatory deformation. Since the amplitude sweeps cover both the linear and the non-linear region the, non-linear elastic component (e3/e1) of the sample was calculated by Fourier Transform, and third-harmonic was extracted using the TA TRIOS software (Yazar et al., 2017).The non-linear elastic component (e3/e1) was then correlated with the lacunarity at the amplitudes of 0.025%, 10%, and 100%.

6.3.3   Preparation of dough samples for imaging

The dough samples were immediately frozen by spraying liquid nitrogen for 10 seconds on-site after the time sweeps were performed. Small pieces of frozen dough (3 mm x 3 mm) were collected from the outer part of the sample, since in the inner part of the plate there is less or no deformation at the center of the geometry during oscillatory measurements. The small pieces of doughs were placed on 'tissue-tek' cryomolds (Fisher Scientific, Hampton, NH, USA) immersed in Optimum Cutting Temperature (OCT) compound (Fisher Scientific, Hampton, NH, USA). The samples then were cryo-sectioned using a LEICA CM 1860 Cryostat (Leica Biosystems, Wetzlar, Germany) at -20 °C. with a thickness of t 10 μm . The 10-μm sections of dough were placed on microscope slides and fixed with methanol. (Bonilla et al., 2019b).

The samples were stained with a mixture of LMW glutenins antibodies, HMW glutenins antibodies (Bonilla et al., 2018), and gliadin antibodies 4F3 (Fisher Scientific, Hampton, NH, USA) conjugated with 525 nm, 585 nm, 655 nm emission wavelength-QDs respectively. The sample is then washed with Phosphate-Buffered Saline PBS (Fisher Scientific, Hampton, NH, USA) three times in order to remove unbound antibodies-QDs complexes.

6.3.4 Confocal Laser Scanning Microscopy analysis

The soft wheat and semolina dough samples were examined with a Confocal Laser Scanning Microscope, Zeiss LSM 880 (Carl Zeiss Microscopy, Oberkochen, Germany) as described in Bonilla et al (2020).

6.3.5 2.5 Quantitative Image Analysis

Co-localization quantitative imaging analysis

The co-localization analyses for this study were run in the 'Zen Blue' software (Carl Zeiss Microscopy, Oberkochen, Germany). The co-localization coefficient has been reported as a measure of the overlay between the location of one gluten subunit relative to a different gluten subunit when staining the three gluten subunits with different quantum dots (Bonilla et al., 2019b). During this analysis, the emission from one detection channel is overlapped with the emission from another detection channel within the exact same detection area (Manders et al., 1993). Since the co-localization is a pair comparison, three colocalization coefficients were taken from each image. The colocalization coefficient between gliadin and HMW glutenins, between gliadins and LMW glutenins, and between HMW glutenins and LMW glutenins was obtained. The variations in co-localization coefficient of different gluten subunits from doughs under different conditions have reported as a quantitative marker of interactions between the gluten subunits during wheat dough mixing. (Bonilla et al., 2019b, 2020).

Quantitative protein network analysis

The three images from each repetition and each sample were studied using the software AngioTool64 software which estimates the area of the protein network formed by each protein subunit, the total number of junctions in the network, and the lacunarity (Bernklau et al., 2016). Lacunarity is a measure of the uniformity of the network. It measures the variance in the size of the gaps of the network. Low variance in the size of the gaps (uniform distribution of the network) is represented by a low lacunarity. High variance in the size of the gaps of the network (less uniform distribution of the network) is presenter by a higher lacunarity value. When the gaps in the gluten network are uniform in size, the lacunarity is low. This low value represents a well-

formed network. When the gaps have a high variability in size, the lacunarity is high and the proteins are forming a much less even network.

6.4   Results

6.4.1   Comparison of amplitude sweeps in the linear and non-linear region for soft wheat and semolina flour doughs

The amplitude sweeps in Figure 23 show the linear and non-linear regions of the storage moduli (G') of soft wheat and semolina flour doughs at three different frequencies. The G' values follow the same trend as a function of strain at the three different frequencies. At a frequency of 1 rad/second G' values are lower and the linear region is longer in contrast to the G' values at 100 rad/sec which are larger with a shorter linear region. At the intermediate frequency of 10 rad/sec, G' values have intermediate magnitudes and the length of the linear region is also intermediate. In both soft wheat and semolina doughs, the linear regions were found to be limited to relatively very small strains between 0.01% to 0.16% at 100 rad/sec, between 0.01% and 0.10 % for 10 rad/sec, and 0.01 to 0.04 % for 1 rad/sec. G' values were higher for semolina dough than soft wheat flour dough in the linear region; for instance, at 0.01% amplitude and 100 rad/sec semolina had a G' value of 4.1 x104 ± 0.2 Pa while soft wheat had a G' value of 2.8 x104 ± 0.2 Pa. This is due to the higher protein content and higher glutenin/gliadin ratio in semolina. Both G' and G" values increased with increasing frequency. At strains above the linear region both G' and G" began to decrease as expected in the non-linear region. The rate of decay at the highest strains was much steeper for the soft wheat flour dough compared to the semolina dough (Table 7). This is also due to the protein quality of the semolina dough studied in this project as described by the glutenin to gliadin ratio which is much higher in semolina flour. The rate of decay of G' did not significantly change with frequency and this is due to the reversible nature of oscillatory flow. The protein network stretched considerably but did not snap excessively resulting in G' values that are close at different frequencies.

In order to subject each dough to oscillatory fatigue we conducted oscillatory time sweeps at a strain of 0.025% in the linear region and then at two other higher strains in the non-linear region. The focus of these experiments was to look at the change in the distribution and interactions

110

between the protein sub-fractions as a function of the deformation amplitude at a constant frequency for the constant time of 100 seconds.
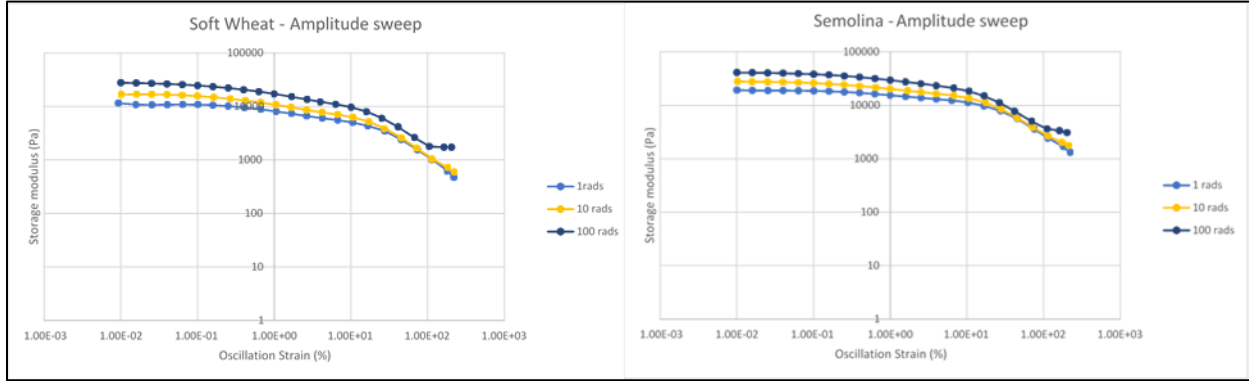
Figure 23. Amplitude sweeps of soft wheat and semolina doughs from 0.01%-200% amplitude strain at 1, 10, and 100 rad/sec.

Table 7. The slopes of the linear regression of the last 6 Points of log G' vs. log % strain in the amplitude sweeps representing the rate of decay of the network structure in the non-linear region at frequencies of 1 rad/sec, 10 rad/sec, and 100 rad/sec for soft wheat and semolina dough

Dough type	1 rad/sec	10 rad/sec	100 rad/sec
Semolina	-0.86	-0.76	-0.83
Soft	-0.96	-0.91	-0.89

Figure 24 shows the oscillatory stress response time sweeps of the soft wheat and semolina doughs subjected to 0.025% (in the linear region) as well as 10%, and 100% strain amplitude in the non-linear region at 10 rad/sec for 100 seconds. The doughs made from both flours, soft wheat and semolina show a constant oscillatory stress wave pattern that does not change throughout the time sweeps when subjected to 0.025% strain amplitude. In the linear region the stress wave is oscillatory and completely reversible. The applied deformation is not sufficient to break the network structure of the doughs; therefore, the stress response is exactly the same after applying the same strain repeatedly.

The oscillatory stress response in both doughs when 10% amplitude strain is applied shows a reduction in the amplitude of the stress response after the first few cycles initially; the10% strain amplitude is in the non-linear region for both doughs, where the deformations generate irreversible changes in the structure of the dough as the deformation time increases. The stress response from the dough stabilizes after 30 seconds of applied strain at 10% strain. It appears that a critical level of mechanical energy is introduced in the first 30 seconds to deform and snap the network until a second level of stronger resistance in the gluten network is reached.

When 100% strain deformation is applied, the amplitude of stress response for the soft wheat dough is reduced from 4000 Pa to 2000 Pa in the first 30 seconds of deformations. The amplitude of the stress response of soft wheat flour keeps decreasing for the following 70 seconds because of the continuation of the breakdown of the network structure. The amplitude of the stress response of semolina dough decreases from 4000 Pa to 2600 Pa in the first 30 seconds and keeps decreasing for the following 70 seconds; after 70 seconds the amplitude of stress is equal to 1800 Pa a reduction in amplitude of about 55%. The drastic reduction in the amplitude of the stress response of the doughs at 100% strain compared to a lesser degree of reduction in stress response at 10% amplitude strain is directly the outcome of the decrease in the storage moduli G' from 10% to 100% in the amplitude sweeps (Figure 23) which correlates well to the network structure of the dough. The larger reduction in the stress response of soft wheat at 100% amplitude strain in the first 30 seconds compared to the stress response of semolina is once more related to soft wheat dough being a weaker network than semolina dough due to lower protein content and the lower protein quality. While these rheological observations are insightful and teach us a lot about the networking behavior of the two flours these is no direct molecular evidence about the mechanism of decay and similarly no evidence whatsoever as to which protein sub fraction may be involved in the change in networking behavior. So far, all the elegant molecular speculations in the literature are based on indirect measurements the results of excellent wet or spectroscopic chemistry (like FTIR and others) and inferences based on the outcome of these indirect measurements (Belton et al., 1995; Georget and Belton, 2006; Li et al., 2006).

In this research we have been using techniques to bind proteins to fluorescent quantum dots and using CLSM to quantitatively image the intensity and extent of the interaction between the

subunits of gluten including gliadin, LMW glutenin and HMW glutenin. We then used very recently developed quantitative techniques to understand the changes in the number of network junctions formed by each gluten subunit and its interaction with the other subunits (co-localization and protein network analysis which give the number of protein junctions as well as lacunarity (which is a measure of the free space in between protein body in the protein network).
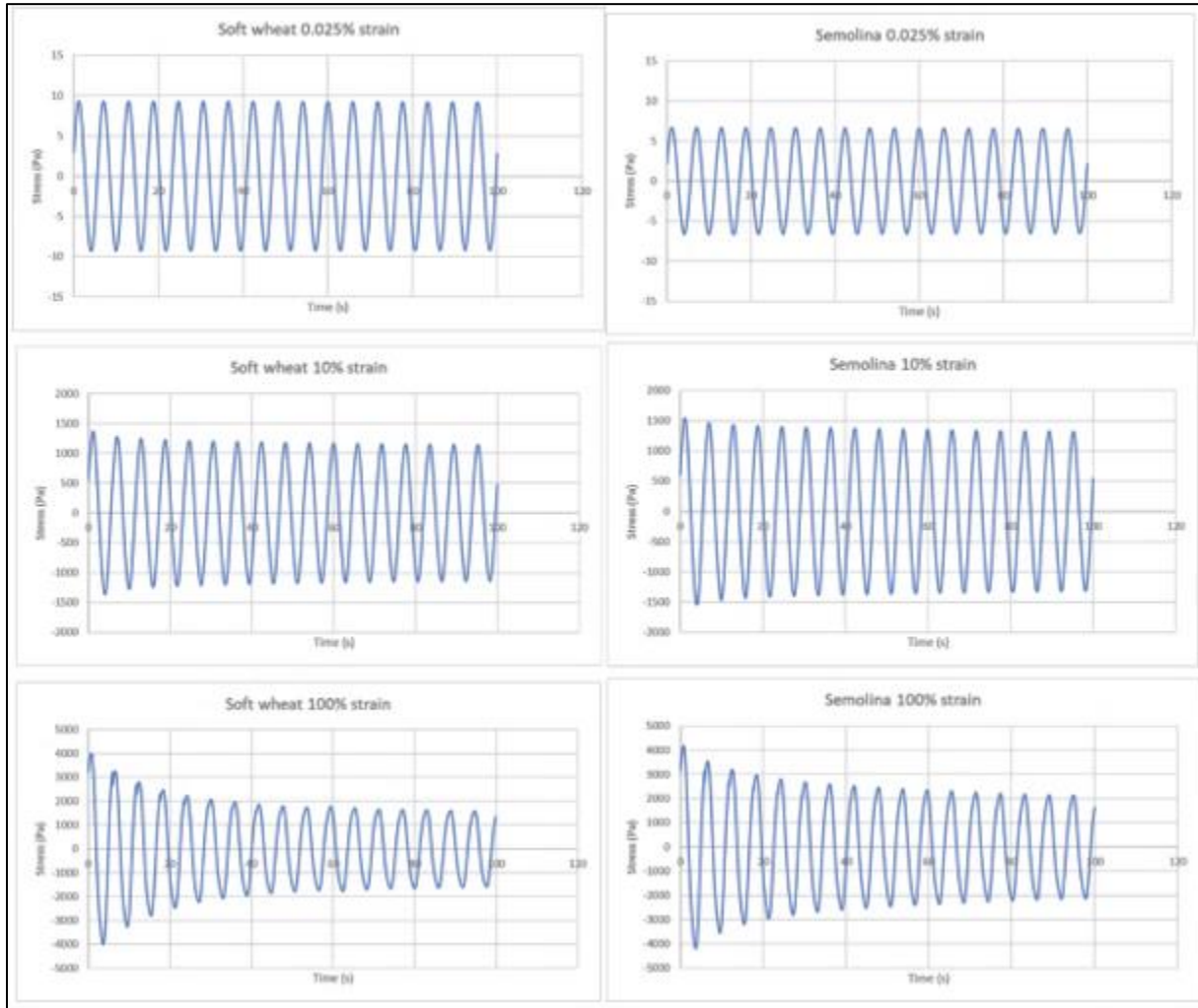
Figure 24. Time sweeps of soft wheat and semolina doughs with 0.025, 10, and 100 applied amplitude strain at 10 rad/sec for 100 seconds

6.4.2   Changes in protein network characteristics in soft wheat dough

Figure 25A shows the protein network parameters for soft flour doughs after their deformation at 0.025%, 10% and 100% amplitude and 10 rad/secs for 100 seconds. The fact that the samples have

been instantaneously frozen at the end of the time sweep enables capturing the networking state of the gluten proteins giving them a minimal time to relax back to their rest configuration. We observe that the network area covered by all three protein subunits, gliadins. LMW glutenins, and HMW glutenins, decreases when the amplitude of the deformation is increased. Clearly this decrease is one of the reasons why the strength of the network diminishes and leads to a decrease in G' in the non-linear region. For HMW glutenins, their network area is reduced from 3.1x104 µm2 to 2.5 µm2 x104 , a reduction in 20% when going from 0.025% strain amplitude to 10% amplitude and continues to decrease to 2.1 x104 µm2 at 100% strain amplitude, a reduction of an extra 11% from its value at 0.025% strain amplitude of 3.1 x104µm2 For LMW glutenins, their network area in is reduced from 4.7 x104µm2 to 3.5 x104 µm2 , a reduction in 25% when going from 0.025% strain amplitude to 10% amplitude and continues to decrease to 2.8 x104µm2 at 100% strain amplitude, a reduction of an extra 14.5% from its value at 0.025% strain amplitude of4.7 x104µm2 HMW glutenins reduce its number of junction points from 181 to 144 (a reduction of 23%) from 0.025% amplitude to 10% amplitude and continues to decrease it to 109 (an additional 22%) at 100% amplitude. LMW glutenins reduce their number of junction points from 354 to 220 (a reduction of 38%) from 0.025% amplitude to 10% amplitude and continues to reduce to 160 (an additional 17%) at 100% amplitude. For HMW glutenins lacunarity increases from 0.425 to 0.551 (an increase of 30%) from 0.025% amplitude to 10% amplitude, and keeps increasing to 0.648 (an additional increase of 22%) at 100% amplitude. For LMW glutenins, their lacunarity increases from 0.286 to 0.410 (an increase of 43%) from 0.025% amplitude to 10% amplitude, and keeps increasing to 0.542 (and additional increase of 46%). In both glutenin fraction it can be seen that their reduction in network parameters is more significant when going from 0.025% amplitude to 10% amplitude.

Gliadins, on the other hand, show reductions of 9% and 10%, in their network area and number of junction points respectively, and increase of 24% in their lacunarity when going from 0.025% to 10% amplitude. However, when going to 100% amplitude., the network area of gliadins and their number of junction points are reduced 22% and 28% more, and their lacunarity is increased 45% more. Opposite to the glutenin fractions, the gliadins reduce their network parameters inn higher more significantly when going from 10% amplitude to 100% amplitude

This data shows the small initial reduction in the sinusoidal stress amplitude response during the time sweeps at 10% strain amplitude compared to 0.025% strain amplitude is mostly driven by breakdown of the LMW glutenins and HMW glutenins, with LMW glutenins having a stronger impact than the HMW glutenins. The reduction in the sinusoidal stress response during the time sweep when going up to 100% strain amplitude is mostly driven by the loss of network in the gliadin subunit. This can be explained by gliadins forming a more molecularly mobile protein network that can recover because of its mobility during oscillatory deformation. This is observed at 10% strain amplitude where again the gliadin network show values that only differ by 9%, 10% and 24% in network area, number of junction points, and lacunarity respectively from the gliadins value at 0.025% amplitude- However, after applying repeated large oscillations of 100% strain amplitude the gliadins do reduce their distribution significantly, having a direct impact in the substantial reduction of stress response of the dough. Figure 25B display one visual representation of the network parameters from each protein subunit after the three different oscillatory strains have been applied to the soft wheat dough.
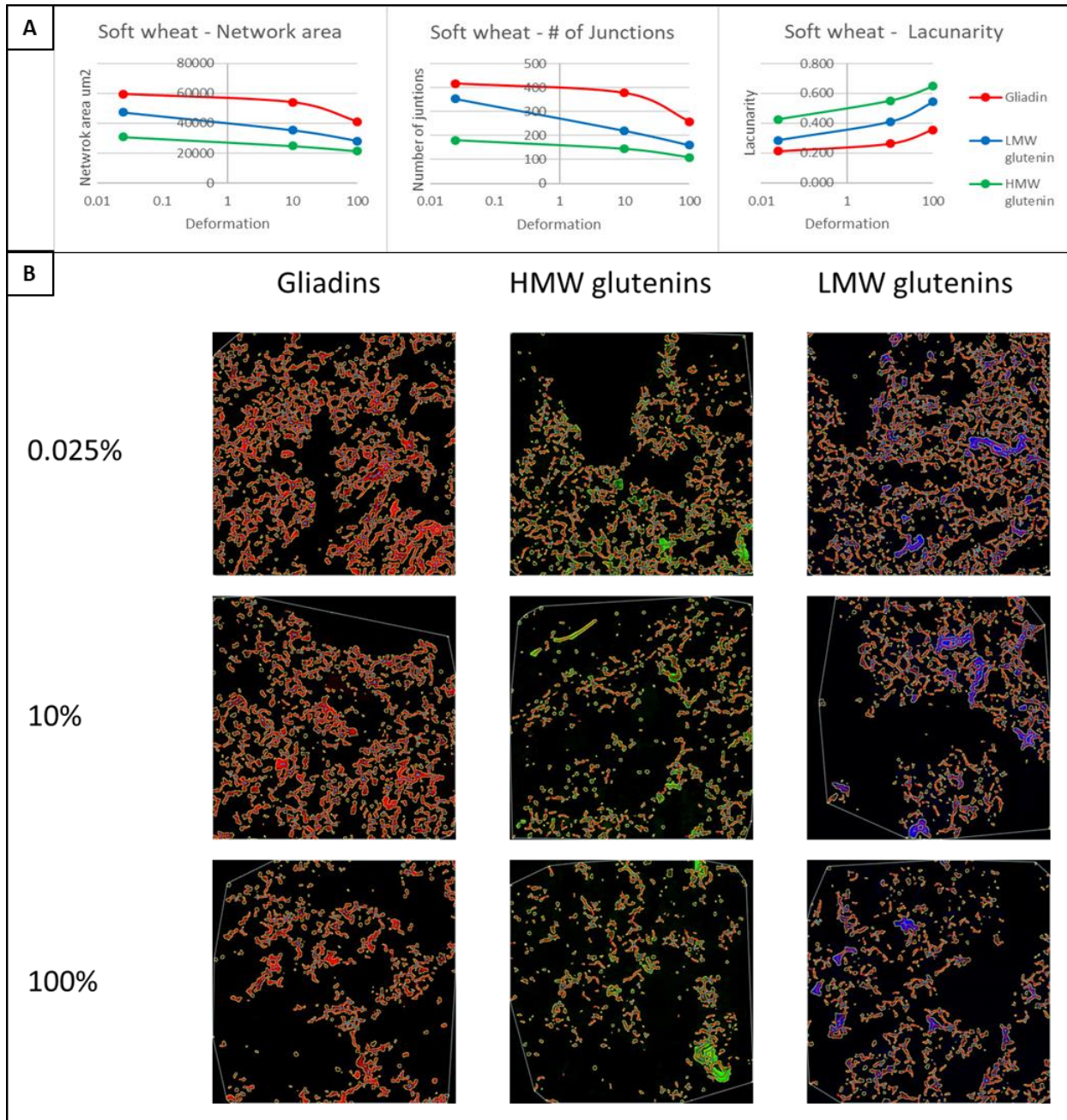
Figure 25. Protein network changes in soft wheat at deformed at different strain amplitudes. A) Protein network parameters at different amplitudes in gliadins, LMW glutenins, and HMW glutenins. B) CLSM images processed with network quantification software

6.4.3 Changes in protein network characteristics in semolina dough

Figure 26A shows the protein network parameters for semolina doughs after their deformation at 0.025%, 10% and 100% amplitude and 10 rad/secs for 100 seconds. The network parameters, network area, number of junctions and are much higher in semolina dough that in soft wheat dough, lacunarity values smaller in semolina dough than in soft wheat doughs. For instance, the highest network area value for gliadin in semolina is 8.7 x104 µm2 while in soft wheat is 5.9 x104 µm2, the highest number of junctions in gliadin network in semolina is 828 and in soft wheat is 418, the lowest lacunarity in semolina is 0.151 and in soft wheat is 0.211. This is due to the higher protein content in semolina (13%) compared to soft wheat (8%), and this difference is clearly seen since both doughs that have been prepared with the same water added level (55%). In semolina dough differently than in soft wheat doughs, gliadins do not reduce their protein network area (0% decrease) and number of junctions (1% decrease), and do not increase their lacunarity (10% decrease) from 0.025% to 10% amplitude. An identical phenomenon is seen with HMW glutenins, from 0.025% to 10% amplitude, 0% decrease in network area, 5% decrease in number of junctions and, 3% decrease in lacunarity. The most significant changes are observed with LMW glutenins. They undergo decreases their network area of 24%, decreases in their number of junctions of 30%, and increases in lacunarity of 33% from 0.025% to 10% strain amplitude. Therefore, these results show that in semolina, in contrast to soft wheat, LMW glutenins are the most significant subunit responsible for the decay in the stress response when going from 0.025% to 10% amplitude.

At100% amplitude the network area formed by LMW glutenins decreases an additional 31% compared to its value at 0.025% amplitude. The network area of HMW glutenins and gliadins decrease 26% and 10% respectively. The number of junction points of LMW glutenins decreases an additional 40% compared to the value at 0.025% amplitude. The junction points of HMW glutenins and gliadins decrease an additional 31% and 18% respectively. And lastly, at 100% amplitude the lacunarity of LMW glutenin increases an additional 133% compared to its value at 0.025% amplitude because the LMW breaks apart under 100% strain. The molecular bonding interactions are not strong enough to maintain the molecular integrity of LMW glutenin. The lacunarity of HMW glutenins increases 39%, and gliadin has an additional 2% decrease from its value at 10% amplitude. These results, show that when going to larger amplitudes (100% amplitude) LMW glutenins are also the main driver for the decay in the amplitude of the sinusoidal

stress response of the dough. However, in the larger amplitude experiment the breakdown of gliadins and HMW glutenins also contribute to the changes in the stress response of the dough.

The rheological breakdown seen in semolina dough from the lowest amplitude (0.025%) to the highest amplitude (100%) were dominated by the changes in the network contributed by LMW glutenins. This is consistent with the results of Bonilla et al (2020), where LMW glutenins were found to be the protein subunit responsible for keeping the dough strength stable in the Brabender farinograph in particular due to its abundance in Semolina flour. In this previous study, the network properties of LMW glutenins did not change during mixing, since mixing allows the glutenin molecules to re-organize themselves constantly, keeping the dough resistance constant. On the other hand, in this current study, significant breakdown of the LMW glutenin has been found since the dough has been intentionally deformed at different amplitudes at least one decade apart. The quantitative image analyses used in this study serve as a 'in situ' and strong and molecular proof that the disruption in the semolina dough is in fact controlled by the breakdown in the LMW glutenins subunits.
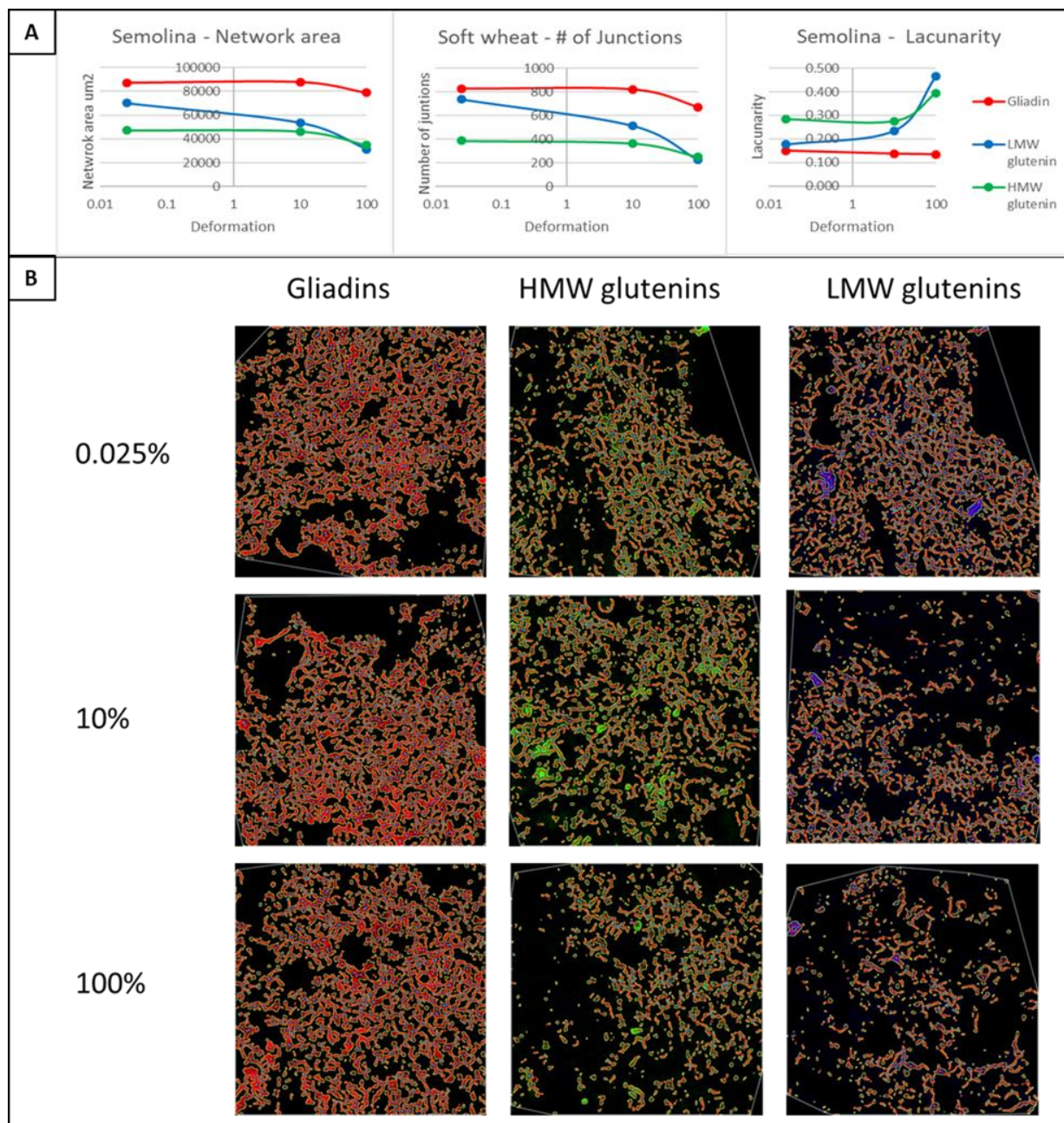
Figure 26. Protein network changes in semolina deformed at different strain amplitudes. A) Protein network parameters at different amplitudes in gliadins, LMW glutenins, and HMW glutenins. B) CLSM images processed with network quantification software

6.4.4 Co-localization coefficient analysis

The co-localization coefficient analysis compliments the previous data by showing where the protein subunits are in the sample and how close they are to one another. This is another measure of the degree of interaction between the subunits. The coefficient ranges from 0 to 1 where 1

119

signifies that the protein subunits are exactly at the same location and 0 signifies that no part of the protein subunits are close to one another. Molecularly a coefficient close to 1 signifies that there a lot of interaction between the protein subunits and a coefficient close to zero signifies that molecular interactions are very low.

In soft wheat, the co-localization coefficient between gliadins and HMW glutenins are originally high showing that HMW glutenins and gliadins interact closely and strongly. The interaction coefficient which is 0.932 decreases to 0.895 from 0.025% to 10% strain amplitude, and then increases back to 0.932 at 100% amplitude (Figure 27). This is thought to be due to the HMW glutenins breaking down at 10% while the gliadins remain largely intact at 10 % amplitude as seen in the protein network analysis results. At 100% amplitude the co-localization increases back to 0.932, since now both HMW glutenins and gliadins both break down seemingly to the same extent showing that gliadins have a major effect on the rheology of the dough at higher amplitudes (100%). The co-localization coefficients of LMW glutenins and gliadin decreases from 0.879 to 0.815, and the co-localization of LMW glutenins and HMW glutenins decrease from 0.898 to 0.185 when the strain amplitude increases from 0.025% to 100% amplitude. This also is consistent with the network parameters related to LMW glutenins decreasing more extensively as strain amplitude increases (from 0.025% to 100%).

In semolina dough, the co-localization of gliadins and HMW glutenins remains constant at all three strain amplitudes (0.97, 0.97, and 0. 97). This matches the proteins network analysis results where it can be seen that the two protein subunits follow the exact same trend in the graphs for protein network area and number of junctions. The co-localization of LMW glutenins with either HMW glutenin or gliadin fluctuates in the same way for both. These results prove the interaction between gliadins and HMW glutenins since the two subunits stick together from 0.025% to 100% amplitudes deformations and the break down in their network happens in the same way from 10% to 100% amplitude. These results confirm that it LMW glutenins are by far the most responsible subunit of the structural integrity in semolina dough.
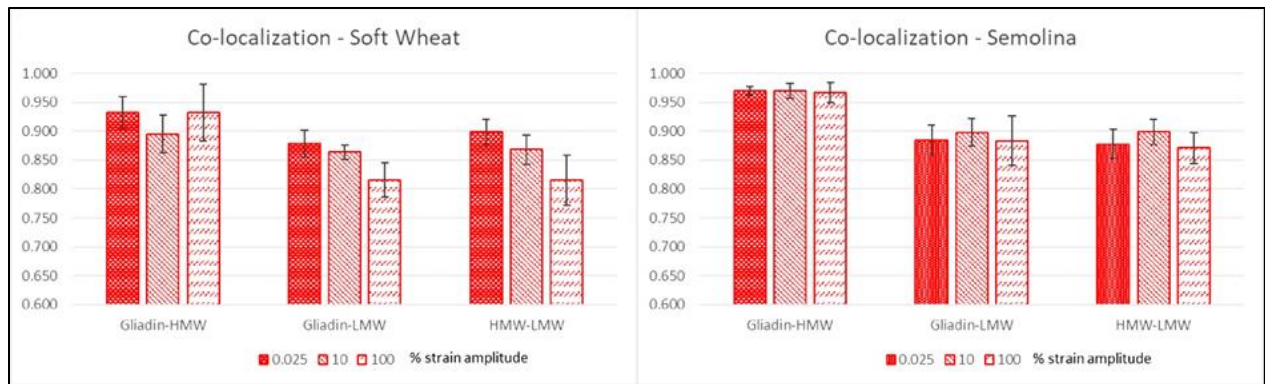
Figure 27. co-localization coefficients of soft wheat and semolina doughs deformed at different strain amplitudes

6.4.5 Correlation between the elastic component of the viscoelastic properties and lacunarity

Figure 28 shows the correlation between the non-linear elastic component (e3/e1) and the lacunarity values of each protein subunits. The elastic component is the response of the amplitude sweep performed from 0.01% strain amplitude to 200% amplitude. The correlation of the specific values of elastic component values at 0.025%, 10%, and 100% strain amplitude and the lacunarity of the gluten subunits at those same amplitude values show different behavior in soft wheat compared with semolina doughs. In soft wheat, the correlations between the lacunarity of gliadin, LMW glutenins, HMW glutenins have a R2 of 0.99, 1.0, and 0.98 respectively, showing that the three gluten subunits are responsible for the decay in the elastic component at the different amplitudes. On the other hand, in semolina dough the correlation between the lacunarity showed by LMW glutenins is significantly higher than the correlation showed by gliadin or HMW glutenins. The lacunarity of LMW glutenins show a correlation with an R2 of 0.99 with the decay in elastic component. The lacunarity of HMW glutenins and gliadins showed an R2 of 0.88 and 0.71 respectively. This shows that LMW glutenins are the most responsible gluten subunits for the decay in the elastic component in semolina dough at different amplitudes. These results together with the protein network analysis and co-localization coefficients compared with the different sinusoidal stress response of the doughs confirmed further that LMW glutenins are the main protein subunit holding together the structural integrity of semolina doughs. In figure 28 the difference between the role of the three gluten subunits in each dough can be compared side by side
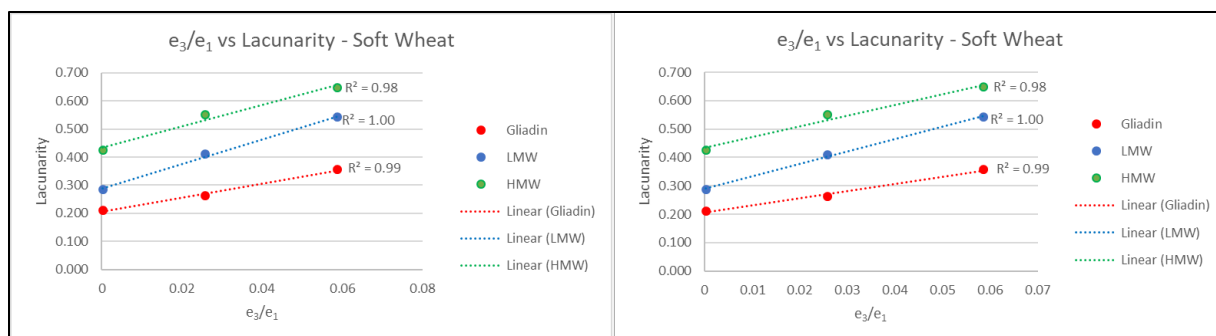
Figure 28. Correlation between the non-linear elastic component (e3/e1) of soft wheat and semolina doughs and the 'lacunarity' of each gluten subunit at the three different amplitudes

6.5   Conclusions

It has been shown that the three different gluten subunits behave and interact differently in soft wheat and semolina doughs. It was found that in soft wheat flour the glutenins (HMW and LMW) are responsible for the decrease in dough stress response at an amplitude of 10%. At 100% amplitude on the other hand the gliadins are much more affected when the soft wheat dough is deformed due to the higher molecular mobility of gliadins.

In the case of semolina doughs, the LMW glutenins were found to be the most responsible subunit keeping the structural integrity of semolina's doughs. The first direct correlation between a well-known rheological parameter with lacunarity was shown, demonstrating further that disruption of LMW glutenins correlates with the decay in the non-linear elastic component e3/e1 of semolina dough. In soft, wheat the disruption of the three gluten subunits correlate with the decay of the non-linear elastic component of the dough.

6.6   References

Belton, P.S., Colquhoun, I.J., Grant, A., Wellner, N., Field, J.M., Shewry, P.R., Tatham, A.S., 1995. FTIR and NMR studies on the hydration of a high-Mr subunit of glutenin. Int. J. Biol. Macromol. 17, 74–80. https://doi.org/10.1016/0141-8130(95)93520-8

Bernklau, I., Lucas, L., Jekle, M., Becker, T., 2016. Protein network analysis — A new approach for quantifying wheat dough microstructure. Food Res. Int. 89, 812–819. https://doi.org/10.1016/j.foodres.2016.10.012

Bohlin, L., Carlson, T.L.G., 1981. Shear stress relaxation of wheat flour dough and gluten. Colloids Surf. 2, 59–69. https://doi.org/10.1016/0166-6622(81)80053-4

Bonilla, J.C., Bernal-Crespo, V., Schaber, J.A., Bhunia, A.K., Kokini, J.L., 2019a. Simultaneous immunofluorescent imaging of gliadins, low molecular weight glutenins, and high molecular weight glutenins in wheat flour dough with antibody-quantum dot complexes. Food Res. Int. 120, 776–783. https://doi.org/10.1016/j.foodres.2018.11.038

Bonilla, J.C., Bozkurt, F., Ansari, S., Sozer, N., Kokini, J.L., 2016. Applications of quantum dots in Food Science and biology. Trends Food Sci. Technol. 53, 75–89. https://doi.org/10.1016/j.tifs.2016.04.006

Bonilla, J.C., Erturk, M.Y., Schaber, J.A., Kokini, J.L., 2020. Distribution and function of LMW glutenins, HMW glutenins, and gliadins in wheat doughs analyzed with 'in situ' detection and quantitative imaging techniques. J. Cereal Sci. 102931. https://doi.org/10.1016/j.jcs.2020.102931

Bonilla, J.C., Ryan, V., Yazar, G., Kokini, J.L., Bhunia, A.K., 2018. Conjugation of Specifically Developed Antibodies for High- and Low-Molecular-Weight Glutenins with Fluorescent Quantum Dots as a Tool for Their Detection in Wheat Flour Dough. J. Agric. Food Chem. 66, 4259–4266. https://doi.org/10.1021/acs.jafc.7b05711

Bonilla, J.C., Schaber, J.A., Bhunia, A.K., Kokini, J.L., 2019b. Mixing dynamics and molecular interactions of HMW glutenins, LMW glutenins, and gliadins analyzed by fluorescent co-localization and protein network quantification. J. Cereal Sci. 102792. https://doi.org/10.1016/j.jcs.2019.102792

Don, C., Lichtendonk, W.J., Plijter, J.J., van Vliet, T., Hamer, R.J., 2005. The effect of mixing on glutenin particle properties: aggregation factors that affect gluten function in dough. J. Cereal Sci. 41, 69–83. https://doi.org/10.1016/j.jcs.2004.09.009

Georget, D.M.R., Belton, P.S., 2006. Effects of Temperature and Water Content on the Secondary Structure of Wheat Gluten Studied by FTIR Spectroscopy. Biomacromolecules 7, 469–475. https://doi.org/10.1021/bm050667j

He, H., Hoseney, R.C., 1991. Gluten, a Theory of How it Controls Breadmaking, in: Gluten Proteins 1990. American Association of Cereal Chemists, St. Paul, Minnesota USA, pp. 1–10.

Hoseney, R.C., Pomeranz, Y., Finney, K.F., 1970. Functional (Breadmaking) and Biochemical Properties of Wheat Flour Components. VII. Petroleum Ether-Soluble Lipoproteins of Wheat Flou. Cereal Chem. 47, 135–140.

Khatkar, B.S., Bell, A.E., Schofield, J.D., 1995. The dynamic rheological properties of glutens and gluten sub-fractions from wheats of good and poor bread making quality. J. Cereal Sci. 22, 29–44. https://doi.org/10.1016/S0733-5210(05)80005-0

Khatkar, B.S., Fido, R.J., Tatham, A.S., Schofield, J.D., 2002. Functional Properties of Wheat Gliadins. II. Effects on Dynamic Rheological Properties of Wheat Gluten. J. Cereal Sci. 35, 307–313. https://doi.org/10.1006/jcrs.2001.0430

Lefebvre, J., Pruska-Kedzior, A., Kedzior, Z., Lavenant, L., 2003. A phenomenological analysis of wheat gluten viscoelastic response in retardation and in dynamic experiments over a large time scale. J. Cereal Sci. 38, 257–267. https://doi.org/10.1016/S0733-5210(03)00025-0

Li, W., Dobraszczyk, B.J., Dias, A., Gil, A.M., 2006. Polymer Conformation Structure of Wheat Proteins and Gluten Subfractions Revealed by ATR-FTIR. Cereal Chem. 83, 407–410. https://doi.org/10.1094/CC-83-0407

Li, W., Dobraszczyk, B.J., Schofield, J.D., 2003. Stress Relaxation Behavior of Wheat Dough, Gluten, and Gluten Protein Fractions. Cereal Chem. 80, 333–338. https://doi.org/10.1094/CCHEM.2003.80.3.333

Manders, E.M.M., Verbeek, F.J., Aten, J.A., 1993. Measurement of co-localization of objects in dual-colour confocal images. J. Microsc. 169, 375–382. https://doi.org/10.1111/j.1365-2818.1993.tb03313.x

Mohamed, A.A., Rayas-Duarte, P., 2003. The effect of mixing and wheat protein/gluten on the gelatinization of wheat starch☆☆Names are necessary to report factually on available data; however, the USDA neither guarantee nor warrants the standard of the product, and the use of the name by the USDA implies no approval of the product to the exclusion of others that may also be suitable. Food Chem. 81, 533–545. https://doi.org/10.1016/S0308-8146(02)00487-9

Morel, M.-H., Redl, A., Guilbert, S., 2002. Mechanism of Heat and Shear Mediated Aggregation of Wheat Gluten Protein upon Mixing. Biomacromolecules 3, 488–497. https://doi.org/10.1021/bm015639p

Onyango, C., Mutungi, C., Unbehend, G., Lindhauer, M.G., 2009. Creep-recovery parameters of gluten-free batter and crumb properties of bread prepared from pregelatinised cassava starch, sorghum and selected proteins. Int. J. Food Sci. Technol. 44, 2493–2499. https://doi.org/10.1111/j.1365-2621.2009.02048.x

Orth, R.A., Bushuk, W., 1972. A Comparative Study of the Proteins of Wheats of Diverse Baking Qualities. Cereal Chem. 49, 268–275.

Popineau, Y., Deshayes, G., Lefebvre, J., Fido, R., Tatham, A.S., Shewry, P.R., 2001. Prolamin Aggregation, Gluten Viscoelasticity, and Mixing Properties of Transgenic Wheat Lines Expressing 1Ax and 1Dx High Molecular Weight Glutenin Subunit Transgenes. J. Agric. Food Chem. 49, 395–401. https://doi.org/10.1021/jf001015j

Redl, A., Morel, M.H., Bonicel, J., Guilbert, S., Vergnes, B., 1999. Rheological properties of gluten plasticized with glycerol: dependence on temperature, glycerol content and mixing conditions. Rheol. Acta 38, 311–320. https://doi.org/10.1007/s003970050183

Yazar, G., Duvarci, O.C., Tavman, S., Kokini, J.L., 2017. LAOS behavior of the two main gluten fractions: Gliadin and glutenin. J. Cereal Sci. 77, 201–210. https://doi.org/10.1016/j.jcs.2017.08.014

CHAPTER 7.   CONCLUSIONS

Specific antibodies for HMW glutenins, and LMW glutenins have been successfully developed and conjugated with quantum dots. The Antibody-QDs complexes have been used along gliadin antibody-QDs complexes to detect LMW glutenins, HMW glutenins, and gliadins in wheat dough samples. Methanol was found to be the best fixative for wheat dough on microscope slides, keeping dough's morphology intact after staining; the autofluorescence of the dough is better controlled with the excitation/emission configuration in the microscope compared to commercially autofluorescence quenchers when using bright QDs as fluorophores. The development of this well-defined methodology for wheat flour dough imaging under the confocal laser scanning microscopy allows the collection of 'high-quality' imagines displaying the distribution of the gluten subunits. The introduction of the co-localization technique moved this project from qualitative description of the images to quantitative data of the interactions of the three different gluten subunits in the images. Moreover, the use of protein network analysis software helped collect data about the network parameters of the gluten subunits. With the use of this staining, microscopy, and image analysis techniques the changes in gluten subunits network and interactions were seen in different stages of mixing for hard wheat, soft wheat, and semolina; the differences of the gluten subunits were also seen under different rheological test for soft wheat and semolina.

New and significant insights were found about the three gluten subunits, especially LMW glutenins, which have been historically less explored in cereal science research compared to gliadins and HMW glutenins. LMW glutenins have been found responsible for the initial decay of dough strength after peak time (mixing time of maximum dough strength) in hard wheat flour mixed at ideal water addition, since they start to interact less with the other two gluten subunits and reduce their network parameters at that time. LMW glutenins also have been found to be the most important gluten subunits in keeping the structural integrity of semolina doughs. These has been demonstrated after none of the gluten subunit change their network parameters during semolina dough extended mixing; however, the network parameters of LMW glutenins subunit decreases much more than the other two subunits when the dough is subjected to disruption at different large amplitudes in the rheometer. HMW glutenins have been found to be responsible for the later decay of dough strength in hard wheat during farinograph mixing at ideal moisture content.

Contrarily to LMW glutenins and gliadins, HMW glutenins do not re-distribute in strong hard wheat flours when it is hydrated below its ideal moisture, this can be explained with their reduced molecular mobility given by its large amount of intra- and inter- molecular disulfide bonds. HMW glutenins interact and move together with gliadins in semolina deformation at large amplitudes. Gliadins, being the most molecular mobile proteins are found more homogenously distributed in general, compared to the glutenins subunits. They only breakdown significantly at the highest deformation amplitude tested (100% strain amplitude), 10% strain amplitude was not enough to disrupt gliadins significantly in either soft wheat dough or semolina dough. The three gluten subunits have been found moving synchronized in four different conditions in this study: first, during hydration of hard wheat flours dough at ideal moisture, building the gluten network and taking the dough to its highest strength; second, in soft wheat flours during its loss of dough strength during mixing with excess of water addition; third, in soft wheat when subjected to different amplitude of deformations in the rheometer; lastly, in semolina dough during prolonged mixing time in the farinograph, where loss of dough strength was not reported. Overall, the use of these new and improved staining, microscopy, and image processing techniques have been used to gain new insights about the role of LMW glutenins, HMW glutenins, and gliadins in wheat doughs.

VITA

JOSE CARLOS BONILLA OLIVA   **Ph.D. Candidate, Purdue University**

- **EDUCATION**

2015-present **PURDUE UNIVERSITY**
West Lafayette, IN, USA
Ph.D. Candidate in Food Science
Food processing and technology development
Department of Food Science

2011-2014   **ZAMORANO UNIVERSITY**
Francisco Morazán, Honduras
Bachelor of Science
Department of Food Science and Technology

- **RESEARCH EXPERIENCE**

2015-present **PURDUE UNIVERSITY**
West Lafayette, IN, USA
Research Assistant
Conducting research studying the structure/function relationships of gluten proteins during wheat dough processing with microscopy and rheological analyses

2014   **PURDUE UNIVERSITY**
West Lafayette, IN, USA
Visiting research scholar
Conducting research on the use of polysaccharides from corn as an encapsulation method for thymol

- **TEACHING EXPERIENCE**

2017   **PURDUE UNIVERSITY**
West Lafayette, IN, USA
Teaching assistant
FS-161 Science of food

2017   **PURDUE UNIVERSITY**
West Lafayette, IN, USA
Invited lecturer
FS-591 Advanced Materials Science Methods for Biomaterials Characterization

AWARDS

- Best Student Poster Award - Protein Division. AACCI annual meeting. November 2019. Denver, CO.
- 2019 Bilsland Dissertation Fellowship Award recipient. Purdue University.
- 1st Place, Global Food Science Competition, November 2018. Wuxi, China.
- 2018 AACCI Walter Bushuk Award - presented to an individual for outstanding contributions in basic and/or applied research in cereal protein chemistry. AACCI annual meeting, October 2018. London, England.
- 1st place, 2018 Student Research Paper Oral Competition – Protein Division. IFT Annual Meeting. July 2018. Chicago, IL.
- 2nd Place, Biological Engineering/Food Processing session at the Agricultural and Biological Engineering Annual Symposium. February 2018. Purdue University.
- 3rd place, Best Student Research Paper Competition, AACCI annual Meeting. October 2017. San Diego, CA.
- Scholarship for Krannert Applied Management Principles Program (Mini-MBA). May 2017. Purdue University.

- **PROFESSIONAL ACTIVITIES**

  - **As a referred journal reviewer**
    Journal of Agriculture and Food Chemistry, 11 manuscripts reviewed.

  - **As a judge for poster competition**
    Purdue Undergraduate Research Conference – College of Agriculture.

- **LEADERSHIP AND INVOLVEMENT**

  - Institute of Food technologists - Protein Division, Student representative, **2018-present**
  - Food Science representative at the College of Agriculture Graduate Student Advisory Council, Purdue University, **2017-present**
  - Institute of Food Technologists Student Association, Purdue Chapter - President **2017-2018**
    - IFTSA Purdue Chapter received '*Chapter of the year recognition*' for the first time
  - President of the Food Science Graduate Student Association (FSGSA), **2017-2018**
  - American Association of Cereal Chemists International Student Association - Student Representative for the Midwest Region, **2017-present**
  - President of the Association of Zamorano Alumni - Purdue Chapter, **2016-2017**
  - Leadership & Professional Development Seminar Series, Purdue Food Science, **2017**

- **MEMBERSHIPS**

  - Phi Tau Sigma **(ΦΤΣ)**, The Honor Society of Food Science, 2019-present
  - Whistler Center for Carbohydrate Research **(WCCR)**, 2014 – present
  - Institute of Food Technologist **(IFT)**, 2015 – present

- Association of Zamorano Alumni **(AGEAP International)**, 2015 – present
- Food Science Graduate Student Association **(FSGSA)**, 2015-present
- American Association of Cereal Chemists International **(AACCI)** – 2016- present

SKILLS

Computer Skills

Software: ImageJ, NIS-Elements, Zeiss-ZEN, I-TASSER, Gen-5, TRIOS, FARINOGRAPH-5, AngioTool64, SAS, MiniTab.

Bioinformatics databases: NCBI, ExPASy, Uniprot.

Language Skills

Spanish- (native language), English

Equipment skills

Confocal Laser Scanning Microscope, Light and Fluorescent Microscope, Rheometer, Farinograph, Mixograph, Texture Analyzer, Differential Scanning Calorimeter, Dynamic Light Scattering, Electrophoresis and Western blot equipment, UV-VIS Spectrophotometer.

PEER-REVIWED PUBLICATIONS

Bonilla, J.C., Erturk, M.Y., Schaber, J.A., Kokini, J.L., **(2020)**. Distribution and function of LMW glutenins, HMW glutenins, and gliadins in wheat doughs analyzed with 'in situ' detection and quantitative imaging techniques. J. Cereal Sci. 102931. https://doi.org/10.1016/j.jcs.2020.102931

Bonilla, J. C., Schaber J., Bhunia, A., & Kokini, J. L. **(2019)**. Mixing dynamics and molecular interactions of HMW glutenins, LMW glutenins, and gliadins analyzed by fluorescent co-localization and protein network quantification. *J. Cereal Sci.*, *89, 102792*

Bonilla, J. C., Bernal-Crespo, V., Schaber, J., Bhunia, A., & Kokini, J. L. **(2019).** Simultaneous immunofluorescent imaging of gliadins, low molecular weight glutenins, and high molecular weight glutenins in wheat flour dough with antibody-quantum dot complexes. Food Research International, 120, 776-783. **DOI**: 10.1016/j.foodres.2018.11.038

Bonilla, J. C., Ryan, V., Yazar, G., Kokini, J. L., & Bhunia, A. **(2018)**. Conjugation of Specifically Developed Antibodies for High- and Low-Molecular-Weight Glutenins with Fluorescent Quantum Dots as a Tool for Their Detection in Wheat Flour Dough. Journal of Agricultural and Food Chemistry, 66 (16), 4259-4266. **DOI:** 10.1021/acs.jafc.7b05711

Bonilla, J. C., Bozkurt, F., Ansari, S., Sozer, N., & Kokini, J. L. **(2016)**. Applications of Quantum Dots in Food Science and Biology. Trends in Food Science & Technology, 53, 75-89. **DOI:** 10.1016/j.tifs.2016.04.006

Bonilla, J.C., Erturk, M.Y., Kokini, J.L., **(2020)**. Understanding the role of gluten subunits (LMW, HMW glutenins and gliadin) in the networking behavior of soft and semolina wheat flour dough and the relationship between linear and non-linear rheology. *Submitted to Food Hydrocolloids*

Turksoy, S., Erturk, M.Y., Bonilla, J., Turasan, H., Kokini, J.L., **(2020)**. Effect of aging at different temperatures on LAOS properties and secondary protein structure of hard wheat flour dough. J. Cereal Sci. 92, 102926. https://doi.org/10.1016/j.jcs.2020.102926

Olivera, N., Rouf, T.B**.**, **Bonilla, J.C.**, Carriazo, J.G., Dianda, N., & Kokini, J.L., **(2019)**. Effect of LAPONITE® addition on the mechanical, barrier and surface properties of novel biodegradable kafirin nanocomposite films. Journal of Food Engineering, 245, 24–32. **DOI**: 10.1016/j.jfoodeng.2018.10.002

Dianda, N., Rouf, T.B., **Bonilla, J.C**., Hedrick, V., Kokini, J., **(2019)**. Effect of solvent polarity on the secondary structure, surface and mechanical properties of biodegradable kafirin films. J. Cereal Sci. 102856. https://doi.org/10.1016/j.jcs.2019.102856

Maldonado, L., Chough, S., **Bonilla, J.,** Kim, K.H., & Kokini, J. L. **(2019).** Mechanism of fabrication and nano-mechanical properties of α-lactalbumin/chitosan and BSA/κ-carrageenan nanotubes through layer-by-layer assembly for curcumin encapsulation and determination of in vitro cytotoxicity. Food Hydrocolloids, 93, 293-307. **DOI**: 10.1016/j.foodhyd.2019.02.040

Turasan, H., **Bonilla, J.,** Bozkurt F., Maldonado L., Li, X., Yilmaz, T., Sadeghi, R., Kokini, J.L **(2020)**. Comparison of the fabrication methods, formation dynamics, structure and delivery performance of solid nanoparticles and hollow layer-by-layer (LbL) edible/biodegradable nanodelivery systems. *Journal of Food Process Engineering (Under review).*

▪ **BOOK CHAPTERS**

Turasan, H., **Bonilla, J**., Jia F., Maldonado L., Malm M., Rouf, T.B., & Kokini, J.L. **(2019).** Advances in Food Functionality and Packaging Using Nanotechnology. Food Applications of Nanotechnology. CRC Press.

▪ **SCIENTIFIC PRESENTATIONS**

- Research E-poster at the Institute of Food Technologist annual meeting. **Chicago, Illinois, June 2019**
- Research poster at the Global Food Science Student Competition. **Wuxi, China, November 2018**
- Oral presentation at the AACCI annual meeting. **London, UK, October 2018**
- Oral presentation at the Institute of Food Technologist annual meeting. **Chicago, Illinois, July 2018**

- Oral presentation at the AACCI annual meeting. **San Diego, California, October 2017**
- Research poster at the Institute of Food Technologist annual meeting. **Las Vegas, Nevada, June 2017**
- Research poster at the Institute of Food Technologist annual meeting. **Chicago, Illinois, July 2016**